RECEIVED
LAWRENCE
RADIATION LABORATORY

MAR 3 1969

LIBRARY AND
DOCUMENTS SECTION

UCRL-18685
cy. 2

A MASS SPECTROMETRIC STUDY OF THE SUBLIMATION OF CHROMIUM TRIOXIDE

Charles Adelbert Washburn
(Ph. D. Thesis)

February 1969

TWO-WEEK LOAN COPY

This is a Library Circulating Copy
which may be borrowed for two weeks.
For a personal retention copy, call
Tech. Info. Division, Ext. 5545

LAWRENCE RADIATION LABORATORY
UNIVERSITY of CALIFORNIA BERKELEY

UCRL-18685
cy. 2

DISCLAIMER

This document was prepared as an account of work sponsored by the United States Government. While this document is believed to contain correct information, neither the United States Government nor any agency thereof, nor the Regents of the University of California, nor any of their employees, makes any warranty, express or implied, or assumes any legal responsibility for the accuracy, completeness, or usefulness of any information, apparatus, product, or process disclosed, or represents that its use would not infringe privately owned rights. Reference herein to any specific commercial product, process, or service by its trade name, trademark, manufacturer, or otherwise, does not necessarily constitute or imply its endorsement, recommendation, or favoring by the United States Government or any agency thereof, or the Regents of the University of California. The views and opinions of authors expressed herein do not necessarily state or reflect those of the United States Government or any agency thereof or the Regents of the University of California.

UCRL-18685

UNIVERSITY OF CALIFORNIA

Lawrence Radiation Laboratory
Berkeley, California

AEC Contract No. W-7405-eng-48

A MASS SPECTROMETRIC STUDY OF THE SUBLIMATION OF CHROMIUM TRIOXIDE

Charles Adelbert Washburn

(Ph.D. Thesis)

February, 1969

TABLE OF CONTENTS

I. INTRODUCTION ---------- 1

II. EXPERIMENTAL ---------- 7

A. Mass Spectrometers ---------- 7

B. Sample Material ---------- 7

III. SPECIES IDENTIFICATION ---------- 8

IV. FRAGMENT IDENTIFICATION ---------- 10

A. Introduction ---------- 10

B. Appearance Potentials ---------- 13

C. Double Cell Experiments ---------- 19

1. Introduction ---------- 29

2. Description of the Double Cell ---------- 31

3. Discussion ---------- 31

V. VAPOR PRESSURE MEASUREMENTS ---------- 51

A. Experimental ---------- 51

B. Behavior of Oxygen ---------- 56

C. Pressure Calibration ---------- 57

1. Ionization Cross Sections ---------- 57

2. Calculation of Relative Partial Pressures ---------- 58

3. Pressure Calibration Factors Based on Weight-Loss Experiments ---------- 64

D. Heats and Entropies of Sublimation and Partial Pressures ---------- 73

E. Total Pressures ---------- 79

F. Stoichiometric Balance ---------- 82

VI. SUMMARY AND CONCLUSIONS ---------- 83

VI.

A. Species Identification---------- 83

B. Cadmium---------- 86

C. Partial Pressures of Chromium-Containing Molecules---------- 86

D. Behavior of Oxygen---------- 87

ACKNOWLEDGEMENT---------- 88

REFERENCES---------- 89

APPENDIX A---------- 92

FIGURE CAPTIONS---------- 96

FIGURES---------- 99

A MASS SPECTROMETRIC STUDY OF THE SUBLIMATION OF CHROMIUM TRIOXIDE

Charles Adelbert Washburn

Inorganic Materials Research Division, Lawrence Radiation Laboratory
Department of Material Science and Engineering, College of Engineering
University of California, Berkeley, California

ABSTRACT

$CrO_{3(s)}$ is metastable, even at room temperature, relative to decomposition to $Cr_2O_{3(s)}$ and $O_{2(g)}$. However the decomposition reaction is strongly kinetically suppressed, and, in fact, $CrO_{3(s)}$ sublimes congruently or nearly congruently below its melting point (196°C). The vapor species in addition to O_2 are Cr_nO_{3n} n = 3, 4, 5, and 6, Cr_nO_{3n-2} n = 3, 4, and 5. In addition, small quantities of Cr_4O_{11} and Cr_3O_8 are probably present in the vapor. The oxygen partial pressure in a Knudsen cell containing 0.5 grams $CrO_{3(s)}$ and fitted with a 1 mm diameter orifice is less than 10^{-10} time the pressure expected from thermodynamics.

In addition to ions corresponding to the molecules mentioned above, ions of the following compositions were detected in the mass spectrum resulting from the sublimation of $CrO_{3(s)}$ but were determined to be fragments of heavier molecules: $Cr_4O_9^+$, $Cr_4O_8^+$, $Cr_4O_7^+$, $Cr_3O_6^+$, $Cr_3O_5^+$, $Cr_3O_4^+$, $Cr_2O_5^+$, $Cr_2O_4^+$, and $Cr_2O_3^+$.

Considerable evidence was found that the chromium containing molecules, unlike oxygen, evaporate with evaporation coefficients near unity and that the gaseous chromium-containing molecules are in equilibrium among themselves but not with oxygen. The partial pressures of the six most important chromium-containing species are given by the following equations between 415.1°K and 468.1°K:

$$\log P_{(CrO_3)_5}\ (\text{atm}) = -\frac{(7.943 \pm 0.240) \times 10^3}{T} + (15.02 \pm 0.54)$$

$$\log P_{Cr_5O_{13}}\ (\text{atm}) = -\frac{(9.373 \pm 0.154) \times 10^3}{T} + (19.13 \pm 0.35)$$

$$\log P_{(CrO_3)_4}\ (\text{atm}) = -\frac{(6.849 \pm 0.150) \times 10^3}{T} + (13.70 \pm 0.34)$$

$$\log P_{Cr_4O_{10}}\ (\text{atm}) = -\frac{(7.983 \pm 0.124) \times 10^3}{T} + (17.17 \pm 0.28)$$

$$\log P_{(CrO_3)_3}\ (\text{atm}) = -\frac{(6.836 \pm 0.152) \times 10^3}{T} + (13.08 \pm 0.34)$$

$$\log P_{Cr_3O_7}\ (\text{atm}) = -\frac{(7.465 \pm 0.095) \times 10^3}{T} + (15.09 \pm 0.22)$$

I. INTRODUCTION

In 1961 Ackermann and Thorn[1] commented: "Unfortunately the vaporization of chromium oxides has not been studied so no discussion of these oxides is given herein." Since then several important papers on the subject have been published. In 1961 Grimley, Burns, and Inghram[2] published a high temperature mass spectrometric study of the vaporization of Cr_2O_3. They found that Cr, CrO, CrO_2, O, and O_2 were the principle gaseous species in equilibrium with Cr_2O_3 and determined the dissociation energies D_o^o (CrO) = 101.7 ± 7 kcal/mol and D_o^o (CrO_2) = 227.1 ± 15 kcal/mol. Grimley, Burns, and Inghram also detected $CrO_{3(g)}$ when oxygen was released into their cell, and on the basis of data at three temperatures, set D_o^o (CrO_3) = 341 ± 20 kcal/mol. The work of Grimley, et al., confirms the work of Wang, et al.,[3] who studied the Langmuir sublimation rate of Cr_2O_3 and found "that the rate of sublimation was slightly higher than predicted for decomposition to the elements" and suggested that small amounts of complex molecules, e.g. CrO and CrO_2, were present in the vapor over Cr_2O_3. The work of Wang and associates also furnished good evidence that Cr_2O_3 is congruently vaporizing. Caplan and Cohen[4] did a qualitative transpiration study on Cr_2O_3 at 1000°C to 1200°C in various atmosphere. They noted an increased rate of weight loss when wet or dry oxygen was used in preference to dry argon.

Glemser, et al.,[5] have published results of transpiration studies on $CrO_{3(s)}$. They used oxygen as a carrier gas and studied the vaporization rate over the range 448 to 468°K. Presenting their results as a vapor pressure equation for the assumed reaction:

$$CrO_{3(s)} = CrO_{3(g)} \qquad (1)$$

they wrote:

$$\log P_{CrO_3(torr)} = -\frac{10.3 \times 10^3}{T} + 20.14 \qquad (2)$$

which, recalculated in atmospheres is:

$$\log P_{CrO_3(atm)} = -\frac{10.30 \times 10^3}{T} + 17.26 \qquad (3)$$

Reaction (1) was postulated because Grimley, et al.,[2] had detected $CrO_{3(g)}$ over $Cr_2O_{3(s)}$ under oxidizing conditions. Multiplying through equation (3) by (-4.576 T) to obtain an equation for ΔF^o_{sub}, we obtain:

$$\Delta F^o_{sub} = 47.2 \times 10^3 - 78.95T \qquad (4)$$

Therefore, Glemser, Muller, and Stockner's data indicates, for reaction (1):

$$\Delta H^o_{sub}(CrO_3) = 47.2 \text{ kcal/mol.}$$

$$\Delta S^o_{sub}(CrO_3) = 78.95 \text{ eu}$$

In 1960 Ackermann, et al.,[6] summarized the available data for the entropy of sublimation of the polymers of MoO_3 and WO_3. These data, together with more recent sublimation entropies for the tungsten trioxide polymers taken from the work of Ackermann and Rauh[7] are summarized in Table I. Comparison of the entropy of sublimation of $(CrO_3)_{(s)}$ deduced from equation (3) with the data in Table I leads to the conclusion that the vapor over $CrO_{3(s)}$ is probably composed not of $CrO_{3(g)}$, but of molecules whose complexity is comparable with that of the trimer and tetramer. Similar considerations led Schafer and Rinke[8] to examine the mass spectrum produced by the vaporization of CrO_3.

The work of Schafer and Rinke was limited to measurements at one

Table I. Literature values of the entropies of sublimation of the polymers of $MoO_{3(s)}$ and $WO_{3(s)}$.

n	ΔS^{o}_{sub}, eu		
	$(MoO_3)_n$[a]	$(WO_3)_n$[b]	$(WO_3)_n$[c]
1	40	40	
2			54.0
3	65	69	53.5
4	76	82	60.8
5	85		

a. Data from reference 6, temperature 1050°K.

b. Data from reference 6, temperature 1400°K.

c. Data from reference 7, temperature 1400°K.

temperature in the neighborhood of the melting point of CrO_3, and does not include evaluation of thermodynamic stabilities. Although most of the ions that they detected were also found in the present study, several prominent differences exist between the two studies:

(a) Schafer and Rinke reported that M268 ($Cr_3O_7^+$) was the most intense peak in the mass spectrum, whereas in the present study M368 ($Cr_4O_{10}^+$) was always the most intense peak (except at some temperatures in the double cell experiments).

(b). Schafer and Rinke reported detecting peaks corresponding to Cr^+, CrO^+, CrO_2^+, and $Cr_2O_2^+$, none of which were detected in this study, even when the double cell was used.

(c) Schafer and Rinke reported metastable peaks corresponding to the decomposition of the ions $Cr_3O_9^+$, $Cr_4O_{12}^+$, and $Cr_5O_{15}^+$ with an electron energy of 16 ev, and additional metastable peaks corresponding to the decomposition of the $Cr_3O_7^+$ and $Cr_4O_{10}^+$ ions when 50 ev electrons were used. In every case they attributed the metastable peaks to decomposition by the loss of two oxygen atoms (or an O_2 molecule). None of these metastable peaks were observed in the present work.

(d) Figure 1 is a plot of the ratio of the intensity of a given peak as measured in this study using 70 ev electrons to the intensity by Schafer and Rinke using 50 ev electrons vs. the mass number of the ion. For some unknown reason, the relative intensities Schafer and Rinke reported for the higher molecular weight species are far less than were found in the current study. A possible explanation is that the graphite used for their Knudsen cell material was very aggressive at reducing CrO_3.

A second mass spectrometric study of the sublimation of $CrO_{4(s)}$ has been published by McDonald and Margrave[9]. They concluded that the only

vapor species present over $CrO_{3(s)}$ were the polymers, $(CrO_3)_n$, with n = 3, 4, or 5. The appearance potentials reported by McDonald and Margrave are listed in Table IV and are, in most cases, in reasonable agreement with the results of this study. Regarding their conclusion that the only species present in the neutral vapor were the polymers, McDonald and Margrave stated: "Appearance potentials show that trimers, tetramers and pentamers of CrO_3 are parent species with $Cr_xO_{3x-2}^+$ and similar ions formed by dissociative ionization. The ionization efficiency curve for the $Cr_4O_{10}^+$ ions did not show breaks or unusual shapes and thus, the ion is assumed to arise from a single precursor." This conclusion is in direct opposition to the conclusions of the present study that the $Cr_xO_{3x-2}^+$ species, and probably the $Cr_xO_{3x-1}^+$ species (not reported by McDonald and Margrave), at low electron energies arise from simple ionization. Evidence of several types bearing on the question of whether the $Cr_nO_{3n-2}^+$ species are fragments of the corresponding Cr_nO_{3n} molecules is discussed later in this thesis.

A point not mentioned in the papers of Schafer and Rinke and of McDonald and Margrave is that the species observed during vaporization of $CrO_{3(s)}$ cannot be the most stable possible vaporization reaction products.

In his review article of 1950, Brewer[10] discussed the probable vaporization behavior of CrO_3. He pointed out ". . . the higher oxides of chromium all lose oxygen without appreciable loss to chromium to form Cr_2O_3." Brewer[10] also noted that the heat of formation then available indicated that even at room temperature $CrO_{3(s)}$ is metastable relative to decomposition to $CrO_{3(s)}$ and oxygen. The redetermination of the heat of formation of $CrO_{3(s)}$ by Margrave and Neugebauer[11] confirmed that this is true. The reported observations of $CrO_{3(s)}$ vaporization to polymers of CrO_3 is inconsistant with the thermodynamic predication of dissociation. An important question to be settled, therefore, is whether or not

the observed vapor species are in metastable equilibrium with solid CrO_3 and with each other.

In addition to his transpiration study using oxygen as the carrier gas, Glemser, together with Muller[12], studied the vaporization of CrO_3 in the presence of wet oxygen or wet nitrogen over the temperature range 135-185°C. They concluded that $CrO_2(OH)_{2(g)}$ was formed under these conditions. Since the mass spectrometric studies of the sublimation of CrO_3 indicate that the vapor contains oxide polymers, it is probable that the reaction of CrO_3 with water vapor produces a complex assortment of polymeric oxyhydroxide molecules.

II. EXPERIMENTAL

A. Mass Spectrometers

An Atlas CH-4 mass spectrometer (240 mm radius, 60° sector, single focusing) equipped with a Knudsen cell was used for all of the studies except the double cell experiments. The Atlas mass spectrometer was equipped with a 16 stage electron multiplier, using copper-beryllium dynodes.

A Nuclide Analysis Associates HT mass spectrometer (12 inch radius 60° sector, single focusing) was used for the double cell studies. The Nuclide mass spectrometer was equipped with a 12 stage electron multiplier, using copper-beryllium dynodes.

B. Sample Material

The chromium trioxide used in this study was Baker and Adamson's reagent grade. A spectrographic analysis detected no metallic impurities.

III. SPECIES IDENTIFICATION

The first scan of the mass spectrum resulting from the vaporization of CrO_3 revealed a bewildering complexity of ions. Fortunately, chromium has four isotopes of appreciable abundance which allowed unambiguous identification of the chemical composition of the observed ions. The relative abundances of Cr_n, n=1 to 6, are tabulated in Appendix A. The Atlas CH4 mass spectrometer was equipped with a "mass meter" which allowed the location of a given peak to within a few mass units. By comparing the relative peak intensities in a given series of peaks with the abundances tabulated in Appendix A, it was possible to identify the number of chromium atoms present in a given series of ions. From the approximate mass number and the number of chromium atoms, it was possible to establish the number of oxygen atoms present in a given series of ions, and hence the chemical composition of the ions.

Table II summarizes the compositions of ions identified in the mass spectrum. Each ion is reported in terms of the mass number of its most abundant isotope. The same ion peaks and the same relative ion intensities (at a given cell temperature) were found with either an Al_2O_3 or a graphite Knudsen cell liner. However, except for the cell exhaustion experiment which used a graphite liner and the double cell experiments which used a stainless steel and copper cell, Al_2O_3 liners were used in all of the quantitative measurements reported in this thesis.

Table II. Identification of chromium-containing ions from a Knudsen cell containing CrO_3.

Composition of ion	Mass Number of most abundant ion	Composition of ion	Mass Number of most abundant ion
$Cr_2O_3^+$	M152 (a)	$Cr_4O_7^+$	M320 (b)
$Cr_2O_4^+$	M168	$Cr_3O_8^+$	M336
$Cr_2O_5^+$	M184	$Cr_4O_9^+$	M352
$Cr_3O_4^+$	M220 (b)	$Cr_3O_{10}^+$	M368
$Cr_3O_5^+$	M236	$Cr_4O_{11}^+$	M384
$Cr_3O_6^+$	M252	$(CrO_3)_4^+$	M400
$Cr_3O_7^+$	M268	$Cr_5O_{13}^+$	M468
$Cr_3O_8^+$	M284	$(CrO_3)_5^+$	M500
$(CrO_3)_3^+$	M300	$(CrO_3)_6^+$	M600 (b)

(a). This ion was present in too low a concentration to allow accurate measurement of its appearance potential.

(b). These ions were detected only in very low concentrations and then only when the sample temperature was high (CrO_3 above its melting point) and the electron energy was of the order of 50 to 70 ev.

IV. FRAGMENT IDENTIFICATION

A. Introduction

The great complexity of the mass spectrum resulting from the vaporization of CrO_3 is in sharp contrast with the mass spectrum resulting from the evaporation of MoO_3 or W_{O_3}.

Berkowitz, Inghram, and Chupka[13] found the following ions and appearance potentials when $MoO_{3(s)}$ was vaporized from a molybdenum cell: $(MoO_3)_3^+$ 10.9 ev; $(MoO_3)_4^+$, 10.9 ev; $(MoO_3)_5^+$, 10.9 ev; MoO_3^+ 13.9 ev; $(MoO_3)_2^+$, 13.5 ev. They concluded that the first three ions represented simple ionization of parent molecules while the last two ions resulted principally from fragmentation of the first three ions, and stated: "Essentially the same results were obtained using electron kinetic energies of 15, 40, and 150 ev."

In their study of the sublimation of molybdenum dioxide from an aluminum oxide Knudsen cell, Burns, DeMaria, Drowart, and Inghram[14] found the following ions and appearance potentials: MoO_3^+, 12.0 ev; $(MoO_3)_2^+$, 12.1 ev; MoO_2^+, 9.4 ev; $(MoO_3)_3^+$, 12.0 ev; $Mo_2O_5^+$, 10. ev; $Mo_2O_4^+$; and $Mo_3O_8^+$, 12.2 ev. They concluded, on the basis of appearance potentials and ionization efficiency curves, that MoO_3^+, $(MoO_3)_2^+$, and $(MoO_3)_3^+$ resulted from simple ionization of the neutral molecules, and that part of the MoO_2^+ ion current resulted from simple ionization of the neutral molecules, and that part of the MoO_2^+ ion current resulted from simple ionization of the neutral molecule. Furthermore, they also concluded that part of the $Mo_2O_5^+$ and $Mo_3O_8^+$ ion peaks resulted from simple ionization of molecules of the same composition, but that "The presence of a parent Mo_2O_4 molecule must be considered doubtful." These authors apparently used 17 ev ionizing electrons.

Berkowitz, Chupka, and Inghram[15] also investigated the sublimation of tungsten trioxide. Here again the equilibrium species were concluded to be the trimer, tetramer, and pentamer of the trioxide. Berkowitz, et al., also noted: "Ion peaks having mass numbers corresponding to WO_3^+ and $W_2O_6^+$ appeared, but were due largely, if not entirely, to dissociative ionization of the higher polymers." Their study was performed with 60 ev electrons.

In their study of the sublimation of $WO_{2.96}$, Ackermann and Rauh[7] observed WO^+, WO_2^+, WO_3^+, $W_2O_5^+$, $W_2O_6^+$, $W_3O_8^+$, $W_3O_9^+$, $W_4O_{11}^+$, $W_4O_{12}^+$, and $W_5O_{15}^+$ ions of which WO^+, WO_2^+, WO_3^+, and most of the $W_2O_5^+$ ions disappeared when electron energies below 30 ev were used. The authors then commented: "Although a part of the $W_2O_6^+$ and $W_3O_8^+$ ion currents could have resulted from fragmentation of the major species W_3O_9, the principal gaseous species above all tungsten oxides studied here appear to be W_2O_6, W_3O_8, W_3O_9, and W_4O_{12}."

Norman and Staley[16] detected WO_2^+, WO_3^+, $W_2O_5^+$, $(WO_3)_2^+$, $W_3O_8^+$, and $(WO_3)_3^+$ ions when a tungsten trioxide-silicate solution was heated in an iridium cell. The appearance potentials found were: WO_2^+, 14.2 ev; WO_3^+, 12.1 ev; $W_2O_5^+$, 15.8 ev; $(WO_3)_2^+$, 13.4 ev; $W_3O_8^+$, 15.5 ev; and $(WO_3)_3^+$, 13.3 ev. They concluded: "It was apparent from a study of the appearance potentials and appearance potential curves that the principal gaseous species under the conditions of the study were WO_3, $(WO_3)_2$, and $(WO_3)_3$, and that $W_3O_8^+$, $W_2O_5^+$, and WO_2^+ were essentially fragment ions." These investigators used 20 ev. electrons for ionization.

The immediate problem in the study of the sublimation of chromium trioxide was to identify the ions that were fragments and to determine

an electron energy that could be used for vapor pressure measurements that was low enough so that fragmentation was negligible but high enough so that the ion intensities were adequate to allow accurate ion intensity measurements.

Several types of experiments can be used to obtain information useful for the identification of parent ion-fragment ion relationships:

I). Measurement of appearance potentials and ionization efficiency curves.

II). Measurements of heats of sublimation (slopes of $I^{+}T$ vs. 1/T plots).

III). Experiments with reduced activity of one or more of the elements present in the solid, specifically:

1. Use of a compound containing chromium and oxygen, with the activity of one or both reduced below its activity in CrO_3.
2. Cell exhaustion experiments.

IV). Experiments that provide for undersaturation of the gas phase while using a solid of unit activity.

1. Use of the double oven technique
2. Use of the nested cell technique

V). Experiments that increase the activity of one of the elements above its activity in the solid, such as by releasing oxygen into the cell.

VI). Molecular beam profile studies.

The Atlas CH_4 mass spectrometer which was used during this phase of the study is equipped with an electro-magnetic molecular beam shutter that does not have a manual over-ride; hence experiments of type VI

were not possible. Attempts were made to examine the spectrum resulting from the evaporation of several compounds that would have an activity of CrO_3 lower than that of $CrO_{3(s)}$. The compounds used included Cr_3O_8 $PbCrO_4$, Na_2CrO_4, and CrO_2. None of these experiments were successful in giving useful information. In every case the oxygen pressure rose so rapidly upon heating that polymers of CrO_3 were not observed in the mass spectrum before the compound had been reduced to a lower oxide. Since each of these solids should have a lower oxygen activity than $CrO_{3(s)}$, these results clearly confirm the prediction from thermochemical measurements that O_2 should be the principal equilibrium gaseous product when $CrO_{3(s)}$ is heated. The observed polymeric gaseous oxides may be in metastable equilibrium with the solid, but they are not the equilibrium reaction products. In addition, an attempt was made to use a reducing cell material but surprisingly, the mass spectrum observed when a graphite cell liner was used for experiments up to the melting point of CrO_3, 196°C, was indistinguishable from that observed when an aluminum oxide cell liner was used. Since graphite is a reducing agent, this result implies that the gaseous oxides as well as the solid CrO_3 do not rapidly establish equilibrium oxygen pressures.

Consequently, identification of the parent-fragment relationships was made by use of appearance potentials, heats of sublimation, nested cell experiments, double cell experiments, and cell exhaustion experiments.

B. Appearance Potentials

Appearance potentials of the chromium containing ions detected in this study are listed in Table III. Both absolute appearance potentials, made using mercury as a standard and taking the spectroscopic ionization

Table III. Appearance potentials of chromium-containing ions in the mass spectrum resulting from the sublimation of CrO_3.

Species	Appearance Potential Relative to $Cr_4O_{10}^+$	Appearance Potential Absolute volts	Species	Appearance Potential Relative to $Cr_4O_{10}^+$	Appearance Potential Absolute volts
$(CrO_3)_5$	-0.8	11.0	Cr_3O_8	4.9	16.7
$(CrO_3)_4$	-0.7	11.1	Cr_4O_8	4.9	16.7
$(CrO_3)_3$	-0.3	11.5	Cr_4O_9	5.5	17.3
Cr_5O_{13}	-0.1	11.7	Cr_2O_4	5.7	17.5
Cr_4O_{10}	0.0	11.8	Cr_3O_5	5.7	17.5
Cr_3O_7	1.0	12.8	Cr_2O_5	7.1	18.9
Cr_4O_{11}	3.5	15.3	Cr_3O_6	7.8	19.6

potential (10.43 ev)[17] of mercury as its appearance potential, and appearance potentials relative to $Cr_4O_{10}^+$ (M368) are tabulated. The appearance potentials of the chromium containing species were determined relative to $Cr_4O_{10}^+$ by use of the extrapolated differences method.[18] The difference between the appearance potential of $Cr_4O_{10}^+$ and Hg^{202+} was then determined by the same technique. As a check on the reliability of using the $Cr_4O_{10}^+$ ion intensity as in 'internal standard,' the appearance potentials of the ions $Cr_3O_7^+$ $(CrO_3)_3^+$, $(CrO_3)_4^+$, $Cr_4O_{13}^+$, and $(CrO_3)_5^+$ were all determined directly relative to Hg^{202+}. The agreement of the direct determination with the indirect determination was within 0.1 ev in all cases except for $Cr_3O_7^+$, where the difference was 0.3 ev. Table IV is a comparison of appearance potential values determined in this study with values reported by Schafer and Rinke[8] and by McDonald and Margrave[9].

Grimley, Burns, and Inghram[2] found the following values for the dissociation energies of chromium oxides.

$D_o^o(CrO)$ = 101 kcal/mol (4.4 ev)

$D_o^o(CrO_2)$ = 227 kcal/mol (4.9 ev/bond)

$D_o^o(CrO_3)$ = 341 kcal/mol (4.9 ev/bond)

Thus the Cr-O bond energy can be taken at about 4.4 ev. Examination of the results of work on other MO_3 polymers (M=Mo,W) shows that the polymerization energy is usually about 85% of the bond energy. The value of $\Delta H^o_{f298}(O_{(g)})$ selected for the revised Circular 500 is 59.553 kcal.[19] These data will be used to consider the energetics of several possible fragmentation processes.

For the reaction:

$$XY + e = X^+ + Y + 2e$$

Table IV. Comparison of observed appearance potentials.

Species	Appearance Potentials (electron volts)		
	Schafer and Rinke[8]	McDonald and Margrave[9]	This study
$(CrO_3)_5^+$		12	11.0
$Cr_5O_{13}^+$		14.2	11.7
$(CrO_3)_4^+$	~ 12 (a)	11.9	11.1
$Cr_4O_{11}^+$		(b)	15.3
$Cr_4O_{10}^+$	~ 12	12.8	11.8
$Cr_4O_9^+$			17.3
$Cr_4O_8^+$			16.7
$(CrO_3)_3^+$	~ 12	12.4	11.5
$Cr_3O_8^+$		(b)	16.7
$Cr_3O_7^+$	~ 12	15.8	12.8
$Cr_3O_6^+$		15.6	19.6
$Cr_3O_5^+$		(b)	17.5
$Cr_2O_5^+$			18.9
$Cr_2O_4^+$	~ 19	19.4	17.5
$Cr_2O_3^+$		17.4	

(a). Schafer and Rinke reported that their values were uncorrected.

(b). These ions were not reported by McDonald and Margrave.

the appearance potential of the X^+, $AP(X^+)$, will be:

$$AP(X^+) = D(X\text{-}Y) + I(X) + K + E \qquad (5)$$

where:

D(X-Y) is the X-Y bond energy

I(X) is the ionization potential of X (from the ground state to the particular ionic state produced).

K, E are the excess energy carried off by the fragments (kinetic and electronic energy).

Stevenson[20] has shown that the equality:

$$AP(X^+) = D(X - Y) + I(X)$$

will hold in nearly all cases if $I(X) < I(Y)$. However, we will not make this assumption, but will always keep the quantity (K + E) on the right side of equations of the form of (5). The quantity (K + E) will not be included explicitly, but its presence will be indicated by the sign $\geq$.

Example I. Assume $(CrO_3)_4^+$ arises from:

$$(CrO_3)_5 + e = (CrO_3)_4^+ + CrO_3 + 2e$$

Then the above considerations lead to the expectation that:

$$AP\ ((CrO_3)_4^+) \geq D((CrO_3)_4 \text{ -- } CrO_3) + I(CrO_3)_4$$

Past experience on a wide range of inorganic systems suggests that the ionization potentials of these complex chromium-oxygen molecules should all be roughly the same. Hence we would except:

$$AP((CrO_3)_4^+) - AP((CrO_3)_5^+ \geq D((CrO_3)_4 \text{ -- } CrO_3)$$

$$\geq 0.85 \times 4.4$$

$$\geq 3.7 \text{ ev}$$

Thus the difference between the appearance potentials of the tetramer and pentamer would be expected to be at least 3.7 ev if the tetramer arises from fragmentation of the pentamer. Experimentally this difference is found to be 0.1 ev. Thus the appearance potential results indicate that $(CrO_3)_4^+$ does not arise from the fragmentation of $(CrO_3)_5$.

Example II.

Assume $Cr_4O_{10}^+$ arises from:

$$(CrO_3)_4 + e = Cr_4O_{10}^+ + 2\,O_{(g)} + 2e$$

In this case:

$$AP(Cr_4O_{10}^+) - AR((CrO_3)_4^+) \geq 2\,D(Cr\text{-}O)$$

$$\geq 8.8 \text{ ev.}$$

If the fragmentation process produces O_2 rather than two oxygen atoms, D_o^o should be subtracted from the above result, yielding $8.8 - 5.2 \geq 3.6$ ev for the difference between the appearance potentials of $Cr_4O_{10}^+$ and $(CrO_3)_4^+$. Experimentally this difference was found to be 0.7 ev. Fragmentation of the tetramer can be reasonably ruled out as the source of $Cr_4O_{10}^+$. Fragmentation of molecules more complex than the tetramer to form $Cr_4O_{10}^+$ would require even larger energies.

Other examples of this type of argument can be found in section D, "Double Cell Experiments" where the conclusions drawn from the appearance potential data are checked against conclusions drawn from the double cell experiments.

From consideration of a large number of examples such as those illustrated, the appearance potential data suggest that the equilibrium species are:

$$(CrO_3)_x \quad x = 3, 4, 5$$

$$(Cr_xO_{3x-2}) \quad x = 3, 4, 5.$$

Likewise, the appearance potential data suggest that the following ions are fragments:

$$Cr_2O_4^+,\ Cr_2O_5^+,\ Cr_3O_5^+,\ Cr_3O_6^+,\ Cr_3O_8^+,\ Cr_4O_9^+,\ \text{and}\ Cr_4O_{11}^+.$$

Of course, if high ionization electron energies are used, contributions to the observed intensities of lower molecular weight species can arise not only from simple ionization, but also from fragmentation of higher molecular weight species.

C. Cell Exhaustion Experiment

Previous experiments had shown that the relative proportions of the various ions composing the mass spectrum resulting from the vaporization of CrO_3 were the same when a graphite cell was used as when an alumina cell was used. Apparently there was a kinetic barrier to reduction of CrO_3 solid and the vapor polymer molecules by graphite at the relatively low temperatures of these experiments.

During attempts to study the vaporization behavior of $PbCrO_4$, a cell exhaustion experiment was performed which produced highly undersaturated vapor conditions. A graphite cell with a tight-fitting graphite lid was used in this experiment. The orifice diameter was approximately 1 mm. A 17 ev beam of electrons was used.

Lead chromate was loaded into the cell and packed; a small quantity of CrO_3 was added on top of the $PbCrO_4$ and the lid was installed. The intended purpose of the CrO_3 was primarily to provide easily detectable vapor at low temperatures to aid alignment of the spectrometer. The plan was to evaporate away the CrO_3 at low temperatures, then to heat to higher temperatures and search for chromium-containing molecules arising from the vaporization of the $PbCrO_4$. The ion intensities were recorded at various times as the CrO_3 was evaporated with the expectation that the undersaturated vapor conditions would provide useful data for fragment identification.

The results of the high temperature portion of the experiment were negative--as the sample was heated above 500°C, the oxygen pressure increased rapidly with temperature and no chromium-containing species were detected.

The cell exhaustion experiment itself was divided into two parts; an isothermal period of over four hours during which the sample was held at 225°C, and a period in which the temperature of the cell was raised in a series of steps to about 400°C. Ionizing electrons of 17 ev energy were used.

The intensity of the ion peaks began to fall shortly after the temperature reached 225°C and continued to fall for several hours while the sample was held at 225°. For example, the intensity of M268 ($Cr_3O_7^+$) was reduced by a factor of 14 and the intensity of M500 ($(CrO_3)_5^+$) decreased by a factor of 34. Obviously, highly undersaturated vapor conditions developed as the CrO_3 in the cell was exhausted. Figure 2 and Table V summarize the variation of the ion intensities of $Cr_3O_7^+$, $Cr_4O_{10}^+$, and $(CrO_3)_4^+$ with time. Ion intensity ratios at various times are listed in Tables VI and

Table V. Ion intensities from the isothermal portion of the cell exhaustion experiment. (Sample temperature = 225°C)

elapsed time hours.	Ion Intensities (a) (arbitrary units)					
	I^+_{268}	I^+_{300}	I^+_{368}	I^+_{400}	I^+_{468}	I^+_{500}
0	0.161	0.185	0.744	0.0495	0.075	4.9×10^{-3}
0.28	0.135	0.155	0.595	0.0390	0.057	3.9×10^{-3}
0.73	0.103	0.119	0.435	0.0285	0.039	2.5×10^{-3}
1.20	0.077	0.088	0.305	0.0198	0.025	1.7×10^{-3}
2.12	0.059	0.068	0.204	0.0134	0.015	1.0×10^{-3}
2.90	0.040	0.046	0.120	0.0081	0.0081	6×10^{-4}
3.73	0.026	0.030	0.069	0.0046	0.0037	2×10^{-4}
4.40	0.013	0.015	0.028	0.0018	0.0011	----------

(a) electron voltage = 17

Table VI. Ion Intensity ratios from the isothermal portion of the cell exhaustion experiment. (Sample Temperature = 225°C).

elapsed time, hours.	Ion Intensity Ratios, $(I^+_{M_i}/I^+_{M_j})$; M_i/M_j						
	$\frac{268}{368}$	$\frac{300}{368}$	$\frac{400}{368}$	$\frac{468}{368}$	$\frac{500}{368}$	$\frac{300}{268}$	$\frac{400}{268}$
0	0.216	0.249	0.067	0.101	6.6×10^{-3}	1.15	0.308
0.28	0.227	0.260	0.0655	0.095	6.6×10^{-3}	1.15	0.290
0.73	0.236	0.274	0.0655	0.090	5.7×10^{-3}	1.15	0.276
1.20	0.253	0.289	0.0650	0.081	5.6×10^{-3}	1.14	0.258
2.12	0.290	0.334	0.0658	0.075	4.9×10^{-3}	1.16	0.228
2.90	0.330	0.383	0.0675	0.068	5.0×10^{-3}	1.16	0.205
3.73	0.381	0.4w8	0.067	0.054	2.9×10^{-3}	1.12	0.180
4.40	0.47	0.53	0.065	0.040	----------	1.14	0.140

Table VII. Ion intensity ratios from the isothermal portion of the cell exhaustion experiment (Sample Temperature = 225°C).

elapsed time hours	Ion Intensity Ratios, $(I^+_{M_i}/I^+_{M_j})$; M_i/M_j					
	$\frac{468}{268}$	$\frac{500}{268}$	$\frac{500}{400}$	$\frac{500}{468}$	$\frac{400}{300}$	$\frac{468}{400}$
0	0.465	3.1×10^{-2}	9.9×10^{-2}	6.5×10^{-2}	0.267	1.52
0.28	0.420	2.9×10^{-2}	1.0×10^{-1}	6.9×10^{-2}	0.251	1.45
0.73	0.380	2.4×10^{-2}	8.8×10^{-2}	6.4×10^{-2}	0.240	1.37
1.20	0.320	2.2×10^{-2}	8.6×10^{-2}	6.9×10^{-2}	0.225	1.24
2.12	0.260	1.7×10^{-2}	7.5×10^{-2}	6.5×10^{-2}	0.197	1.14
2.90	0.205	1.5×10^{-2}	7.4×10^{-2}	7.4×10^{-2}	0.180	1.00
3.73	0.140	0.8×10^{-2}	4.4×10^{-2}	5.4×10^{-2}	0.16	0.81
4.40	0.085	---------	----------	---------	0.12	0.61

VII.

A serious question that must be asked is whether equilibrium existed among the various chromium containing molecules under the conditions of severe undersaturation. Strong evidence that equilibrium did exist can be found by considering the five independent equilibria that can be written involving the six chromium-containing gaseous species that were detected in this experiment. Several choices of these five equilibria can be made, among which is the following:

I. $(CrO_3)_{3(g)} + (CrO_3)_{5(g)} = 2(CrO_3)_{4(g)}$

$$K_I = \frac{P^2_{(CrO_3)_4}}{P_{(CrO_3)_3} \times P_{(CrO_3)_5}} \sim \frac{I^2_{400+}}{I_{300+} \times I_{500+}}$$

II. $Cr_3O_{7(g)} + Cr_5O_{13(g)} = 2Cr_4O_{10(g)}$

$$K_{II} = \frac{P_{Cr_4O_{10}}}{P_{Cr_3O_7} \times P_{Cr_5O_{13}}} \sim \frac{I^2_{368+}}{I_{268+} \times I_{468+}}$$

III. $Cr_3O_{7(g)} + (CrO_3)_{4(g)} = (CrO_3)_{3(g)} + Cr_4O_{10(g)}$

$$K_{III} = \frac{P_{(CrO_3)_3} \times P_{Cr_4O_{10}}}{P_{Cr_3O_7} \times P_{(crO_3)_4}} \sim \frac{I_{300+} \times I_{368+}}{I_{268+} \times I_{400+}}$$

IV. $(CrO_3)_{4(g)} + Cr_5O_{13(g)} = Cr_3O_{7(g)} + 2(CrO_3)_{3(g)}$

$$K_{IV} = \frac{P_{Cr_3O_7} \times P_{(CrO_3)_3}}{P_{(CrO_3)_4} \times P_{Cr_5O_{13}}} \sim \frac{I_{268+} \times I^2_{300+}}{I_{400} \times I_{468}}$$

V. $2Cr_5O_{13(g)} = Cr_3O_{7(g)} + Cr_4O_{10(g)} + (CrO_3)_{3(g)}$

$$K_V = \frac{P_{Cr_3O_7} \times P_{Cr_4O_{10}} \times P_{(CrO_3)_3}}{P^2_{Cr_5O_{13}}} \quad \frac{I_{268+} \times I_{368+} \times I_{300+}}{I^2_{468+}}$$

In the above equations, the equilibrium constants have been written as proportional to ion intensity products. In general, the partial pressures will be proportional to the products of the ion intensities and the absolute temperature.[21] If care is taken to calculate and compare equilibrium constants only at a single temperature, the equilibrium constants can be written as being proportional to their respective ion intensity products. Ion intensity products are listed as a function of time in Table VIII. It is apparent from Table VIII that the six species $(CrO_3)_x$, Cr_xO_{3x-2}, x = 3, 4, and 5 were in equilibrium throughout the isothermal portion of the experiment even though the individual ion intensities were reduced by factors as large as 34 below their saturation values. The data corresponding to the longest times should be discounted because the extremely low ion intensities corresponding to these points had high inherent errors.

The constancy of the ion intensity factors cannot, by themselves, be taken as conclusive evidence that all of these species result from simple ionization of molecules of the same compositions as the respective ions. For example, if each of the species in equilibrium constant K_{II} (involving the ions of M268, M368, and M468) resulted from fragmentation of the corresponding $(CrO_3)_x$ polymer molecules (masses M_{300}, M400, and M500 respectively), then the ion intensity product $I_{368}^2/[I_{268} \times I_{468}]$ would be constant as long as the ion intensity product $I_{400}^2/[I_{300} \times I_{500}]$ remained constant. (However in this particular case the heat of vaporization data show that $Cr_4O_{13}^+$ (M468) is not a fragment of Cr_5O_{15} (M500), hence the constancy of K_{II} is evidence that $Cr_3O_7^+$ and $Cr_4O_{10}^+$ are not fragments of $(CrO_3)_3$ and $(CrO_3)_4$, respectively.) In fact, the ion ratios I_{400}/I_{368}, I_{300}/I_{268}, and I_{500}/I_{468} behave differently than the other intensity ratios during the isothermal series (Tables VI and VII). The constancy of these

Table VIII. Ion intensity products from the isothermal portion of the cell exhaustion experiment.

elapsed time hours	$K_I = \frac{I_{400^+}^2}{I_{300^+} \; I_{500^+}}$	$K_{II} = \frac{I_{368^+}^2}{I_{268^+} \; I_{468^+}}$	$K_{III} = \frac{I_{300^+} \; I_{368^+}}{I_{268^+} \; I_{400^+}}$	$K_{IV} = \frac{I_{268^+} \; I_{300^+}^2}{I_{400^+} \; I_{468^+}}$	$K_V = \frac{I_{268} \; I_{368} \; I_{300}}{(I_{468^+})^2}$
0	2.70	4.56×10^1	1.72×10^1	1.42	3.94×10^2
0.28	2.52	4.64×10^1	1.76×10^1	1.47	3.90×10^2
0.73	2.73	4.71×10^1	1.76×10^1	1.31	3.5×10^2
1.20	2.62	4.91×10^1	1.76×10^1	1.22	3.4×10^2
2.12	2.64	4.60×10^1	1.76×10^1	1.34	3.5×10^2
2.90	2.4	4.50×10^1	1.73×10^1	1.27	3.3×10^2
3.73	3.6	4.89×10^1	1.68×10^1	1.34	3.9×10^2
4.40	----	5.31×10^1	1.73×10^1	1.39	4.3×10^2

ion ratios was originally interpreted as evidence that a large part of the ion currents of M268, M368, and M468 were due to fragmentation of molecules of molecular weights 300, 400, and 500 respectively. However, further experiments showed that when 17 ev electrons are used for ionization this interpretation is not correct and that $Cr_3O_7^+$, $Cr_4O_{10}^+$, and $Cr_5O_{13}^+$ arise primarily from simple ionization of the corresponding molecules.

After the ion intensities dropped to levels too low for accurate measurements with the sample at 225°C, the cell temperature was raised in a series of steps, resulting in even more highly undersaturated vapor. In the extreme case, the ratio I_{268}/I_{300} was 2.7 compared with the saturation value of 0.157. Ions corresponding to $(CrO_3)_4^+$, $Cr_5O_{13}^+$, and $(CrO_3)_5^+$ soon became undetectable, but ions corresponding to $Cr_3O_7^+$, $(CrO_3)_3^+$ and $Cr_4O_{10}^+$ remained detectable for several steps of temperature increases. The results are summarized in Table IX for the ion intensity ratios I_{300}/I_{268}, I_{500}/I_{468}, and $I_{400}/_{368}$. The continual decline of these ratios cannot be explained in terms of fragmentation.

If one argues that the decrease of, for instance, the ratio I_{300}/I_{268} as the temperature is raised is due to fragment contributions to M268 from molecules such as $(CrO_3)_4$ and $(CrO_3)_5$ as well as $(CrO_3)_3$, two difficulties are immediately encountered. First the intensities of M400 and M500 would be expected to decrease relative to M300 as the more highly undersaturated vapor conditions develop, and this expectation is verified by the data. Hence the contributions of higher molecular weight species to M268 should decrease as the temperature is increased, causing the intensity of M268 to approach a constant value relative to M300, but it does not. Secondly, the data taken under isothermal conditions show a constant ratio of the intensity of M268 only relative to M300. This fact

Table IX. Cell exhaustion experiment; Ion intensity ratios I^+_{300}/I^+_{268}, I^+_{400}/I^+_{368} and I^+_{500}/I^+_{468} as cell temperature is increased.

Temp. °C	Ion Intensity Ratios		
	$\frac{I^+_{300}}{I^+_{268}}$	$\frac{I^+_{400}}{I^+_{368}}$	$\frac{I^+_{500}}{I^+_{468}}$
225	1.15	0.066	0.065
265	0.87	0.033	-----
266	0.84	0.033	-----
285	0.82	0.026	-----
295	0.79	0.0235	0.023
304	0.72	0.0206	-----
325	0.73	------	-----
370	0.48	------	-----
405	0.34	------	-----

means that the higher molecular weight species cannot be making significant contributions to M268. Hence the isothermal portion of the cell exhaustion experiment shows that $Cr_3O_7^+$ is independent of $Cr_4O_{10}^+$, $(CrO_3)_4^+$, $Cr_5O_{13}^+$ and $(CrO_3)_5^+$, while the series of data recorded with rising temperature shows that $Cr_3O_7^+$ is independent of $(CrO_3)_3^+$. Similar arguments apply regarding the questions of possible relationships between the ion pairs $Cr_4O_{10}^+$ - - $(CrO_3)_4^+$ and $Cr_5O_{13}^+$ - - $(CrO_3)_5^+$.

The cell exhaustion experiment confirms that $(CrO_3)_x^+$ and $Cr_xO_{3x-2}^+$, x = 3, 4, 5 are all independent species.

D. Double Cell Experiments

1. Introduction

Two series of intensity measurements (Series C and Series E) were made using a double Knudsen cell to produce undersaturated vapor. In both of these series, the lower cell was held at an approximately constant temperature, while the upper cell was heated to produce undersaturated vapor effusing from the upper cell into the ion source.

The low cell (which held solid or liquid CrO_3) was held at 189 ± 3°C during the Series C measurements, with the upper cell being varied from 201 to 430°C. In the series E measurements, the lower cell was held at 194 ± 6°C, while the upper cell temperature was varied from 177 to 382°C.

The measurements of Series C were made using 17.5 and 25 ev ionizing electrons, while those of Series E were made using 21 and 25 ev electrons. Only the six low appearance potential peaks (M268, M300, M368, M400, M468, and M500) could be studied with 17.5 ev electrons, while intensities of all chromium-containing species that have been detected were recorded using 25 ev electrons. The intensities of all chromium-containing species except $Cr_2O_3^+$ (M152) and $Cr_2O_5^+$ (M184) were measured with 21 ev electrons.

The value of the double cell method lies in the fact that if an ion of mass Mx is a fragment of a molecule of mass My, or if both of these are fragments of a parent of mass Mz, the intensity ration I_x^+/I_y^+ will be a constant value regardless of the pressure of the neutral molecules of mass My or Mz. However, if Mz and My both result from simple ionization of molecules of the same composition as the respective ions, or if one of them results from fragmentation of a molecule of mass Mz, or if both Mx and My are fragments, but of different parent molecules, the ratio I_x^+/I_y^+ will change as the chemical potentials of their component elements are changed by varying the temperature of the upper Knudsen cell.

It is true that nearly nothing is known about the temperature dependence of mass spectra.[22,23] But thermal energy, kT, at 800°K is 0.067 ev, while thermal energy at 500°K is 0.042 ev. The difference (0.025 ev) is so small relative to typical bond energies (4 to 5 ev) or to the electron energies (10 ev and higher) that the cell temperature differences used in these experiments are unlikely to have appreciable influence on the fragmentation cross sections. The assumption that fragmentation patterns are temperature-independent over relatively narrow temperature ranges is made on this basis.

Possible temperature effects on the fragmentation patterns could be avoided by holding the upper cell at a fixed temperature (above the highest temperature reached by the lower cell) and varying the degree of undersaturation in the upper cell by adjusting the temperature of the lower cell. This approach was attempted, but the relatively narrow temperature range reachable by the lower cell together with difficulties in holding the upper cell temperature constant led to abandonment of this variation

of the double cell method.

In the discussion of the double cell results, the fragment-parent relationships deduced from the double cell results are checked against the measured appearance potentials to determine if the two kinds of results are compatible. During the discussion of appearance potentials, the assumption is frequently made that large Cr_xO_y molecules all have approximately the same ionization potentials (within a few electron volts). This assumption was verified for the molecules Cr_3O_7, $(CrO_3)_3$, Cr_4O_{10}, $(CrO_3)_4$, Cr_5O_{13}, and $(CrO_3)_5$.

2. Description of the Double Cell

Figure 3 shows a sketch of the double cell at a scale of 2:1. The entire assembly was fabricated from stainless steel except for the barrel of the lower cell which was of copper. A screen of 80 mesh platinum gauze was inserted into the upper cell. A disc of 0.10" thick platinum spot-welded to the platinum gauze prevented effusion directly from the lower cell to the orifice of the upper cell.

Heating wires were wrapped around the upper cell, the connecting tube, and the lower cell. Platinum/platinum-10 rhodium thermocouples were spot welded to the upper and lower cells.

3. Discussion

In this section a molecule is referred to by its composition (e.g., $(CrO_3)_5$), while the ions of this molecule may be referred to either by indicating their composition (e.g., $(CrO_3)_5^+$) or by indicating the mass number of the most abundant ion (the peak studied) of that composition (e.g., M500 for $(CrO_3)_5^+$ or M400 for $(CrO_3)_4^+$).

$(CrO_3)_5^+$ (M500)

The pentamer of CrO_3 was the highest molecular weight species detected in this study at temperatures below the melting point of CrO_3, 196°C. In early single-cell experiments above the melting point of CrO_3, indication of a series of low intensity peaks at about M600 was observed. Presumably these peaks corresponded to $(CrO_3)_6^+$. It was not possible to detect these peaks as long as the temperature of the sample was held below about 210°C.

Pressures were too low in the ionization chamber for $(CrO_3)_5^+$ to have been formed by an ion-neutral molecule addition reaction. The appearance potential, isothermal intensity variation relative to other ion peaks, and calculated enthalpy of sublimation relative to those of other vapor species all are consistent with the conclusion that $(CrO_3)_5^+$ appears as a result of simple ionization of a neutral molecule of the same composition, rather than by fragmentation of a heavier parent molecule.

$Cr_5O_{13}^+$ (M468)

Column 1 of Table X is a listing of the ratio I_{468}/I_{500} as a function of temperature difference between the upper and lower cells, as obtained from the series C 17.5 double cell experiments. There is no evidence in the double cell results that $Cr_5O_{13}^+$ is a fragment of $(CrO_3)_5$. The difference of the heats of sublimation of Cr_5O_{13} and $(CrO_3)_5$ is about 6 kcal, which is three times as large as the sum of the standard deviations in the heats.

Thus both $(CrO_3)_5^+$ and $Cr_5O_{13}^+$ ions result from simple ionization of molecules of the same composition as the respective ions.

Table X. Ion intensity ratios calculated from data of double cell series C17.5.

Point No.	$T_U - T_L$ [a] °C	(1) $\frac{I_{468}}{I_{500}}$	(2) $\frac{I_{400}}{I_{500}}$	(3) $\frac{I_{400}}{I_{468}}$	(4) $\frac{I_{368}}{I_{500}}$	(5) $\frac{I_{368}}{I_{468}}$	(6) $\frac{I_{368}}{I_{400}}$	(7) $\frac{I_{300}}{I_{500}}$	(8) $\frac{I_{300}}{I_{468}}$	(9) $\frac{I_{300}}{I_{400}}$	(10) $\frac{I_{300}}{I_{368}}$
8-C	15	8.2	7.8	0.96	74	9.1	9.5	15	1.8	1.9	0.20
7-C	38	12.5	9.4	0.76	125	10	13.2	26	2.1	2.8	0.21
9-C	42	7.3	9.6	1.3	136	18.5	14.2	31	4.2	3.3	0.23
1-C	63	18	12	0.67	214	11.6	17.3	60	3.3	4.9	0.28
6-C	69	22	13	0.62	270	12.5	20.4	83	3.9	6.2	0.31
2-C	80	28	12	0.42	292	10.7	25	83	3.0	7.1	0.29
5-C	109	52	18	0.35	716	13.9	39	250	4.8	14	0.35
3-C	132	---	---	-----	----	19.4	63	---	6.9	22	0.35
10-C	162	---	---	-----	----	17	84	---	7.0	35	0.41
4-C	165	---	---	-----	-----	20	84	---	7.7	32	0.38
11-C	216	---	---	-----	-----	25	125	---	13	67	0.53
12-C	246	---	---	-----	-----	37	----	---	22	---	0.59

(a) $T_U - T_L$ = upper cell temperature minus lower cell temperature.

Table XI. Ion intensity ratios calculated from data of double cell series C17.5.

Point No.	$T_U - T_L$ (a) °C	(1) $\frac{I_{268}}{I_{500}}$	(2) $\frac{I_{268}}{I_{468}}$	(3) $\frac{I_{268}}{I_{400}}$	(4) $\frac{I_{268}}{I_{368}}$	(5) $\frac{I_{268}}{I_{300}}$
8-C	15	8.9	1.1	1.1	0.12	0.60
7-C	38	18	1.4	1.9	0.14	0.67
9-C	42	22	3.0	3.0	0.16	0.71
1-C	63	43	2.4	3.5	0.20	0.72
6-C	69	61	2.8	4.6	0.22	0.73
2-C	80	69	2.5	5.9	0.24	0.83
5-C	109	250	4.8	14	0.35	1.00
3-C	132	---	10	33	0.52	1.5
10-C	162	---	11	57	0.67	1.6
4-C	165	---	12	52	0.62	1.6
11-C	216	---	28	140	1.1	2.1
12-C	246	----	63	----	1.7	2.9

(a) $T_U - T_L$ = Upper cell temperature minus lower cell temperature.

$(CrO_3)_4^+$ (M400)

Values of the ratio I_{400}/I_{500} are listed in column two of Table X. These data show that the tetramer is not correlated with the pentamer.

Ratios of I_{400}/I_{468} from Series C17.5 are listed in column three of Table X. The results clearly show that the tetramer is not a fragment of Cr_5O_{13}. The difference in their heats of sublimation is approximately 11 kcal, some seven times the sum of the standard deviations in the heats.

$(CrO_3)_4^+$ ions also result from simple ionization of neutral molecules of the same composition as the ions.

$Cr_4O_{11}^+$ (M384) and $Cr_4O_{10}^+$ (M368)

The measured difference in appearance potentials between $Cr_4O_{11}^+$ and $(CrO_3)_4^+$ is 4.2 ev which is in good agreement with the value of 4.4 ev which is predicted if $Cr_4O_{11}^+$ is a fragment of $(CrO_3)_4$. But the data from series E 21 columns 1 and 2 of Table XII show that M384 is not correlated with M468, or M500 when 21 ev electrons are used for ionization. Figure 4 shows that M384 is not correlated with M400. Figure 5 plots the intensity ratio I_{384}/I_{368} obtained in series E21, and E25. The $Cr_4O_{11}^+$ intensity is about 1% of the $Cr_4O_{10}^+$ intensity when 21 ev ionizing electrons are used.

If $Cr_4O_{10}^+$ were formed as a fragment of Cr_4O_{11}, as Fig. 5 suggests, then the following line of argument developing the difference in the ionization potentials of M368 and M384 should be approximately correct.

Assume: Cr_4O_{11} is the parent of $Cr_4O_{10}^+$.

$$Cr_4O_{11} + e = Cr_4O_{11}^+ + 2e$$

$$AP[Cr_4O_{11}^+] \simeq IP[Cr_4O_{11}]$$

$$Cr_4O_{11} + e = Cr_4O_{10}^{+} + O + 2e$$

$$AP[Cr_4O_{10}] \geqslant IP[Cr_4O_{10}] + D_o^o(CrO)$$

so: $AP[Cr_4O_{11}^{+}] - AP[Cr_4O_{10}^{+}] + D_o^o(Cr\text{-}O) \geqslant IP[Cr_4O_{11}] - IP[Cr_4O_{10}]$

Thus the above assumption implies that

$$IP[Cr_4O_{11}] - IP[Cr_4O_{10}] = 3.5 + 4.4 = 7.9 \text{ ev}$$

which is an extraordinarily large difference in ionization potentials for two molecules of as similar composition as Cr_4O_{11} and Cr_4O_{10}. Taking the appearance potential of the assumed parent, Cr_4O_{11}, as its ionization potential, the above conclusion implies that the ionization potential of Cr_4O_{10} would be less than or equal to 7.5 ev if it is formed as the result of fragmentation of Cr_4O_{11}.

A possible, but very unlikely, source of the $Cr_4O_{11}^{+}$ ion is a molecule-ion reaction occuring in the ion source:

$$Cr_4O_{10}^{+} + O_2 = Cr_4O_{11}^{+} + O$$

This reaction would imply that the appearance potential difference should be approximately:

$$\begin{aligned} AP[Cr_4O_{11}^{+}] - AP[Cr_4O_{10}^{+}] &= D_o^o(O_2) - D_o^o(Cr\text{-}O) \\ &= 5.4 - 4.4 \\ &= 1.0 \text{ ev.} \end{aligned}$$

The actual value was found to be 3.5 ev.

Figure 6 presents a comparison of the appearance potential curves of M368, M384, and M400, all with the intensities adjusted to make the upper parts of the curves approximately parallel. These data leave little

Table XII. Ion intensity ratios from double cell run E-25 (25 ev electrons).

Point No.	T_U-T_L (a) °C	$\frac{I_{384}}{I_{500}}$	$\frac{I_{384}}{I_{468}}$	$\frac{I_{352}}{I_{400}}$
10-E	-11	1.1	0.14	0.072
3-E	4		0.13	0.11
19-E	5	1.5		0.086
2-E	28		0.14	0.13
18-E	29	2.8		0.10
17-E	30	3.2		0.14
9-E	43	3.5	0.19	0.14
16.E	46	6.0	0.17	0.18
1-E	52		0.15	0.19
4-E	76		0.20	0.16
15-E	88		0.24	0.21
8-E	97		0.25	0.27
5-E	108		0.23	0.29
6-E	122		0.22	0.32
14-E	134		0.21	0.28
7-E	153		0.30	0.30
11-E	171		0.39	0.32
13-E	176		0.54	0.41
12-E	189		0.55	0.56

(a) T_U-T_L = temperature difference between upper and lower cells.

doubt that more than one process contributes to the ion intensities of M368 when electron energies of five volts or so above the threshold are used. But the curves do not indicate the nature of the reactions.

If the process that produces most of the $Cr_4O_{10}^+$ at 21 ev and above is assumed to be:

$$Cr_4O_{11} + e^- = Cr_4O_{10}^+ + O + 2e^-$$

the appearance potential that would correspond to this process can be estimated as about 14.3 ev by comparison with the appearance potential of $(CrO_3)_4^+$ (Table IV) and the shape of the ionization efficiency curve for $(CrO_3)_4^+$. Then:

$$Cr_4O_{11} + e^- = Cr_4O_{10}^+ + O + 2e^- \qquad \Delta E = +14.3 \text{ ev}$$

$$Cr_4O_{10}^+ + 2e^- = Cr_4O_{10} + e^- \qquad \Delta E = -11.8 \text{ ev}$$

$$Cr_4O_{11} = Cr_4O_{10} + O \qquad \Delta E \cong 2.5 \text{ ev}$$

compared to 4.4 ev for the dissociation energy of one Cr-O bond. However, the Cr-O bonds from which this value (4.4 ev) is calculated involve oxygens which are bonded to one Cr atom only, while the polymers must contain some oxygens that are bonded to two Cr atoms. It is possible that the Cr_4O_{10} molecules, while having less oxygen than Cr_4O_{11}, may have more oxygen atoms which are bonded to two Cr atoms with a consequent gain in stability.

From this discussion, the probability that some neutral Cr_4O_{11} exists in the vapor effusing from the Knudsen cell seems high, but the Cr_4O_{11} probably is not the source of the $Cr_4O_{10}^+$ when electron energies under about 20 ev are used. At 25 ev, the $Cr_4O_{10}^+$ may result mainly from dissociative ionization of Cr_4O_{11}.

The data listed in columns 4, 5 and 6 of Table X show that M368 ($Cr_4O_{10}^+$) is not correlated with M400 ($(CrO_3)_4^+$,) M468 ($Cr_5O_{13}^+$), or M500 ($(CrO_3)_5^+$) if an ionizing electron energy of 17.5 ev is used.

If M368 did arise from M400 (the ion intensity ratios indicate that it does not) due to the reaction:

$$(CrO_3)_4 + e = Cr_4O_{10}^+ + O_2 + 2e$$

The expected appearance potential difference would be:

$$\begin{aligned} AP[Cr_4O_{10}^+] - AP[(CrO_3)_4^+] &\geq 2\ D_o^o(Cr\text{-}O) - D_o^o(O_2) \\ &\geq 2(4.4) - 5.2 \\ &\geq 3.6 \text{ ev.} \end{aligned}$$

The measured value for this appearance potential difference is 0.7 ev.

Thus $Cr_4O_{10}^+$ observed at less than 20 ev arises from simple ionization of neutral molecules of the same composition as the ion.

$Cr_4O_9^+$ (M352)

As Fig. 7 shows, M352 is correlated with M368 (and therefore with M384) when 25 ev electrons are used.

If Cr_4O_{11} is the parent of $Cr_4O_9^+$:

$$Cr_4O_{11} + e^- = Cr_4O_9^+ + O_2 + 2e^-.$$

This reaction would have an expected appearance potential difference of:

$$\begin{aligned} AP[Cr_4O_9^+] - AP[Cr_4O_{10}^+] &\geq D_o^o\ (Cr\text{-}O) \\ &\geq 4.4 \text{ ev.} \end{aligned}$$

The actual difference in appearance potentials of M368 and M352 is 5.5 ev.

Figure 8 plots the ion intensity ratio I_{352}/I_{384} as recorded with 21 ev electrons. At 21 ev, M352 is seen to be about as well correlated with M384 as with M368. The data listed in column three of Table XII shows that M352 is not correlated with M400.

It is not possible to say for certain whether $Cr_4O_{10}^+$ or $Cr_4O_{11}^+$ is the principal parent of $Cr_4O_9^+$, but $Cr_4O_{11}^+$ is the more probable.

At electron energies of 21 ev, the M352 ion intensity is less than 1% of the M368 ion intensity.

$Cr_4O_8^+$ (M336)

Figure 9 shows that M368 is probably the parent of M336. Presumably the formation reaction is:

$$Cr_4O_{10} + e \rightarrow Cr_4O_8^+ + O_2 + 2e$$

This reaction leads to the following relationships between the appearance potentials:

$$AP(Cr_4O_8^+) - AP(Cr_4O_{10}^+) \geq 2D_o^o\ (Cr\text{-}O) - D_o^o(O_2)$$

$$\geq 3.6 \text{ ev}$$

The actual difference in the appearence potentials of $Cr_4O_8^+$ and $Cr_4O_{10}^+$ is 4.9 ev.

With an ionizing electron energy of 21 volts, the M336 intensity is less than 2% of the M368 intensity.

Figure 10 shows, of course, that M336 appears to be correlated with M384. If M384 were the parent of M336, the formation reaction presumably would be:

$$Cr_4O_{11} + e \rightarrow Cr_4O_8^+ + O_2 + O + 2e$$

This reaction leads to the following expected relationship between the appearance potentials:

$$AP(Cr_4O_8^+) - AP(Cr_4O_{11}^+) \geq 3\ D_o^o(Cr\text{-}O) - D_o^o(O_2)$$

$$\geq 8.0 \text{ ev}$$

The actual difference in the appearance potentials of $Cr_4O_8^+$ and $Cr_4O_{10}^+$ is 4.9 ev.

With an ionizing electron energy of 21 volts, the M336 intensity is less than 2% of the M368 intensity.

Figure 10 shows of course, that M336 appears to be correlated with M384. If M384 were the parent of M336, the formation reaction presumably would be:

$$Cr_4O_{11} + e \rightarrow Cr_4O_8^+ + O_2 + O + 2e$$

This reaction leads to the following expected relationship between the appearance potentials:

$$AP(Cr_4O_8^+) - AP(Cr_4O_{11}^+) \geq 3\ D_o^o(Cr\text{-}O) - D_o^o(O_2)$$

$$\geq 8.0 \text{ ev.}$$

The actual difference in the appearance potentials of M384 and M336 is 1.4 ev.

Thus $Cr_4O_8^+$ is a fragment, and its parent is probably Cr_4O_{10}.

$(CrO_3)_3^+$ (M300)

The data listed in columns 7 through 10 of Table X show that the trimer is not correlated with $Cr_4O_{10}^+$, $(CrO_3)_4^+$, $Cr_4O_{13}^+$, or $(CrO_3)_5^+$. Similar results were found in all four sets of double cell data, recorded using electron voltages ranging from 17.5 to 25 ev.

$Cr_3O_8^+$ (M284) and $Cr_3O_7^+$ (M268)

Figure 11 shows the ratio I_{284}/I_{300} calculated from intensity data recorded at 21 and 25 ev. The 21 ev data show a temperature trend, the value of I_{284}/I_{300} increasing with temperature. The 25 ev data show little if any temperature trend, indicating correlation of M284 to M300 at ionizing electron energies of 25 ev.

Figure 12 shows the ratio I_{284}/I_{268} calculated from data recorded at 21 and 25 ev. The data taken with 25 ev electrons show a clear temperature trend indicating independence of M268 from M284 when 25 ev ionizing electrons were used. However, this is probably an artifact since M284 is correlated with M300 at this electron energy. The 21 ev data show a reduced temperature trend.

A possible explanation for this behavior is that some Cr_3O_8 is present in the neutral vapor, but at an ionizing electron energy of 25 ev, a predominant contribution to the M284 peak is made by fragmentation of the trimer.

If the trimer (M300) is the parent of $Cr_3O_8^+$ (M284), the formation reaction would presumably be:

$$(CrO_3)_3 + e = Cr_3O_8^+ + O + 2e$$

Which implies an appearance potential difference of:

$$AP\ Cr_3O_8^+ - AP\ CrO_3)_3^+ \geq D_o^o(Cr\text{-}O)$$

$$\geq 4.4 \text{ ev.}$$

The actual difference was found to be 5.2 ev.

Figure 12 can be interpreted as indicating that the principle source of M268 when 21 ev electrons are used is fragmentation of M284. If this were so, the following line of argument should indicate the approximate

difference to be expected in the appearance potentials of M268 and M284: Assume that Cr_3O_8 is the parent of $Cr_3O_7^+$:

$$Cr_3O_8 + e = Cr_3O_8^+ + 2e$$

$$AP\ Cr_3O_8^+ = IP\ Cr_3O_8$$

$$Cr_3O_8 + e = Cr_3O_7^+ + O + 2e$$

$$AP[Cr_3O_7^+] = IP[Cr_3O_7^+] + D_o^o(Cr\text{-}O) + (K + E)$$

so: $$AP[Cr_3O_8^+] - AP[Cr_3O_7^+] + D_o^o(Cr\text{-}O) + (K + E) \cong IP[Cr_3O_8] - IP[Cr_3O_7]$$

Thus the assumption that Cr_3O_8 is the parent of $Cr_3O_7^+$ implies that:

$$IP[Cr_3O_8] - IP[Cr_3O_7] \geqq 3.9 + 4.4$$

$$\geqq 8.3 \text{ ev.}$$

This value (8.3 ev) is an extraordinarily large difference in ionization potentials for two molecules of as similar composition as Cr_3O_8 and Cr_3O_7. This means that the ionization potential of Cr_3O_7 would have to be about 8.3 ev. It is extremely unlikely that Cr_3O_8 is the parent of the $Cr_3O_7^+$ measured at low electron energies.

As was the case with the question of a M368-M384 realtionship, a possible but unlikely source of $Cr_3O_8^+$ is a molecule-ion reaction occuring in the ion source:

$$Cr_3O_7^+ + O_2 = Cr_3O_8^+ + O$$

This reaction implies that the appearance potential difference should be approximately:

$$AP[Cr_3O_8^+] - AP[Cr_3O_7^+] = D_o^o(O_2) - D_o^o(Cr\text{-}O)$$

$$= 5.2 - 4.4$$

$$= 1.1 \text{ ev.}$$

The actual difference is 3.9 ev.

Figure 13 presents a plot of the appearance potential curves of M268, M284 and M300. Clearly, more than one process is contributing to the M268 and M284 ion intensities, but these curves do not eliminate the possibility that M268 and M284 near their thresholds, are due to simple ionization of neutral molecules of the same composition as the respective ions.

An extrapolation that assumes the high intensity region of the $Cr_3O_7^+$ ionization efficiency curve results from fragmentation of Cr_3O_8 with a curvature like that of the $Cr_3O_8^+$ ionization efficiency curve at low intensities gives an appearance potential of about 16.5 ev for $Cr_3O_7^+$ being formed by the process:

$$\begin{array}{lcl} Cr_3O_8 + e^- = Cr_3O_7^+ + 2e^- + O & & \Delta E = 16.5 \text{ ev} \\ \underline{Cr_3O_7^+ + 2e^- = Cr_3O_7 + e^-} & & \underline{\Delta E = -12.8 \text{ ev}} \\ Cr_3O_8 = Cr_3O_7 + O & & \Delta E \approx 3.7 \text{ ev} \end{array}$$

compared to an expected value of 4.4 ev. If the Cr_3O_7 molecule has more oxygen atoms with bonds to two Cr atoms than does Cr_3O_8, the difference between the predicted value and that calculated is reasonable.

The data indicate that at an ionizing electron energy of 25 ev, the principal part of the M284 peak is due to fragmentation of M300. However, a small quantity of Cr_3O_8 may be present in the neutral vapor effusing from the Knudsen cell. Fragmentation of Cr_3O_8 is probably not an important source of M368 at low electron energies, but may become an

important source at electron energies above 25 ev. With an ionizing electron energy of 21 ev, the M284 peak was less than 1.5% as intense as the M268 peak.

The double cell data with 17.5 ev electrons (Columns 1 through 5 of Table XI) indicate that $Cr_3O_7^+$ observed at low voltages is independent of $(CrO_3)_3^+$, $Cr_4O_{10}^+$, $(CrO_3)_4^+$, Cr_5O_{13}, and $(CrO_3)_5^+$ (all of which have been previously concluded to arise by simple ionization of molecules of the same composition as the ions). The appearance potential of $Cr_3O_7^+$ is only 1.3 ev above that of $(CrO_3)_3^+$. If $Cr_3O_7^+$ resulted from fragmentation of the trimer, the minimum appearance potential difference would be expected to be:

$$(CrO_3)_3 + e = Cr_3O_7^+ + O_2 + 2e$$

$$AP[Cr_3O_7^+] - AP[(CrO_3)_3^+] \geq 2D_o^o(Cr\text{-}O) - D_o^o(O_2)$$

$$\geq 3.6 \text{ ev.}$$

This argument does not, of course, eliminate the possibility that M300 makes substantial contributions to the M268 ion intensity at electron energies a few volts above the M268 threshold. Indeed, the long tail of the M268 ionization efficiency curve in Fig. 13 is evidence that more than one process (one of which is probably fragmentation of Cr_3O_8 or $(CrO_3)_3$) does contribute to the M268 ion intensity at electron energies a few volts above threshold. Figure 14, which is a plot of I_{268}/I_{300} with electron energies of 17.5, 21, and 25 ev, also indicates that M300 does contribute to M268 at sufficiently high electron energies. The decreasing slope of I_{268}/I_{300} ratio in Fig. 14 as the electron energy is raised would be expected if M300 were contributing to the M268 ion intensity at 21 and 25 ev. The ratio of $(CrO_3)_3/Cr_3O_7$ in the neutral vapor

will decrease as the upper cell temperature is increased, so at higher electron energies (and thus at larger contributions of fragments of M300 to the M268 ion intensity), the slope of the I_{268}/I_{300} ratio should be less than its slope at lower energies.

At low electron energies, $Cr_3O_7^+$ results from simple ionization of molecules of the same composition, but at higher electron energies, significant contribution is made to the M268 ion intensity by fragments of M284 and/or M300.

$Cr_3O_6^+$ (M252)

Figure 15 based on double cell data obtained with an ionizing electron energy of 21 ev, indicates that M252 is much more closely correlated with M268 (which appears to arise mainly from fragmentation of Cr_3O_8 at this electron energy) than with M300. The formation of $Cr_3O_6^+$ by fragmentation of Cr_3O_8 would be expected to lead to: $AP[Cr_3O_6^+] - AP[Cr_3O_8^+] = 3.4$ ev, the actual difference being 2.9 ev. The formation of $Cr_3O_6^+$ by framentation of Cr_3O_7 would be expected to lead to $AP[Cr_3O_6^+] - AP[Cr_3O_7^+] = 4.4$ ev, the actual difference being 5.8 ev. Thus, appearance potentials do not help decide whether Cr_3O_7 or Cr_3O_8 is the parent of $Cr_3O_6^+$.

However, the 25 ev data (Fig. 16) indicates that both Cr_3O_7 and $(CrO_3)_3$ may act as parents of $Cr_3O_6^+$ at an ionizing electron energy of 25 ev. The temperature dependence of the ratio I_{252}/I_{300} in Fig. 16 is greatly reduced compared with that of Fig. 15. The ratio I_{252}/I_{268} shows a decreasing trend with increasing temperature at 25 ev, as would be expected if some of the M252 ions resulted from fragmentation of M300 molecules (M300 becomes less important relative to M268 as the temperature of the upper cell is increased).

The formation reaction of $Cr_3O_6^+$ from $(CrO_3)_3$ would presumably be:

$$(CrO_3)_3 + e = Cr_3O_6^+ + O_2 + O + 2e$$

The difference in appearance potentials would thus be expected to be:

$$AP[Cr_3O_6^+] - AP[(CrO_3)_3^+] \geq 3\,D_o^o(Cr\text{-}O) - D_o^o(O_2)$$

$$\geq 8.0 \text{ ev.}$$

The actual difference was found to be 7.1 ev.

The intensity of the M252 peak was about 1% of the intensity of the M268 peak when 21 ev ionizing electrons were used.

At electron energies near its threshold, $Cr_3O_6^+$ apparently is a fragment of Cr_3O_7 or Cr_3O_4 but as the electron energy is increased, $(CrO_3)_3$ may become an important parent of $Cr_3O_6^+$.

$Cr_3O_5^+$ (M236)

Figure 17 is a plot of I_{236}/I_{268} and I_{236}/I_{300} based on data obtained with 21 and 25 ev electrons.

The 21 ev data in particular show that M236 is correlated with M268 but not with M300. This indicates that at electron energies of 21 ev or less, Cr_3O_7 is the predominant parent of M236. For formation from Cr_3O_7 the reaction presumably is:

$$Cr_3O_7 + e = Cr_3O_5^+ + O_2 + 2e$$

The expected appearance potential difference is thus:

$$AP[Cr_3O_5^+] - AP[Cr_3O_7^+] \geq 2\,D_o^o(Cr\text{-}O) - D_o^o(O_2)$$

$$\geq 2(4.4) - 5.2$$

$$\geq 3.6 \text{ ev.}$$

The actual difference was 4.7 ev.

As the electron energy is increased from 21 to 25 ev, the temperature dependence of I^+_{236}/I^+_{300} is sharply decreased. This is a strong indication that at 25 ev M300 has become a significant parent of M336. Note (Fig. 18) that at 25 ev the ratio I_{236}/I_{268} decreases slightly with increasing temperature, as would be expected if M300 makes a significant contribution to the M236 ion intensity.

The M236 ion intensity is about 1% of the M268 ion intensity at an ionizing electron energy of 21 ev. Near its threshold, $Cr_3O^+_5$ is a fragment of Cr_3O_7, but at higher electron energies $(CrO_3)_3$ may become an important parent of $Cr_3O^+_5$.

$Cr_2O^+_5$ (M184)

Figure 19 shows that M184 is a fragment of M300, not of M268 or M368. All of these data are based on 25 ev ionizing electrons. Largely because of the high appearance potential of M184, the intensity of the M184 ion current was too low to allow accurate measurements at 21 ev. The appearance potential of $Cr_2O^+_5$ is 7.4 ev above that of $(CrO_3)^+_3$.

The intensity of the M184 peak was of the order of 0.5% of the M300 peak when 25 ev ionizing electrons were used. The double cell data indicate that $Cr_2O^+_5$ (M184) is a fragment of $(CrO_3)_3$.

$Cr_2O^+_4$ (M168).

Figure 20 presents the ion intensity ratio I^+_{168}/I^+_{268}, I^+_{168}/I^+_{368} and I^+_{168}/I^+_{300} calculated from the double cell data of Series E using 25 volt electrons. These data indicate that M168 is correlated with M300. The appearance potential of M168 is 6.0 ev above that of M300.

The ion intensity of M168 was about 10% of the M300 ion intensity when 21 ev ionizing electrons were used. The double cell data indicate that $(CrO_3)_3$ is the parent of $Cr_2O_4^+$.

$Cr_2O_3^+$ (M152)

Intensity data on M152 were recorded only at 25 ev; its intensity was too low to record when 21 ev electrons were used. Because of its low intensity, no reliable appearance potential was determined for M152.

Figure 21 presents the ion intensity ratios I_{152}/I_{268} and I_{152}/I_{300}. From these figures, M152 appears to be correlated with M268, but it cannot be said for certain that Cr_3O_7 is the parent of $Cr_2O_3^+$. The intensity of the M152 peak was less than 1% of the intensity of the M268 peak when 25 ev ionizing electrons were used.

4. Summary and Conclusions

The double cell experiments indicate that the following ions are formed by simple ionization of neutral molecules of the same composition as the ion when an ionizing electron energy near the threshold for these ions is used:

$Cr_3O_7^+$
$(CrO_3)_3^+$
$Cr_4O_{10}^+$
$(CrO_3)_4^+$
$Cr_5O_{13}^+$
$(CrO_3)_5^+$

In addition to the molecules corresponding to the above ions, small quantities of Cr_3O_8 and Cr_4O_{11} probably are present in the vapor from the

Knudsen cell.

The following ions were found to arise from molecules with molecular weights larger than the respective ions:

$Cr_2O_3^+$

$Cr_2O_4^+$

$Cr_2O_5^+$

$Cr_3O_5^+$

$Cr_3O_6^+$

$Cr_4O_8^+$

$Cr_4O_9^+$

These conclusions based on double cell data are consistent with the appearance potential data.

V. VAPOR PRESSURES MEASUREMENTS

A. Experimental

Aluminum oxide Knudsen cell liners were chosen for this work because of their inertness. Although heating chromium trioxide in aluminum oxide discolors the aluminum oxide, no evidence of gross attack or deterioration of the aluminum oxide was found. Aluminum oxide cells supplied by Morganite Refractories and Coors Porcelain Company were used; no difference in behavior was noted between cells from the two suppliers.

The Al_2O_3 Knudsen cell was held in a massive aluminum cell holder which was designed to have a relatively large heat capacity to damp out temperature drift. The cell was heated by insulated resistance wire which was wrapped around the outside surface of the cell holder. Figure 22 is a cross section of the cell holder and cell.

The cell holder was supported on three sections of mullite or alumina tubing. Either of these materials offered much lower thermal conductivity than the more conventional refractory metal supports.

Two Pt/Pt-10% Rh (type S) thermocouples were attached to the cell holder opposite one another, one near the top of the cell holder, the other near the bottom. To assume good thermal contact between the cell holder and thermocouples, the thermocouples were inserted 4 to 5 millimeters into holes drilled through the wall of the cell holder, where they were held in place by tapered aluminum pins. The type S thermocouple wires were led out of the vacuum chamber through ceramic lead-throughs. The temperature of the thermocouples was measured with a Leeds and Northrup potentiometer, model number 8686, serial number 1690549. The same potentiometer was used for calibration of thermocouples as well as experimental

temperature measurements.

The thermocouples were calibrated in place under vacuum conditions by comparison with a calibrated chromel-alumel thermocouple placed inside the Knudsen cell. The chromel-alumel thermocouple was calibrated at the tin point; two successive cooling curves produced identical arrests. The arrests occurred at an indicated temperature less than 0.1°C below the established tin point, 231.9°C.[24] The tin used for calibration purposes was Baker and Adamson's reagent grade, 99.9+ Sn.

To assure that the chromel-alumel thermocouple would accurately indicate the temperature of the cell, it was necessary to devise a means of assuring excellent thermal contact between the thermocouple and the cell. This was done by fusing reagent grade lead in the alumina cell and freezing the end (two to four millimeters) of the chromel-alumel thermocouple in the lead. Calibration tests performed after annealing for several days at 250°C (while frozen in lead) showed that this treatment did not affect the calibration of the chromel-alumel thermocouple. Therefore, during calibration tests the chromel-alumel thermocouple was held frozen in lead in an aluminum oxide cell which was in turn held in the aluminum cell holder. The spectrometer was pumped down to about 10^{-5} torr. The average of the readings of the two types S thermocouples was compared with the reading of the chromel-alumel thermocouple at a series of temperatures over the range of interest. A typical set of readings is shown below.

Typical comparison of type S thermocouple readings and chromel-alumel thermocouple reading

temperature measured with chromel-alumel t.c. inside the alumina cell, °C.	average of temperature measured with two Pt/Pt-10Rh t.c.'s in cell holder, °C.
14.2	16.0
178.4	180.0
237.4	239.3
135.1	137.1
14.1	15.8

Within the reproducibility of the readings (0.2°C), no temperature trend of the apparent temperature difference between the chromel-alumel thermocouple and the average of the two type S thermocouples was discernable. Hence a correction (in this typical case) of -14 microvolts (about -2°C) was applied to the average of the readings of the type S thermocouples. This calibration procedure was repeated whenever the experimental arrangement was changed.

The two type S thermocouples frequently gave slightly different readings. The difference between the readings persisted to room temperature, where isothermal conditions existed because the Knudsen cell chamber is surrounded by a water-cooled jacket. Hence the difference in the readings is attributed to differences between the two thermocouples. The apparent difference was typically equivalent to about one degree. Simple heat transfer calculations indicated that the cell holder was massive enough to assure essentially isothermal conditions. The absolute accuracy of the temperature measurements was placed at ± 2°C.

Cadmium was selected as an appropriate material with which to verify

the experimental arrangement. Cadmium has a vapor pressure in the range expected for the system under investigation, and its vapor pressure is known with considerably accuracy.[25] Baker and Adamson reagent grade cadmium was used; powder was obtained by filing a cadmium stick.

Fourteen data points were recorded over the temperature range from 431.5° to 513.6°K. The electron multiplier was used to detect the ion current of Cd^{114+}, the cadmium ions being produced by 70 ev electrons at an emission current of 40 microampere. Data were recorded at decreasing temperatures, then increasing temperatures, then decreasing temperatures. Table XIII lists the temperatures, the intensities of the Cd^{114+} ion signal, and the products of the intensities and the temperatures. The heat of sublimation is equal to 4.576 times the slope of the $\log(I^{+}T)$ vs. 1/T plot (Fig. 23). The freehand line drawn through the data has a slope of 26.8 kcal/mole, and a least-squares computer calculation gave a slope of 26.70 ± 0.25 kacl/mole. These values should be compared with the following values selected by Hultgren, et al.,[25]

$$\Delta H^{\circ}_{400} = 26.580 \pm 0.150$$

$$\Delta H^{\circ}_{500} = 26.413 \pm 0.150 \text{ kcal/mol}$$

The slope of a line drawn through a plot (vs. 1/T) of the logarithms of their selected pressures from 416° to 530°K is 26.55 kcal/mol. The agreement is interpreted as being satisfactory verification of the temperature calibration and measurement system and the experimental arrangement.

It is of interest to note that the total vapor pressure of cadmium at the lowest temperature used in this test (431.5°K) is 2.8×10^{-8} atmospheres.[25] Since the isotopic abundance of Cd^{114} is 28.86%, pressures

Table XIII

Cadmium 114 Vapor Pressure Data

°K	I^{114+}(volts)	$(I^{+}T)$
508.4	1.11	5.64×10^{2}
491.0	0.385	1.89×10^{2}
481.8	0.263	1.27×10^{2}
462.3	0.0837	3.87×10^{1}
449.6	0.0378	1.70×10^{1}
429.7	0.0096	4.1
440.2	0.0201	8.85
459.1	0.0698	3.20×10^{1}
476.5	0.189	9.01×10^{1}
490.4	0.442	2.16×10^{2}
502.7	0.883	4.19×10^{2}
513.6	1.332	6.84×10^{2}
506.4	0.918	4.65×10^{2}
492.4	0.414	2.04×10^{2}

as low as 8.1×10^{-9} atmospheres were measured.

The vapor pressure of cadmium at the highest temperature used in ths test is 4.5×10^{-6} atmospheres.[25] Using the simple hard spheres formula for the mean free path of atoms in a gas[26] and an assumed cadmium atom diameter of 2.98 Å,[27] the mean free path corresponding to this condition was calculated to be about 4.0 centimeters. Since the diameter of the orifice was 0.1 centimeter, the Knudsen condition for effusive flow was satisfied.

B. Behavior of Oxygen

As was mentioned in the introduction, $CrO_{3(s)}$ is metastable relative to $Cr_2O_{3(s)}$ even at room temperature. The pressure of oxygen in equilibrium with $CrO_{3(s)}$ and $Cr_2O_{3(s)}$ at 450°K was calculated from the heat of formation of $CrO_{3(s)}$ reported by Neugebauer and Margrave[11] and the estimated entropy of $CrO_{3(s)}$ given by Wicks and Block[28] to be about 700 atmospheres. All other data necessary for the calculation were taken from Lewis, Randall, Pitzer, and Brewer.[29] At 450°K, the pressure of oxygen observed in this study when about 0.5 gm of $CrO_{3(s)}$ powder was heated in a Knudsen cell with a 1 mm diameter orifice was approximately 6×10^{-8} atmospheres. The vaporization data indicate a remarkably high kinetic barrier to the equilibrium decomposition.

At temperatures just below the melting point of CrO_3, oxygen was released from CrO_3 in very intense bursts of short duration and apparently random time intervals. At temperatures above the melting point, the bursts became so intense that measurements could not be made. In the case of the cell exhaustion experiment (which was carried out above the melting point of CrO_3) the combination of a small quantity of CrO_3 mixed with a

large quantity of $PbCrO_4$ (which was probably inert) prevented this problem.

No detailed studies were made to learn if the observed chromium-containing species have evaporation coefficients appreciably less than unity. However, one piece of evidence indicates that the chromium-containing species have evaporation coefficients near unity (or at least that all of the chromium-containing species have about the same evaporation coefficients). Two experiments were performed with the lid of the Knudsen cell liner and the cover of the Knudsen cell holder removed. In one of these experiments the sample was powdered CrO_3, in the other the sample was CrO_3 which had been melted and allowed to freeze in the Knudsen cell liner. The relative ion intensities were not changed significantly in these experiments from those in experiments with the lid in place using powdered CrO_3.

One experiment was performed in which 40 mg of CrO_3 were loaded into a new cell which was then heated in the mass spectrometer at a temperature below the melting point of CrO_3. After evaporating to "dryness" the cell and lid were reweighed (together with the residue). Over 99% of the original mass of the CrO_3 was lost by evaporation. This experiment provided further evidence of the high degree of kinetic suppression of the decomposition of $CrO_{3(s)}$ to $Cr_2O_{3(s)}$ and indicates that the uncatalyzed sublimation reaction is congruent.

C. Pressure Calibration

1. Cross-Sections for Ionization by Electron Impact

Three simple choices of relative cross-sections are possible: 1) the much used, but much criticized[30,31] cross-sections of Otvos and Stevenson[32]; 2) cross-sections assumed to be proportional to the total number of electrons in the molecule; and 3) the cross-sections assumed to be proportional to the number of valence electrons in the molecule.

Table XIV compares the cross-sections obtained by these three assumptions, all adjusted so that the cross-section of Cr_3O_7 is taken as unity. Table XIV shows that, for these chromium-containing molecules, the relative Otvos-Stevenson cross sections are nearly the same as those obtained by assuming that the ionization cross-section is proportional to the total number of electrons. The difference between the first two sets of cross-sections and the set based on the assumption of proportionality between ionization cross-section and the number of valence electrons in the molecule is not great. There is no really substantive information to guide a choice in assumptions for complex inorganic molecules. Furthermore, all three of these methods of deriving relative cross-sections use the assumption that the ionization cross-section is equal to the sum of the atomic cross-sections; this has been shown not to be literally true.[33] However, we note the comment of Inghram and Drowart[34]: "Thus, until further theoretical and experimental work is done, it is felt that the most consistent way of treating the data is to use both the additivity postulate and the ionization cross-sections given by Otvos and Stevenson." Consequently, the Otvos-Stevenson cross-sections have been rather arbitrarily adopted for this work.

2. Calculation of Relative Partial Pressures

The partial pressure of a particular vapor species can be calculated from the ion intensity of one of its isotopes, $I^+_{Cr_xO_y}$ by use of the following equation:

$$P_{Cr_xO_y} = \frac{\left(I^+_{Cr_xO_y} \; T\right) \left(K\right)}{\left(E-A_{Cr_xO_y}\right) \; \sigma_{Cr_xO_y} \; S_{Cr_xO_y} \; G_{Cr_xO_y}} \qquad (6)$$

Table XIV. Relative ionization cross-sections calculated by three different assumptions (normalized to $\sigma_{Cr_3O_7} = 1.00$).

Species	Otvos-Stevenson	proportional to total number of electrons	proportional to number of valence electrons
O_2	0.075	0.118	0.286
Cr_3O_7	1.00	1.00	1.00
$(CrO_3)_3$	1.08	1.06	1.29
Cr_4O_{10}	1.36	1.35	1.43
$(CrO_3)_4$	1.43	1.41	1.72
Cr_5O_{13}	1.72	1.70	1.86
$(CrO_3)_5$	1.79	1.77	2.14

where:

K = instrument calibration factor (independent of ion species and sample temperature).

T = absolute temperature of the solid in the Knudsen cell.

E = energy of the ionizing electrons.

$A_{Cr_xO_y}$ = appearance potential of the ion $Cr_xO_y^+$.

$\sigma_{Cr_xO_y}$ = relative ionization cross section of Cr_xO_y.

$S_{Cr_xO_y}$ = isotopic abundance of the particular isotope of of Cr_xO_y whose intensity is being measured.

$G_{Cr_xO_y}$ = relative electron multiplier gain of species Cr_xO_y.

The calculation of

$$\left[\frac{1}{\left(E-A_{Cr_xO_y}\right)\left(\sigma_{Cr_xO_y}\right) \quad S_{Cr_xO_y} \quad G_{Cr_xO_y}} \right]$$

for various species involved is summarized in Tables XV, XVI and XVII for 13.5, 15.5 and 16.4 ev electron energies. The relative electron multiplier gains (normalized to $G_{Cr_4O_{10}}$) were calculated from several sets of experimental gain checks except for $G_{(CrO_3)_5}$, which could not be measured because of the low intensity of $(CrO_3)_5^+$. Consequently the assumption $G_{(CrO_3)_5} = G_{(CrO_3)_4}$ was made. Also the assumption was made that $G(O_2) = G(Cr_4O_{10})$. One experimental gain check was made which indicated that this assumption is accurate to within 25%, but because of the low intensity of O_2^+ the gain check was not very reliable.

Two mass spectrometer runs were made with the same cell and orifice which were used in the weight loss experiment. The data of Run C were

Table XV. Calculation of $\left[\frac{1}{(E-A)\ S\ \sigma\ G}\right]$ for 13.5 ev electrons.

Species	(E-A)	S	G	σ	$[(E-A)\ S\ \sigma\ G]^{-1}$
Cr_3O_7	0.6	0.5940	1.06	107.4	2.46×10^{-2}
$(CrO_3)_3$	1.4	0.5940	1.23	114.0	8.58×10^{-3}
Cr_4O_{10}	1.2	0.5048	1.00	145.4	1.14×10^{-2}
$(CrO_3)_4$	1.7	0.5048	1.12	152.0	6.84×10^{-3}
Cr_5O_{13}	1.5	0.4326	0.923	183.4	9.11×10^{-3}
$(CrO_3)_5$	1.9	0.4326	1.12	190.0	5.72×10^{-3}

Table XVI Calculation of $\left[\frac{1}{(E-A)\ S\ \sigma\ G}\right]$ for 15.5 ev electrons.

Species	(E-A)	S	G	σ	$[(E-A)\ S\ \sigma\ G]^{-1}$
Cr_3O_7	2.6	0.5940	1.06	107.4	5.69×10^{-3}
$(CrO_3)_3$	3.4	0.5940	1.23	114.0	3.53×10^{-3}
Cr_4O_{10}	3.2	0.5048	1.00	145.4	4.26×10^{-3}
$(CrO_3)_4$	3.7	0.5048	1.12	152.0	3.14×10^{-3}
Cr_5O_{13}	3.5	0.4326	0.923	183.4	3.90×10^{-3}
$(CrO_3)_5$	3.9	0.4326	1.12	190.0	2.79×10^{-3}

Table XVII. Calculation of $\left[\frac{1}{(E-A)\ S\ \sigma\ G}\right]$ for 16.4 ev electrons.

Species	(E-A)	S	G	σ	$[(E-A)\ S\ \sigma\ G]^{-1}$
Cr_3O_7	3.5	0.5940	1.06	107.4	4.22×10^{-3}
$(CrO_3)_3$	4.3	0.5940	1.23	114.0	2.79×10^{-3}
Cr_4O_{10}	4.1	0.5048	1.00	145.4	3.32×10^{-3}
$(CrO_3)_4$	4.6	0.5048	1.12	152.0	2.53×10^{-3}
Cr_4O_{13}	4.4	0.4326	0.923	183.4	3.10×10^{-3}
$(CrO_3)_5$	4.8	0.4326	1.12	190.0	2.26×10^{-3}
O_2	3.9	1.00	(1.00)	6.58	3.90×10^{-2}

recorded using 15.5 and 16.4 ev electrons, while those of run D were recorded using 13.5 and 16.4 ev electrons. An incomplete set of points were taken in run C15.5, hence the scatter of this set of data is relatively high. Oxygen intensities were recorded only in the 16.4 ev runs. The multiplier gain during run C was 3.38×10^6 (for $Cr_4O_{10}^+$) while the multiplier gain during run D was 3.77×10^6 (for $Cr_4O_{10}^+$). For convenience in comparing data, a factor of 0.898 was applied to all of the run D data to normalize it to the same gain as was encountered in run C.

In order to obtain relative pressures of the various vapor species, the product:

$$P' = \frac{P^\circ}{K} = \frac{I^+_{Cr_xO_y} \; T}{E\text{-}A_{Cr_xO_y} \quad \sigma_{Cr_xO_y} \quad S_{Cr_xO_y} \quad G_{Cr_xO_y}}$$

was calculated by machine for each point in these four sets of data. The slope of the log (P°/K) vs 1/T relationship was also calculated. This slope, multiplied by 4.5758, is the heat of vaporization of the particular species. The intercept of the log (P°/K) vs 1/T line was also calculated. This intercept, when multiplied by 4.5758, gives not the entropy of sublimation ΔS°_{sub}, but a quantity $\Delta S'$. The following expressions demonstrate the relationship between $\Delta S'$ and ΔS_{sub}:

$$-4.5758 \log P^\circ = \frac{\Delta H_{sub}}{T} - \Delta S^\circ_{sub} \qquad (7)$$

but here: $P^\circ = P' \times K$, hence:

$$-4.5758 \log P' = \frac{\Delta H^\circ_{sub}}{T} - \Delta S' \qquad (8)$$

and:

$$-4.5758 \log K = \Delta S' - \Delta S^\circ_{sub} \qquad (9)$$

3. Pressure Calibration Factors Based on Weight-Loss Experiments

Two weight-loss runs were performed using the same Knudsen cell and lid as were used in the temperature-dependent partial pressure measurement runs. The lid had been lapped by the use of diamond paste to fit the cell. The cell and sample were first heated for 24 hours, cooled in vacuum, transferred to a weighing bottle and weighed, heated for the first run, weighed again by the same procedure, heated for the second run, then weighed again. The conditions of these two weight loss runs and their results are listed in Table XVIII.

The equation relating the pressure of an unknown substance, $P_{Cr_xO_y}$ to the pressure (P°_{std}) and ion intensity (I^{+}_{std}) of a standard substance is:

$$P_{Cr_xO_y} = I^{+}_{Cr_xO_y} T \left(\frac{E-A_{std}}{E-A_{Cr_xO_y}}\right)\left(\frac{P^{\circ}_{std}}{I^{+}_{std}T_{std}}\right)\left(\frac{\sigma_{std}}{\sigma_{Cr_xO_y}}\right)\left(\frac{S_{std}}{S_{Cr_xO_y}}\right)\left(\frac{G_{std}}{G_{Cr_xO_y}}\right) \quad (10)$$

$$= \frac{I^{+}_{Cr_xO_y} T}{\left(E-A_{Cr_xO_y}\right)} \left\{\frac{K}{\left(\sigma_{Cr_xO_y}\right) S_{Cr_xO_y} G_{Cr_xO_y}}\right\} \quad (11)$$

where:

I^{+}_{i} = ion intensity of species i at temperature T_i (°K)

E = energy of ionizing electrons, volts.

A_i = appearance potential of ion i.

P°_{std} = vapor pressure of standard substance at T_{std}

σ_i = ionization cross-section of species i.

S_i = isotopic abundance of species i.

G_i = relative multiplier gain of species i.

K = pressure calibration factor (same for all 'unknown' species).

Table XVIII Conditions and results of $CrO_{3(s)}$ weight-loss experiments.

	Expt. No. 1	Expt. No. 2
Temperature, °K	455.1	441.7
time, sec.	2.30×10^5	2.02×10^5
gms. CrO_3 vaporized	0.21381	0.06435
orifice area, cm^2	0.0351	0.0351
orifice L/R	2.44	2.44
Clausing Factor, W_o	0.4682	0.468°
apparent $CrO_{3(g)}$ pressure, (atm.)	2.77×10^{-6}	9.31×10^{-7}

For a Knudsen experiment

$$P = M\left(\frac{2\pi RT}{M}\right)^{1/2} = \frac{M}{44.33}\left(\frac{T}{M}\right)^{1/2} \qquad (12)$$

where:

m = weight loss per unit area per unit time.

$m = \frac{m'}{aW_o t}$

m' = grams evaporated in t seconds from an orifice of area a (cm^2) and Clausing Factor W_o.

M_i = molecular weight of vapor species i.

The total rate of weight loss ($gm/cm^2/sec$) when several species are present will be given by:

$$m = \frac{44.33}{\sqrt{T}} \sum_i P_i \sqrt{M_i} \qquad (13)$$

Where the summation is over all vapor species effusing from the cell. Using the factor in equation (11), exclusive of K, the relative pressures P' of the vapor species can be calculated.

Since:

$$P_i^o = P_i' \times K$$

$$m = \frac{44.33K}{\sqrt{T}} \sum_i P_i' \sqrt{M_i} \qquad (14)$$

$$K = \frac{M' \sqrt{T}}{44.33 \sum_i P_i' \sqrt{M_i}} \qquad (15)$$

$$K = \frac{M' \sqrt{T}}{44.33 (a W_o t) \sum_i P_i' \sqrt{M_i}} \qquad (16)$$

Using the values listed in Table XV for the first weight loss experiment:

$$K = \frac{0.21381 \quad (454.4)^{1/2}}{(0.0351)\ (0.4682)\ (2.30 \times 10^{-5})\ (44.33)[\sum_i P_i' \sqrt{M_i}]}$$

$$= \frac{2.72 \times 10^{-5}}{\sum P_i' \sqrt{M_i}}$$

Four sets of relative pressure data are available for use to evaluate $P_i' \sqrt{M_i}$: the data taken with 16.4 volt and 15.5 volt ionizing electrons in run C and the 13.5 and 16.4 ev data of run D. The ion intensities from these two experiments are tabulated in Tables XIX, XX, XXI and XXII. Because of the low ionization cross-section of oxygen, the oxygen ion intensities were measured only at 16.4 ev.

Exactly the same calculation was carried out using the data obtained in the second weight-loss experiment. In this case:

$$K = \frac{9.21 \times 10^{-6}}{\sum_i P_i' \sqrt{M_i}}$$

Table XXIII present the eight K-values based upon the first and second weight-loss experiments. As is seen in Table XXIII, the K-values calculated using the 13.5 ev data are roughly 1/3 larger than the K-values based on the 16.4 ev data. The most important reasons for this are, first the possible fragment contributions to the $Cr_4O_{10}^+$ and $Cr_4O_7^+$ ion peaks when 16.4 ev electrons were used. The second factor to be considered is the fact that the uncertainties in the appearance potentials and non-linearity of the ionization efficiency curves near the threshold are more important (since (E-A) will be smaller) in evaluating the 13.5 ev data than the 16.4 ev data.

Table XIX. Ion Intensity Data, Knudsen Cell Run C 15.5. All intensity data are in volts ouput from the electron multiplier.

Temp. °K	I_{268}	I_{300}	I_{368}	I_{400}	I_{468}	I_{500}
444.9	7.90×10^{-3}	1.58×10^{-2}	6.16×10^{-2}	1.18×10^{-2}	5.40×10^{-3}	9.60×10^{-4}
457.8	2.55×10^{-2}	5.05×10^{-2}	2.04×10^{-1}	3.57×10^{-2}	2.20×10^{-3}	3.40×10^{-3}
466.7	4.42×10^{-2}	7.88×10^{-2}	3.76×10^{-1}	5.21×10^{-2}	4.41×10^{-2}	5.90×10^{-3}
428.0	1.60×10^{-3}	4.30×10^{-2}	1.21×10^{-2}	3.30×10^{-3}	8.00×10^{-4}	2.30×10^{-4}
415.1	5.70×10^{-4}	1.40×10^{-3}	3.45×10^{-3}	1.10×10^{-3}	1.70×10^{-4}	6.00×10^{-5}
434.5	3.20×10^{-3}	7.00×10^{-3}	2.40×10^{-2}	5.60×10^{-3}	1.80×10^{-3}	4.50×10^{-4}
435.6	3.75×10^{-3}	7.95×10^{-3}	2.90×10^{-2}	6.45×10^{-3}	2.20×10^{-3}	5.00×10^{-4}
442.9	7.40×10^{-3}	1.68×10^{-2}	5.72×10^{-2}	1.26×10^{-2}	5.10×10^{-3}	1.05×10^{-3}
451.6	1.50×10^{-2}	3.22×10^{-2}	1.19×10^{-1}	2.34×10^{-2}	1.23×10^{-2}	2.30×10^{-3}
457.3	2.40×10^{-2}	4.05×10^{-2}	2.01×10^{-1}	3.65×10^{-2}	2.16×10^{-2}	3.80×10^{-3}
447.0	1.01×10^{-2}	2.21×10^{-2}	8.05×10^{-2}	1.68×10^{-2}	7.40×10^{-3}	1.40×10^{-3}
436.0	3.95×10^{-3}	1.01×10^{-2}	3.30×10^{-2}	7.90×10^{-3}	2.70×10^{-3}	5.00×10^{-4}
426.1	1.70×10^{-3}	4.40×10^{-3}	1.31×10^{-2}	3.40×10^{-3}	8.50×10^{-4}	2.50×10^{-4}
424.4	1.25×10^{-3}	3.25×10^{-3}	9.15×10^{-3}	2.60×10^{-3}	5.00×10^{-4}	1.00×10^{-4}
416.8	6.00×10^{-4}	1.50×10^{-3}	4.25×10^{-3}	1.15×10^{-3}	2.00×10^{-4}	----------
468.1	4.63×10^{-2}	7.50×10^{-2}	3.80×10^{-1}	4.85×10^{-2}	4.55×10^{-2}	5.50×10^{-3}

Table XX Ion Intensity Data, Knudsen Cell Run C 16.4. All intensity data are in volts output from the electron multiplier.

Temp °K	I_{268}	I_{300}	I_{368}	I_{400}	I_{468}	I_{500}	I_{32}
454.2	3.80×10^{-2}	5.50×10^{-2}	2.61×10^{-1}	3.80×10^{-1}	2.24×10^{-2}	3.70×10^{-3}	1.80×10^{-3}
4.60	7.33×10^{-2}	9.03×10^{-2}	4.52×10^{-1}	5.95×10^{-2}	4.18×10^{-2}	6.30×10^{-3}	3.50×10^{-3}
465.7	9.45×10^{-2}	1.25×10^{-1}	6.65×10^{-1}	7.95×10^{-2}	6.47×10^{-2}	8.10×10^{-3}	5.90×10^{-3}
418.3	1.40×10^{-3}	2.40×10^{-3}	7.60×10^{-3}	1.80×10^{-3}	4.00×10^{-4}	---------	---------
426.0	2.95×10^{-3}	4.85×10^{-3}	1.73×10^{-2}	3.45×10^{-3}	9.00×10^{-4}	2.00×10^{-4}	---------
444.9	1.59×10^{-2}	2.10×10^{-2}	1.04×10^{-1}	1.47×10^{-2}	7.80×10^{-3}	1.25×10^{-3}	8.00×10^{-4}
457.8	4.90×10^{-2}	6.65×10^{-2}	3.45×10^{-1}	4.33×10^{-2}	3.02×10^{-2}	4.50×10^{-3}	2.20×10^{-3}
466.7	9.30×10^{-2}	1.23×10^{-1}	6.75×10^{-1}	7.65×10^{-2}	6.55×10^{-2}	8.70×10^{-3}	4.70×10^{-3}
428.0	3.05×10^{-3}	5.30×10^{-3}	1.89×10^{-2}	4.10×10^{-3}	1.05×10^{-3}	2.50×10^{-4}	---------
415.1	1.05×10^{-3}	1.90×10^{-3}	5.55×10^{-3}	1.30×10^{-3}	2.00×10^{-4}	---------	---------
434.5	6.25×10^{-3}	1.05×10^{-2}	4.35×10^{-2}	7.05×10^{-3}	2.75×10^{-3}	6.00×10^{-4}	---------
435.6	8.10×10^{-3}	1.17×10^{-2}	5.10×10^{-2}	8.40×10^{-3}	3.20×10^{-3}	6.00×10^{-4}	---------
442.9	1.67×10^{-2}	2.70×10^{-2}	1.16×10^{-1}	1.97×10^{-2}	8.40×10^{-3}	1.60×10^{-3}	---------
451.6	3.15×10^{-2}	4.80×10^{-2}	2.29×10^{-1}	3.40×10^{-2}	1.89×10^{-2}	3.30×10^{-3}	1.70×10^{-3}
457.3	5.20×10^{-2}	7.70×10^{-2}	3.80×10^{-1}	5.20×10^{-2}	3.40×10^{-2}	5.40×10^{-3}	---------
447.0	2.16×10^{-2}	3.30×10^{-2}	1.48×10^{-1}	2.40×10^{-2}	1.19×10^{-2}	1.25×10^{-3}	1.20×10^{-3}
436.0	9.30×10^{-3}	1.50×10^{-2}	5.90×10^{-2}	1.11×10^{-2}	4.00×10^{-3}	8.00×10^{-4}	---------
426.1	3.80×10^{-3}	6.30×10^{-3}	2.35×10^{-2}	4.90×10^{-3}	1.30×10^{-3}	3.00×10^{-4}	---------
424.4	2.95×10^{-3}	4.85×10^{-3}	1.73×10^{-2}	3.50×10^{-3}	9.50×10^{-4}	2.00×10^{-4}	---------
416.8	1.50×10^{-3}	2.30×10^{-3}	8.70×10^{-3}	1.70×10^{-3}	3.50×10^{-4}	---------	---------
468.1	1.07×10^{-1}	1.32×10^{-1}	8.08×10^{-1}	8.20×10^{-2}	8.05×10^{-2}	9.00×10^{-3}	7.20×10^{-3}

Table XXI. Ion intensity data, Knudsen cell run D 13.5. All intensity data are in volts output from the electron multiplier

Temp °K	I_{268}	I_{300}	I_{368}	I_{400}	I_{468}	I_{500}
453.4	3.45×10^{-3}	1.47×10^{-2}	4.69×10^{-2}	1.25×10^{-2}	5.90×10^{-3}	--------
453.6	3.50×10^{-3}	1.36×10^{-2}	4.70×10^{-2}	1.18×10^{-2}	6.12×10^{-3}	1.30×10^{-3}
443.6	2.25×10^{-3}	8.10×10^{-3}	2.76×10^{-2}	7.37×10^{-3}	3.10×10^{-3}	6.50×10^{-4}
448.9	3.35×10^{-3}	1.23×10^{-2}	4.27×10^{-2}	1.04×10^{-2}	5.00×10^{-3}	1.05×10^{-3}
454.1	4.95×10^{-1}	1.61×10^{-2}	6.26×10^{-2}	1.35×10^{-2}	8.05×10^{-3}	1.40×10^{-3}
463.9	1.07×10^{-2}	3.22×10^{-2}	1.31×10^{-1}	2.49×10^{-2}	1.92×10^{-2}	2.95×10^{-3}
435.6	4.50×10^{-4}	2.85×10^{-3}	7.60×10^{-3}	2.78×10^{-3}	7.80×10^{-4}	2.50×10^{-4}
440.9	8.00×10^{-4}	4.15×10^{-3}	1.22×10^{-2}	4.02×10^{-3}	1.30×10^{-3}	3.50×10^{-4}
449.0	2.75×10^{-3}	1.11×10^{-2}	3.72×10^{-2}	1.01×10^{-2}	4.55×10^{-3}	9.30×10^{-4}
458.9	6.50×10^{-3}	2.20×10^{-2}	8.50×10^{-2}	1.82×10^{-2}	1.17×10^{-2}	2.05×10^{-3}
461.5	7.48×10^{-3}	2.48×10^{-2}	1.01×10^{-1}	2.15×10^{-2}	1.41×10^{-2}	2.40×10^{-3}
462.6	8.16×10^{-3}	2.56×10^{-2}	1.06×10^{-1}	2.02×10^{-2}	1.53×10^{-2}	2.57×10^{-3}
427.6	----------	1.43×10^{-3}	4.30×10^{-3}	1.25×10^{-3}	3.20×10^{-4}	---------
440.2	1.15×10^{-3}	4.10×10^{-3}	1.44×10^{-2}	3.65×10^{-3}	1.45×10^{-3}	2.50×10^{-3}
432.3	6.00×10^{-4}	2.43×10^{-3}	7.30×10^{-3}	2.22×10^{-3}	6.00×10^{-4}	--------
436.0	9.60×10^{-4}	3.60×10^{-3}	1.20×10^{-2}	3.13×10^{-3}	1.10×10^{-3}	1.30×10^{-4}
454.4	3.30×10^{-3}	1.24×10^{-2}	4.45×10^{-2}	1.05×10^{-3}	5.40×10^{-3}	1.15×10^{-3}
455.4	3.55×10^{-3}	1.19×10^{-2}	4.45×10^{-2}	9.60×10^{-3}	5.63×10^{-3}	1.10×10^{-3}
463.1	6.25×10^{-3}	2.06×10^{-2}	7.80×10^{-2}	1.64×10^{-2}	1.10×10^{-2}	2.00×10^{-3}
444.3	1.10×10^{-3}	4.30×10^{-3}	1.46×10^{-2}	3.73×10^{-2}	1.50×10^{-3}	2.80×10^{-4}
442.8	2.75×10^{-3}	9.60×10^{-3}	3.70×10^{-2}	8.34×10^{-3}	4.45×10^{-3}	9.00×10^{-4}

Table XXII Ion Intensity Data, Knudsen Cell Run D 16.4. All intensity data are in Volts output from the electron multiplier

Temp °K	I_{268}	I_{300}	I_{368}	I_{400}	I_{468}	I_{500}	I_{32}
453.4	4.83×10^{-2}	6.40×10^{-2}	3.47×10^{-1}	4.43×10^{-2}	3.05×10^{-2}	4.50×10^{-3}	1.20×10^{-3}
453.6	4.70×10^{-2}	5.75×10^{-2}	3.48×10^{-1}	4.05×10^{-2}	3.10×10^{-2}	4.22×10^{-3}	2.00×10^{-3}
443.6	2.48×10^{-2}	3.15×10^{-2}	1.74×10^{-1}	2.30×10^{-2}	1.29×10^{-2}	2.00×10^{-3}	7.00×10^{-4}
448.9	3.75×10^{-2}	4.48×10^{-2}	2.67×10^{-1}	3.20×10^{-2}	2.14×10^{-2}	3.00×10^{-3}	8.00×10^{-4}
454.1	5.38×10^{-2}	5.92×10^{-2}	3.84×10^{-1}	4.05×10^{-2}	3.22×10^{-2}	4.15×10^{-3}	1.40×10^{-3}
463.9	1.11×10^{-1}	1.19×10^{-1}	8.20×10^{-1}	7.60×10^{-2}	7.82×10^{-2}	8.55×10^{-3}	2.65×10^{-3}
435.6	1.08×10^{-2}	1.44×10^{-2}	6.82×10^{-2}	1.09×10^{-2}	4.70×10^{-3}	8.50×10^{-4}	---------
440.9	1.44×10^{-2}	2.17×10^{-2}	1.07×10^{-1}	1.49×10^{-2}	7.62×10^{-3}	1.10×10^{-3}	4.00×10^{-4}
449.0	3.25×10^{-2}	4.40×10^{-2}	2.40×10^{-1}	3.25×10^{-2}	2.00×10^{-2}	3.05×10^{-3}	5.30×10^{-4}
458.9	6.60×10^{-2}	8.15×10^{-2}	5.00×10^{-1}	5.60×10^{-2}	4.76×10^{-2}	6.00×10^{-3}	1.30×10^{-3}
461.5	7.81×10^{-2}	9.25×10^{-2}	5.75×10^{-1}	6.10×10^{-2}	5.80×10^{-2}	7.05×10^{-3}	1.30×10^{-3}
462.3	8.33×10^{-2}	9.63×10^{-2}	6.63×10^{-1}	6.40×10^{-2}	6.45×10^{-2}	7.22×10^{-3}	1.60×10^{-3}
442.8	2.98×10^{-2}	3.67×10^{-2}	2.29×10^{-1}	2.57×10^{-2}	---------	2.58×10^{-3}	2.50×10^{-4}
427.6	3.92×10^{-3}	5.40×10^{-3}	2.72×10^{-2}	4.00×10^{-3}	1.50×10^{-3}	----------	----------
440.4	1.23×10^{-2}	1.55×10^{-2}	9.93×10^{-2}	1.12×10^{-2}	6.30×10^{-3}	9.00×10^{-4}	2.20×10^{-4}
432.3	6.50×10^{-3}	9.00×10^{-3}	4.50×10^{-2}	6.75×10^{-3}	---------	5.00×10^{-4}	----------
436.0	9.60×10^{-3}	1.18×10^{-2}	6.55×10^{-2}	8.20×10^{-3}	4.23×10^{-3}	8.00×10^{-4}	2.00×10^{-4}
454.0	3.63×10^{-2}	4.63×10^{-2}	2.69×10^{-1}	3.20×10^{-2}	---------	3.25×10^{-3}	4.20×10^{-4}
455.4	3.75×10^{-2}	4.40×10^{-2}	2.83×10^{-1}	3.05×10^{-2}	----------	3.18×10^{-3}	2.00×10^{-4}
463.1	6.52×10^{-2}	7.61×10^{-2}	4.93×10^{-1}	4.92×10^{-2}	---------	5.48×10^{-3}	9.00×10^{-4}
444.3	---------	1.55×10^{-2}	9.15×10^{-2}	1.17×10^{-2}	----------	1.02×10^{-3}	3.50×10^{-4}

Table XXIII. Summary of pressure calibration factors (K-values)

Partial Pressure Expt.	K-value	
	Weight-loss Run No. 1	Weight-loss Run No. 2
C15.5	3.25×10^{-6}	3.30×10^{-6}
C16.4	2.35×10^{-6}	2.46×10^{-6}
D13.5	3.79×10^{-6}	3.40×10^{-6}
D16.4	2.52×10^{-6}	2.56×10^{-6}

Average K = 2.95×10^{-6}

D. Heats and Entropies of Sublimation and Partial Pressures

Tables XXIV through XXX list heats and entropies of sublimation for the various species. In addition to the data from experiments C15.5, C16.4, D13.5 and D16.4, heat of sublimation data from experiments E13.5 and E16.4 are also included. The "E" series experiments were performed using a smaller orifice. The orifice used in the E series (r = 0.0546 cm) had an effective area 5.53 times smaller than the orifice used in the C and D experiments. The change in orifice had no significant effect on the measured heats.

Standard deviations of the heats and entropies are significantly smaller in the C16.4 data than in any of the other data. Because of this, the C16.4 data was used as a basis for calculating vapor pressure curves. It might be argued that it the C16.4 data are to be used for the final pressure calculations, then the calibration factor from the C16.4 data (2.40×10^{-6}) should be used rather than the average of the eight values (2.95×10^{-6}) which was used. If this is done, all of the reported entropies would be reduced by 0.42 ev. This entropy difference is equivalent to a pressure difference of less than 25%.

Table XXXI summarizes the selected heats and entropies of sublimation of the various species. Figure 24 plots the partial pressures over the temperature range 420-470°K.

McDonald and Margrave[9] reported heats and entropies of sublimation for $(CrO_3)_x$, x = 3, 4, 5. Their values for $(CrO_3)_5$ were based on the average of two runs for $Cr_5O_{13}^+$ (which they assumed to be a fragment of $(CrO_3)_5$). Their values for $(CrO_3)_3$ were based on the average of two runs for $Cr_3O_7^+$ (assumed to be a fragment of $(CrO_3)_3$) and one run for $(CrO_3)_3^+$.

Table XXIV. Partial Heats and Entropies of Sublimation of Cr_3O_7.

Expt. No.	ΔH^o_{sub} kcal	Std. Deviation of ΔH^o_{sub}	ΔS^o_{sub} eu	Std. Deviation of ΔS^o_{sub}
C15.5	34.16	0.43	44.75	0.99
C16.4	34.58	0.51	45.62	1.16
D13.5	36.18	2.62	47.94	5.83
D16.4	33.21	1.67	42.75	3.73
E13.5	36.03	1.07		
E16.4	35.79	0.64		

Table XXV. Heats and Entropies of Sublimation of $(CrO_3)_3$

Expt. No.	ΔH^o_{sub} kcal	Std. Deviation of ΔH^o_{sub}	ΔS^o_{sub} eu	Std. Deviation of ΔS^o_{sub}
C15.5	31.28	0.69	38.85	1.58
C16.4	32.43	0.56	40.75	1.27
D13.5	32.47	1.73	40.21	3.85
D16.4	31.58	1.85	38.68	4.12
E13.5	33.31	1.11		
E16.4	33.78	1.37		

Table XXVI. Partial Heats and Entropies of Sublimation of Cr_4O_{10}.

Expt. No.	ΔH^o_{sub} kcal	Std. Deviation of ΔH^o_{sub}	ΔS^o_{sub} eu	Std. Deviation of ΔS^o_{sub}
C15.5	35.67	0.53	50.68	1.20
C16.4	36.53	0.57	53.28	1.28
D13.5	35.74	1.99	50.54	4.44
D16.4	35.32	1.45	50.83	3.23
E13.5	37.24	0.70		
E16.4	37.23	0.82		

Table XXVII. Heats and Entropies of Sublimation of $(CrO_3)_4$.

Expt. No.	ΔH^o_{sub} kcal	Std. Deviation of ΔH^o_{sub}	ΔS^o_{sub} eu	Std. Deviation of ΔS^o_{sub}
C15.5	30.02	0.81	34.18	1.85
C16.4	31.34	0.69	37.36	1.55
D13.5	28.99	3.60	31.92	8.03
D16.4	30.08	1.84	44.45	4.11
E13.5	31.01	1.30		
E16.4	32.64	1.37		

Table XXVIII. Partial Heats and Entropies of Sublimation of Cr_5O_{13}.

Expt. No.	ΔH^o_{sub} kcal/mol	Std. Deviation of ΔH^o_{sub}	ΔS^o_{sub} eu	Std. Deviation ΔS^o_{sub}
C15.5	42.51	0.78	61.03	1.77
C16.4	42.89	0.71	62.24	1.60
D13.5	42.35	2.22	60.58	4.95
D16.4	42.65	1.04	62.16	2.33
E13.5	41.30	0.99		
E16.4	42.56	0.91		

Table XXIX. Heats and Entropies of Sublimation of $(CrO_3)_5$.

Expt. No.	ΔH^o_{sub} kcal/mol	Std. Deviation of ΔH^o_{sub}	ΔS^o_{sub} eu	Std. Deviation of ΔS^o_{sub}
C15.5	35.54	1.26	41.42	2.84
C16.4	36.35	1.10	43.43	2.48
S13.5	31.73	5.45	33.08	12.11
D16.4	33.99	2.22	38.29	4.94
E13.5	35.52	3.20		
E16.4	39.02	2.36		

Table XXX. Partial Heat and Entropy of Activation for Sublimation of O_2 from $CrO_{3(s)}$.

Expt. No.	ΔH^o_{sub} kcal/mol	Std. Deviation of ΔH^o_{sub}	ΔS^o_{sub} eu	Std. Deviation of ΔS^o_{sub}
C16.4	35.42	1.92	45.87	4.18
D16.4	29.40	6.19	30.81	13.71

Table XXXI. Selected Partial Heats and Entropies of Sublimation of Species Effusing from a Knudsen Cell Containing $CrO_{3(s)}$.[a]

Species	Partial Heat of Sublimation Kcal/mol	Std. Deviation of Heat of Sublimation Kcal/mol	Partial Entropy of Sublimation eu	Std. Deviation of Entropy of Sublimation eu
Cr_3O_7	34.58	0.51	45.62	1.16
$(CrO_3)_3$	32.43	0.56	40.75	1.27
Cr_4O_{10}	36.53	0.57	53.28	1.28
$(CrO_3)_4$	31.34°	0.69	37.36	1.55
Cr_5O_{13}	42.89	0.71	62.24	1.60
$(CrO_3)_5$	36.35	1.10	43.43	2.48
O_2[b]	35.42	1.92	45.87	4.18

Likewise, the value they report for $(CrO_3)_4$ is based on two runs for $Cr_4O_{10}^+$ and one run for $(CrO_3)_4^+$.

The values they reported are tabulated and compared with the results of this study in Table XXXII. Note that if the value McDonald and Margrave report for ΔH^o_{sub} $(CrO_3)_5$, 44 ± 5 kcal, is compared with the value found in this study, ΔH^o_{sub} $(CrO_3)_5$ = 36.35 ± 1.10, the agreement is poor, but when compared with the value found in this study for ΔH^o_{sub} (Cr_5O_{13}) = 42.89 ± 0.71, the agreement is very good. Similar comparisons should be made with the entropy values and the reported heat values. In every case, the values reported by McDonald and Margrave are in much better agreement with the values found in this study for the corresponding Cr_xO_{3x-2} than with the values for the $(CrO_3)_x$.

E. Total Pressure

Figure 25 presents the total pressure as determined in experiment C16.4 of this study. Also included in this figure are a curve corresponding to Glemser's[5] measured pressure (based on $CrO_{3(g)}$) as being the gaseous species) and a line corresponding to Glemser's pressures divided by four (to approximately account for the complexity of the vapor).

Table XXXIII compares the total entropy and heat of sublimation as determined in this study with the values derived from Glemser's vapor pressure equation and those reported by McDonald and Margrave. Glemser's entropy values apparently should be reduced by 4.576 log 4 to account for vapor complexity, but this does not significantly decrease the deviation between the two studies.

Table XXXII. Comparison of partial heats and entropies of sublimation with the results of McDonald and Margrave.

Species	Second Law Partial Heats of Sublimation kcal/mol		Second Law Partial Entropies of Sublimation kcal/mol	
	M and M	This Study	M and M	This Study
$(CrO_3)_5$	44 ± 5	36.35 ± 1.10	62 ± 13	43.43 ± 2.48
Cr_5O_{13}		42.89 ± 0.71		62.24 ± 1.60
$(CrO_3)_4$	39 ± 2	31.34 ± 0.69	56 ± 5	37.36 ± 1.55
Cr_4O_{10}		36.53 ± 0.57		53.28 ± 1.28
$(CrO_3)_3$	36 ± 2	32.43 ± 0.56	48 ± 5	40.75 ± 1.27
Cr_3O_7		34.58 ± 0.51		45.62 ± 1.16

Table XXXIII. Comparison of reported heats and entropies of sublimation of $CrO_{3(s)}$.

	This Study	Glemser, Stocker, and Muller	McDonald and Margrave
Heat of Sublimation kcal/mol	35.26 ± 0.67	47.2	40 ± 2
entropy of sublimation, eu	51.36 ± 1.51	78.95	not reported

F. Stoichiometric Balance

If the assumption is made that $CrO_{3(s)}$ vaporizes congruently in this experiment (as it must nearly do), then the sum of the number of moles of Cr_3O_7, Cr_4O_{10} and Cr_5O_{13} effusing from the cell should equal the number of moles of O_2 effusing from the cell. The experimentally determined value of the ratio of the sum of the number of moles of Cr_nO_{3n-2} species to the number of moles of oxygen is 4.6 at the midpoint of the temperature range. If the oxygen data from run C16.4 is combined with the data for the Cr_nO_{3n-2} species from run D13.5, the value of this ratio is found to be 4.9, which is not significantly different from the earlier value.

Four factors adversely affect the accuracy of the oxygen pressure data:

1) The oxygen ion current was always small so that no accurate electron multiplier gain could be measured for O_2. The assumption was made that $G_{O_2} = G_{Cr_4O_{10}}$.

2) There is probably much more uncertainty in the oxygen ionization cross-section relative to the cross-section for the chromium-containing species than from one chromium-containing species to another.

3) Background oxygen intensities were approximately 10%-50% of the total oxygen intensities. This made measurement of the oxygen ion intensity difficult--background may have been overcorrected for.

4) The low oxygen ion intensity produced very scattered data. This is evidence by the high standard deviations of the partial heat and entropy of sublimation of oxygen. Once again it should be emphasized that the entropy and heat of sublimation of O_2 are activation, not equilibrium, values.

VI. SUMMARY AND CONCLUSIONS

A. Species Identification

Double cell experiments, cell exhaustion experiments, and heat of sublimation measurements indicate that at low electron energies, the ionic species $(CrO_3)_n^+$ and $Cr_nO_{3n-2}^+$ (n = 3, 4, and 5) all result from simple ionization of molecules of the same composition as the ions. In addition, O_2^+ and $(CrO_3)_6^+$ were observed in small quantities and small quantities of Cr_nO_{3n-1} (n = 3 or 4) may be present in the vapor. These conclusions are to be contrasted with those of McDonald and Margrave who decided ions of species other than of the $(CrO_3)_n^+$ type are fragments. It may be well to summarize the evidence that neutral species of formulas Cr_nO_{3n-2} are important vapor species.

1. Appearance potentials

The appearance potential differences of the ion pairs in question are reported in the two studies as follows:

ion pair	appearance potential difference (volts) this study	McDonald and Margrave
$AP[(CrO_3)_5^+] - AP[Cr_5O_{13}^+]$	-0.7	< - 2.2
$AP[(CrO_3)_4^+] - AP[Cr_4O_{10}^+]$	-0.7	- 0.9
$AP[(CrO_3)_3^+] - AP[Cr_3O_9^+]$	-1.3	- 3.4

Because both studies found the ion $Cr_4O_{10}^+$ to be the most abundant ion in the mass spectrum arising from CrO_3, the ion pair $(CrO_3)_4^+ - Cr_4O_{10}^+$ is of the most interest. The small appearance potential difference found in

both studies for the $(CrO_3)_4^+ - Cr_4O_{10}^+$ ion pair, when combined with data for the Cr-O bond energy[2] and the dissociation energy of $O_{2(g)}$, tends to indicate that fragmentation is not involved in this case.

2. Ionization efficiency curves

The ionization efficiency curves for $(CrO_3)_4^+$ and $Cr_4O_{10}^+$ are shown in Fig. 6. The curve for $Cr_4O_{10}^+$ appears to show a tail, indicating that more than one ionization process is involved in the formation of this ion. Figure 26 is an extrapolated difference plot[18] comparing the ionization efficiency curves of $(CrO_3)_4^+$ and $Cr_4O_{10}^+$. Unlike the results reported by McDonald and Margrave, there is clear evidence here that more than one process does contribute to the $Cr_4O_{10}^+$ ion current. Figure 13 is a plot of the ionization efficiency curves of $(CrO_3)_3^+$ and $Cr_3O_7^+$, and Fig. 27 is an extrapolated differences plot for these ions. The evidence indicates that more than one source contributes to the $Cr_3O_7^+$ ion current. The case of the ion pair $(CrO_3)_5^+ - Cr_5O_{13}^+$ shows somewhat different behavior. Figure 28 is an extrapolated differences plot for this pair of ions, and it shows no break. An extrapolated differences plot which shows no break is subject to two very different interpretations: (1) both ions result from simple ionization only, or (2) both ions arise from the same parent (one can be the parent of the other) and have only one source. For comparison purposes, Fig. 29 shows the extrapolated differences plot for the ion pair $(CrO_3)_3^+ - (CrO_3)_4^+$, two ions which both studies conclude arise from simple ionization of molecules of the same composition as the ions.

3. Experiments with undersaturated vapor conditions

Table IX lists the ion intensity ratios I_{300}^+/I_{268}^+, I_{400}^+/I_{368}^+ and

I^+_{500}/I^+_{468} (corresponding to the principle peaks of $I^+_{Cr_xO_{3x}}/I^+_{Cr_xO_{3x-2}}$ with x = 3, 4, and 5 respectively) during a cell exhaustion experiment as the temperature of the cell was being raised with the activity of $(CrO_{3(l)})$ less than unity. The sharp temperature trend is strong evidence that the ion pairs in question are not correlated. Other evidence that the species $Cr_nO_{3n-2}^+$ do not arise from fragmentation of the corresponding Cr_nO_{3n} molecules was found in the results of a series of double cell experiments. Column 1 of Table X is a list of the ratio I^+_{468}/I^+_{500} vs temperature of the upper cell (the lower cell was held at a fixed temperature). Similar lists for the ion ratios I^+_{368}/I^+_{400} and I^+_{300}/I^+_{268} during double cell experiments appear in Table X and XI. All of these data demonstrate that the species $Cr_nO_{3n-2}^+$ do not arise from fragmentation of the respective molecules of the type Cr_nO_{3n}: The data from the cell exhaustion experiment and the double cell experiments are considered to be much more reliable evidence of the parent-fragment relationships than appearance potentials or ionization efficience curves.

4. Heats of vaporization

As noted in the abstract and in Table XXXI the heats of sublimation of the various ions differed appreciably, which indicates that they are not correlated. The clearest case is for the ion pair $(CrO_3)^+_5$ - $Cr_5O^+_{13}$ for which the heats of sublimation were found to be 36.35 ± 1.10 and 42.89 ± 0.71 respectively.

As in any mass spectrometric study, the possibility of strongly temperature-dependent fragmentation cross-sections exists. The above species-fragment identifications have been made by assuming that the

fragmentation cross-sections are not highly temperature dependent.

B. Cadmium

The ion intensity of Cd^{114+} was measured from 431.5°K to 513.6°K with the same Knudsen cell and temperature measurement system used in the measurement of the partial pressures of the chromium-containing ions. The measured second-law heat of sublimation of Cd was 26.70 ± 0.25 kcal/mol, in good agreement with the following values selected by Hultgren[25]:

$$\Delta H^{o}_{400} = 26.580 \pm 0.150 \text{ kcal/mol.}$$

$$\Delta H^{o}_{500} = 26.413 \pm 0.150 \text{ kcal/mol.}$$

The direct verification of the system by measurement of the heat of sublimation of cadmium lends considerable confidence to the temperature-dependent parts of the partial pressure equations reported below.

C. Partial Pressures of Chromium-Containing Molecules

The following equations for the partial pressures of the various chromium-containing molecules are based on ion intensity measurements made from 415.1°K to 468.1°K:

$$\log P_{(CrO_3)_5} \text{ (atm)} = -\frac{(7.943 \pm 0.240) \times 10^3}{T} + (15.02 \pm 0.54)$$

$$\log P_{Cr_5O_{13}} \text{ (atm)} = -\frac{(9.373 \pm 0.154) \times 10^3}{T} + (19.13 \pm 0.35)$$

$$\log P_{(CrO_3)_4} \text{ (atm)} = -\frac{(6.849 \pm 0.150) \times 10^3}{T} + (13.70 \pm 0.34)$$

$$\log P_{Cr_4O_{10}} \text{ (atm)} = -\frac{(7.983 \pm 0.124) \times 10^3}{T} + (17.17 \pm 0.28)$$

$$\log P_{(CrO_3)_3} \text{ (atm)} = -\frac{(6.836 \pm 0.152) \times 10^3}{T} + (13.08 \pm 0.34)$$

$$\log P_{Cr_3O_7} \text{ (atm)} = -\frac{(7.465 \pm 0.095) \times 10^3}{T} + (15.09 \pm 0.22)$$

The pressures are dependent, of course, on estimated relative cross sections. The methods of estimation which were used are usually claimed to be reliable within a factor of two or three, but the claim is imperfectly supported.

D. Behavior of Oxygen

In this system, oxygen is not even approximately in equilibrium with the solid. The measured O_2 pressure is less than 10^{-10} times the calculated pressure. Futhermore, oxygen is probably not in equilibrium with the various chromium-containing gaseous species, although they appear to be in equilibrium with each other, since their relative pressures gave good fits to equilibrium constants expressions during cell exhaustion experiments in which ion intensities decreased by more than a factor of 10.

ACKNOWLEDGEMENTS

I would like to express my appreciation to Professor Alan W. Searcy for his guidance and for making laboratory space and equipment available for this work.

This work was performed under the auspices of the United States Atomic Energy Commission.

REFERENCES

1. R. J. Ackermann and R. J. Thorn, Vaporization of Oxides, in Progress in Ceramic Science (Pergamon Press, New York, 1961), Vol. I, p.39.
2. R. T. Grimley, R. P. Burns, and M. G. Inghram, J. Chem. Phys. 34, 664 (1961).
3. Ke-Chin Wang, L. H. Draper, V. V. Dadape, and J. L. Margrave, J. Am. Cer. Soc. 43, 509 (1961).
4. D. Caplan and M. Cohen, J. Electrochem. Soc. 108, 438 (1961).
5. O. Glemser, A. Muller, and U. Stocker, z.a.a.c. 333, 25 (1964).
6. R. J. Ackermann, R. J. Thorn, C. Alexander, and M. Tetenbaum, J. Phys. Chem. 64, 350 (1960).
7. R. J. Ackermann and E. G. Rauh, J. Phys. Chem. 67, 2596 (1963).
8. H. Schafer and K. Rinke, Naturforsch. 20b, 702 (1965).
9. J. D. McDonald and J. L. Margrave, J. Inorg. Nucl. Chem. 30, 665 (1968).
10. L. Brewer, Chem. Revs. 52, 1 (1953).
11. C. A. Neugebauer and J. L. Margrave, J. Phys. Chem. 61, 1429 (1957).
12. O. Glemser and A. Muller, z.a.a.c. 334, 150 (1964).
13. J. Berkowitz, M. G. Inghram, and W. A. Chupka, J. Chem. Phys. 26 842 (1957).
14. R. P. Burns, G. DeMaria, J. Drowart and R. T. Grimley, J. Chem. Phys. 26, 842 (1957).
15. J. Berkowitz, W. A. Chupka, and M. G. Inghram, J. Chem. Phys. 27, 85 (1957).
16. J. H. Norman and H. G. Staley, J. Chem. Phys. 43, 3804 (1965).
17. C. E. Moore, National Bureau of Standards Circular 467 (U.S.G.P.O., Washington, May 1, 1958).

18. J. W. Warren and C. A. McDowell, Disc. Faraday Soc. 10, 53 (1951).

19. D. D. Wagman, et al., National Bureau of Standards Technical Note 270-3 (U.S.G.P.O., Washington, January 1968).

20. D. P. Stevenson, Disc. Faraday Soc. 10, 35 (1951).

21. R. T. Grimley, Mass Spectrometry, in The Characterization of High Temperature Vapors (John Wiley and Sons, New York, 1967) p. 195.

22. R. M. Reese, V. H. Dibeler, and F. L. Mohler, J. Res. National Bureau of Standards, 46, 79 (1951).

23. J. Berkowitz, H. A. Tasman and W. A. Chupka, J. Chem. Phys. 36, 2170 (1962).

24. W. F. Roeser and S. T. Lonberger, National Bureau of Standards Circular 590 (U.S.G.P.O., Washington, February 6, 1958).

25. R. Hultgren, et al., "Selected Values of Thermodynamic Properties of Metals and Alloys" mimeographed revision sheet for cadmium issued September, 1966 (Department of Mineral Technology, University of California, Berkeley, 1966).

26. R. D. Present, Kinetic Theory of Gases (McGraw-Hill Book Company, Inc., New York, 1958).

27. H. J. M. Bowen, et al., Tables of Interatomic Distances and Configurations in Molecules and Ions, (The Chemical Society, London, 1958).

28. C. E. Wicks and F. E. Block, U. S. Bureau of Mines Bulletin 605, (U.S.G.P.O., Washington, 1963).

29. G. N. Lewis and M. Randall, Thermodynamics, Second Edition revised by K. S. Pitzer and L. Brewer (McGraw-Hill Book Company, Inc., New York, 1961).

30. F. W. Lampe, J. L. Franklin, and F. H. Field, J. Am. Chem. Soc. 79, 546 (1956).

31. J. B. Mann, J. Chem. Phys. 46, 1646 (1967).

32. J. W. Otvos and D. P. Stevenson, J. Am. Chem. Soc. 78, 546 (1956).

33. L. J. Kieffer and G. H. Dunn, Rev. Mod. Phys. 38, 1 (1966).

34. M. G. Inghram and J. Drowart, Mass Spectrometry Applied To High Temperature Chemistry, in Proceedings of International Symposium on High Temperature Technology, Asilomar, Calif., 1959, (McGraw-Hill Book Company, Inc., New York).

APPENDIX A.

ISOTOPIC ABUNDANCES, Cr_n, n = 1 -5.

1. Cr

Mass No.	Isotopic Abundance % of total	% of max.
50	4.31	5.15
52	83.76	100
53	9.55	11.40
54	2.38	2.84

2. Cr_2

Mass No.	Isotopic Abundance % of total	% of max.
100	0.1858	0.264
102	7.220	10.29
103	0.8232	1.17
104	70.362	100
105	15.998	22.8
106	4.899	6.96
107	0.4546	0.645
108	0.0566	0.0805

3. Cr_3

Isotopic Abundance

Mass No.	% of total	% of max.
150	0.0080	0.0135
152	0.4669	0.786
153	0.0532	0.0897
154	9.0846	15.31
155	2.0685	3.49
156	59.397	100
157	20.159	33.95
158	7.3082	12.31
159	1.2294	2.08
160	0.2073	0.349
161	0.0162	0.0273
162	0.0014	0.0024

4. Cr_4

Mass No.	Isotopic Abundance % of total	% of max.
200	$< 10^{-3}$	
202	0.027	
203	0.003	
204	0.784	1.55
205	0.179	0.35
206	10.184	20.18
207	3.471	6.88
208	50.478	100
209	22.464	44.51
210	9.469	18.75
211	2.209	4.38
212	0.466	0.93
213	0.61	0.12
214	0.008	
215	10^{-3}	
216	$< 10^{-3}$	

5. Cr_5

Mass No.	Isotopic Abundance % of total	% of max.
250	1.5×10^{-5}	
252	1.4×10^{-3}	
253	1.7×10^{-4}	
254	0.06	0.14
255	0.01	
256	1.10	2.54
257	0.38	0.88
258	10.74	24.82
259	4.86	11.23
260	43.26	100
261	24.00	55.47
262	11.32	26.16
263	3.30	7.63
264	0.83	1.92
265	0.15	0.35
266	0.02	
267	2.7×10^{-3}	
268	1.5×10^{-4}	
269	10^{-6}	
270	$< 10^{-6}$	

FIGURE CAPTIONS

1. Comparison of Ion currents at high electron energies reported by Schafer and Rinke[8] with the results of this study.
2. Ion currents of M268, M368, and M400 during the constant temperature.
3. Schematic diagram of the double cell.
4. Double cell results. I_{384}/I_{400} vs. difference in temperature between the upper and lower cells. Series E 21.
5. Double cell results. I_{384}/I_{368} vs. difference in temperature between the upper and lower cells. Series E 21 and E 25.
6. Ionization efficiency curves for the principle peaks of $Cr_4O_{10}^+$ (M368), and $(CrO_3)_4^+$ (M400).
7. Double cell results. I_{352}/I_{368} vs. difference in temperature between the upper and lower cells. Series E 21 and E 25.
8. Double cell results. I_{352}/I_{384} vs. difference in temperature between the upper and lower cells. Series E 21.
9. Double cell results. I_{336}/I_{384} vs. difference in temperature between the upper and lower cells. Series E 21 and E 25.
10. Double cell results. I_{336}/I_{384} vs. difference in temperature between upper and lower cells. Series E 21 and E 25.
11. Double cell results. I_{284}/I_{300} vs. difference in temperature between the upper and lower cells. Series E 21 and E 25.
12. Double cell results. I_{284}/I_{268} vs. difference in temperature between the upper and lower cells. Series E 21 and E 25.
13. Ionization efficiency curves for the principle peaks of $Cr_3O_7^+$ (M268) $Cr_3O_8^+$ (M384) and $(CrO_3)_3^+$ (M300).
14. Double cell results. I_{268}/I_{300} vs. difference in temperature between the upper and lower cells. Series C 17.5, E 21, and E 25.

15. Double cell results. I_{252}/I_{268} and I_{252}/I_{300} vs. difference in temperature between the upper and lower cells. Series E 21.
16. Double cell results. I_{252}/I_{268} and I_{252}/I_{300} vs. difference in temperature between the upper and lower cells. Series E 25.
17. Double cell results. I_{236}/I_{268} and I_{236}/I_{300} vs. difference in temperature between the upper and lower cells. Series E 21.
18. Double cell results. I_{236}/I_{268} and I_{236}/I_{300} vs. difference in temperature between the upper and lower cells. Series E 25.
19. Double cell results. I_{184}/I_{268}, I_{184}/I_{300} and I_{184}/I_{368} vs. difference in temperature between the upper and lower cells. Series C 25.
20. Double cell results. I_{168}/I_{268}, I_{168}/I_{300}, and I_{168}/I_{368} vs. difference in temperature between the upper and lower cells. Series E 25.
21. Double cell results. I_{152}/I_{268} and I_{152}/I_{300} vs. difference in temperature between the upper and lower cells. Series E 25.
22. Schematic diagram, Knudsen cell and cell holder.
23. Plot of log $[(I^{+}_{Cd}\ 114)] \times T$ vs. 1/T.
24. Partial pressures of chromium-containing molecules and oxygen in a Knudsen cell containing $CrO_{3(s)}$ vs. 1/T.
25. Total pressure of vapor species in a Knudsen cell containing $CrO_{3(s)}$ vs. 1/T.
26. Extrapolated differences plot for the principle peaks of the ion pair $(CrO_3)^{+}_{4}$ - $Cr_4O^{+}_{10}$.
27. Extrapolated differences plot for the principle peaks of the ion pair $(CrO_3)^{+}_{3}$ - $Cr_3O^{+}_{7}$.

28. Extrapolated differences plot for the principle peaks of the ion pair $(CrO_3)_5^+ - Cr_5O_{13}^+$.

29. Extrapolated differences plot for the principle peaks of the ion pair $(CrO_3)_3^+ - (CrO_3)_4^+$.

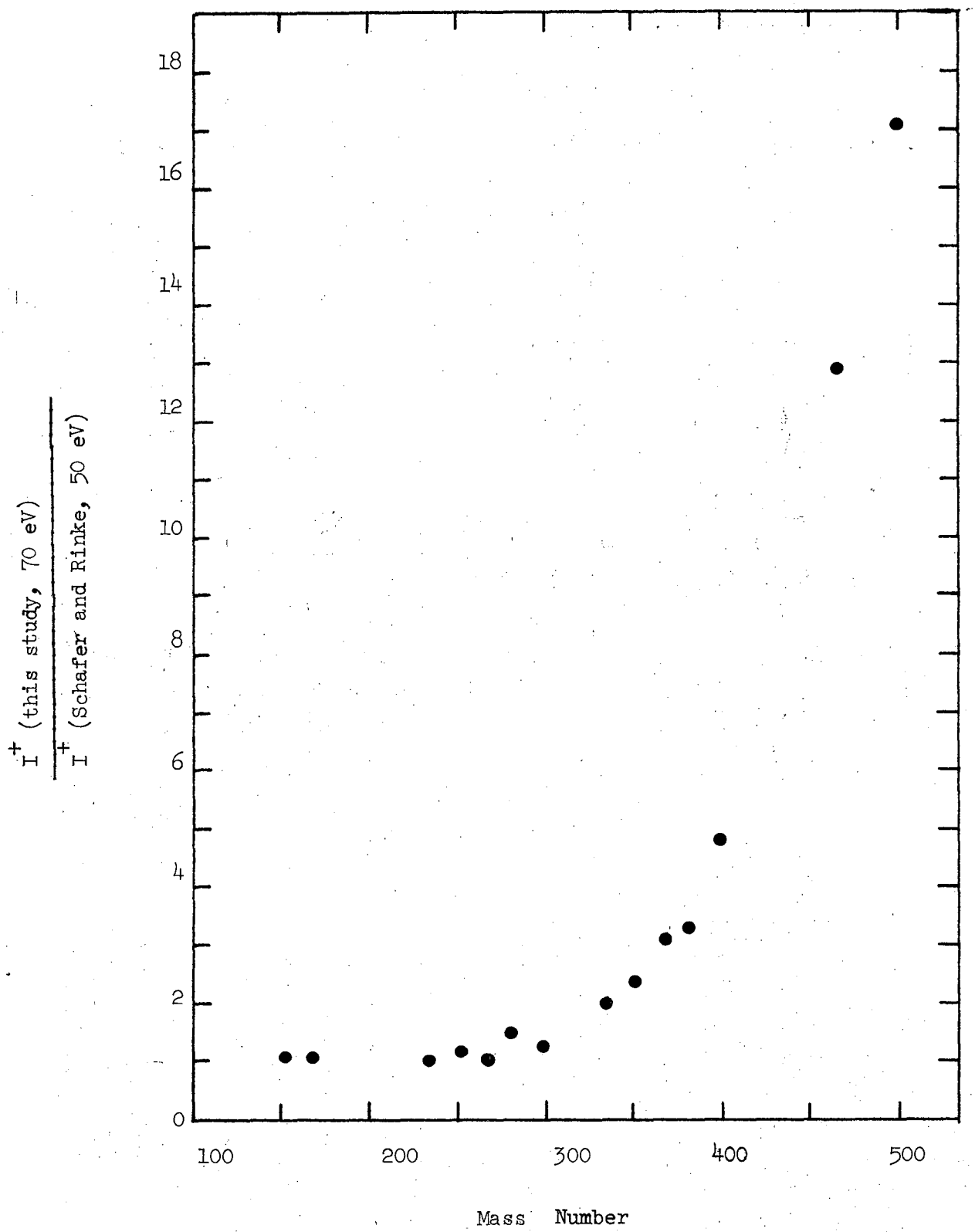
18
16
14
12
10
8
6
4
2
0
100
200
300
400
500
Mass Number
$\frac{I^+ \text{ (this study, 70 eV)}}{I^+ \text{ (Schafer and Rinke, 50 eV)}}$

Figure 1

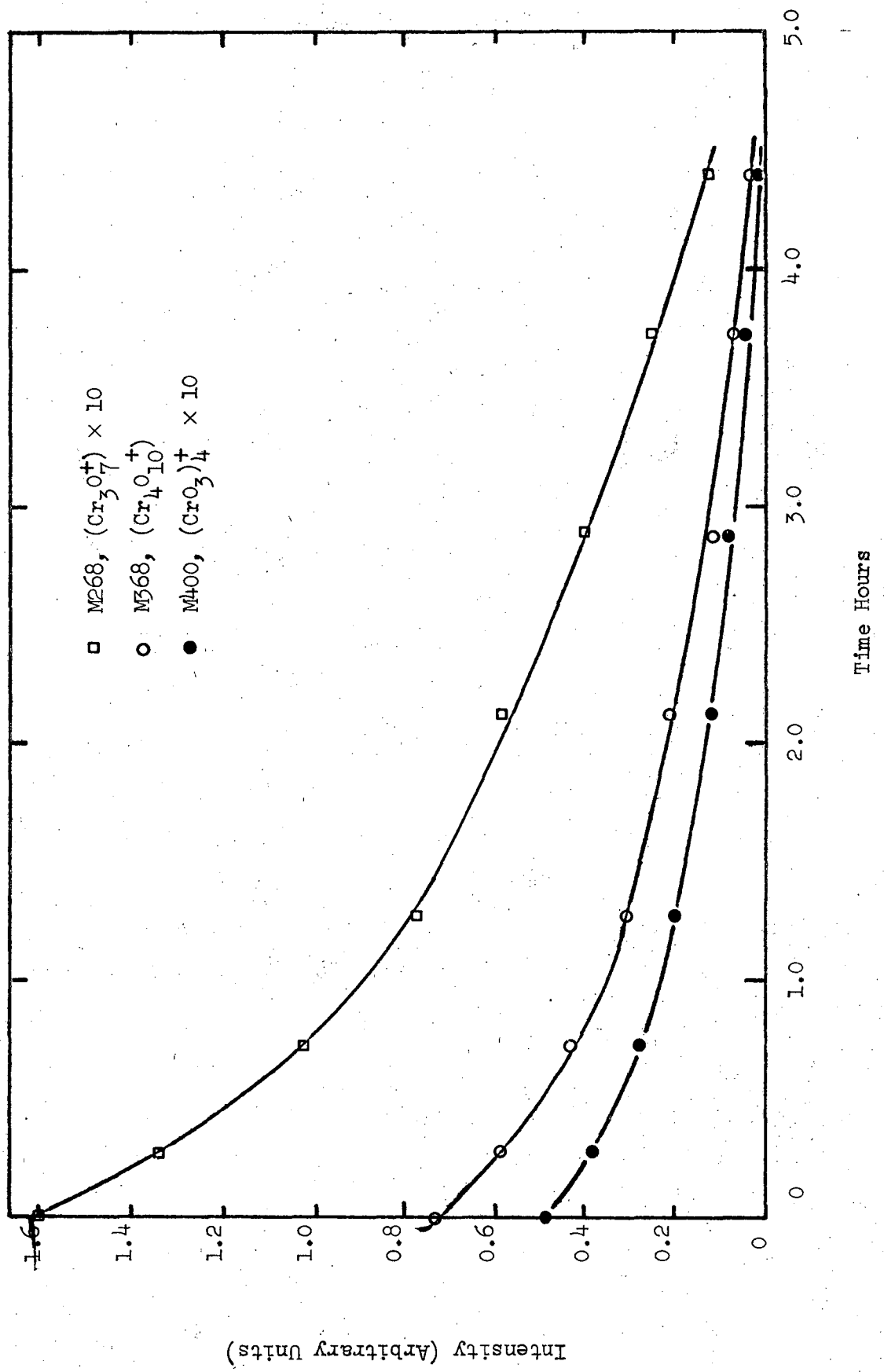
M268, $(Cr_3O_7^+)$ × 10
M368, $(Cr_4O_{10}^+)$
M400, $(CrO_3)_4^+$ × 10
Time Hours
Intensity (Arbitrary Units)
0
1.0
2.0
3.0
4.0
5.0
0.2
0.4
0.6
0.8
1.0
1.2
1.4
1.6

Figure 2

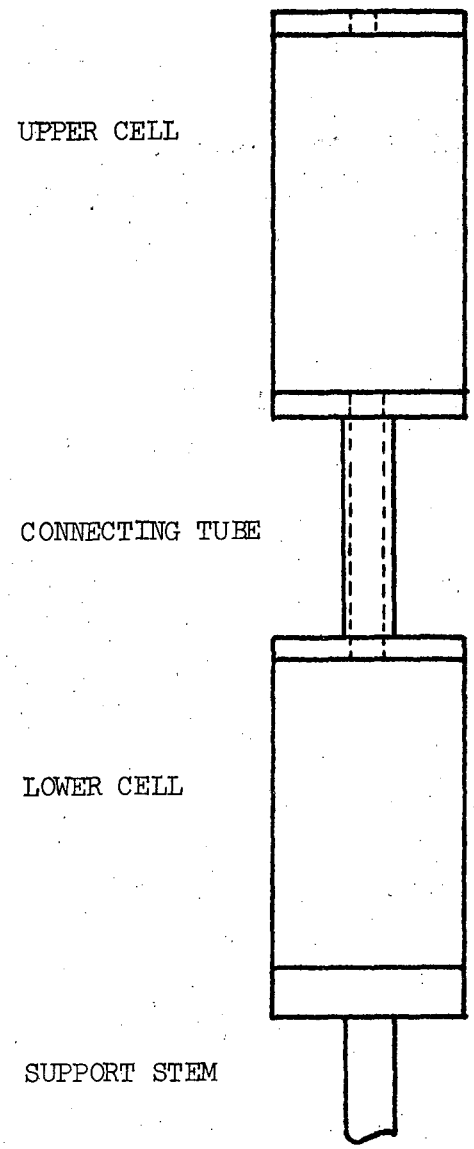

Figure 3

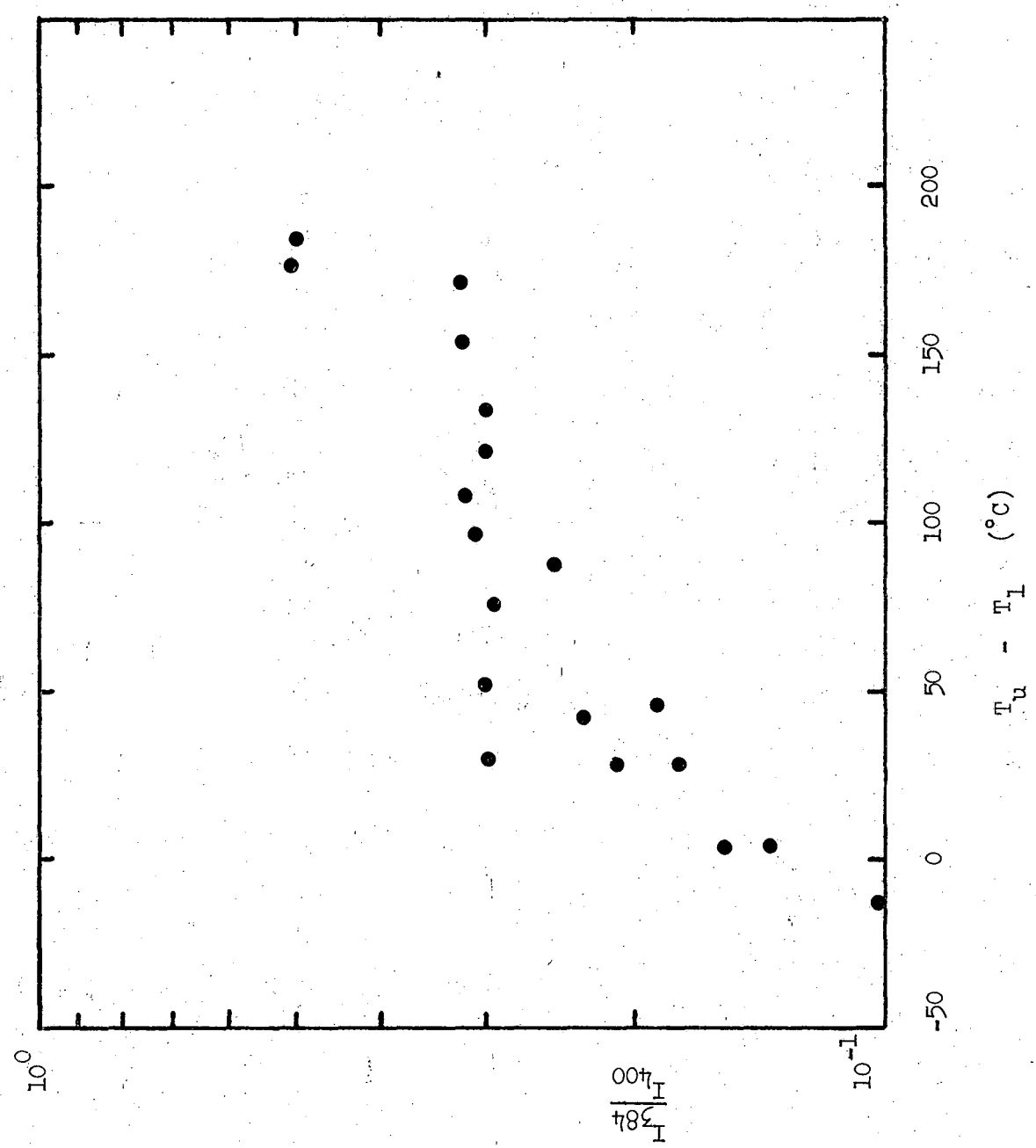

Figure 4

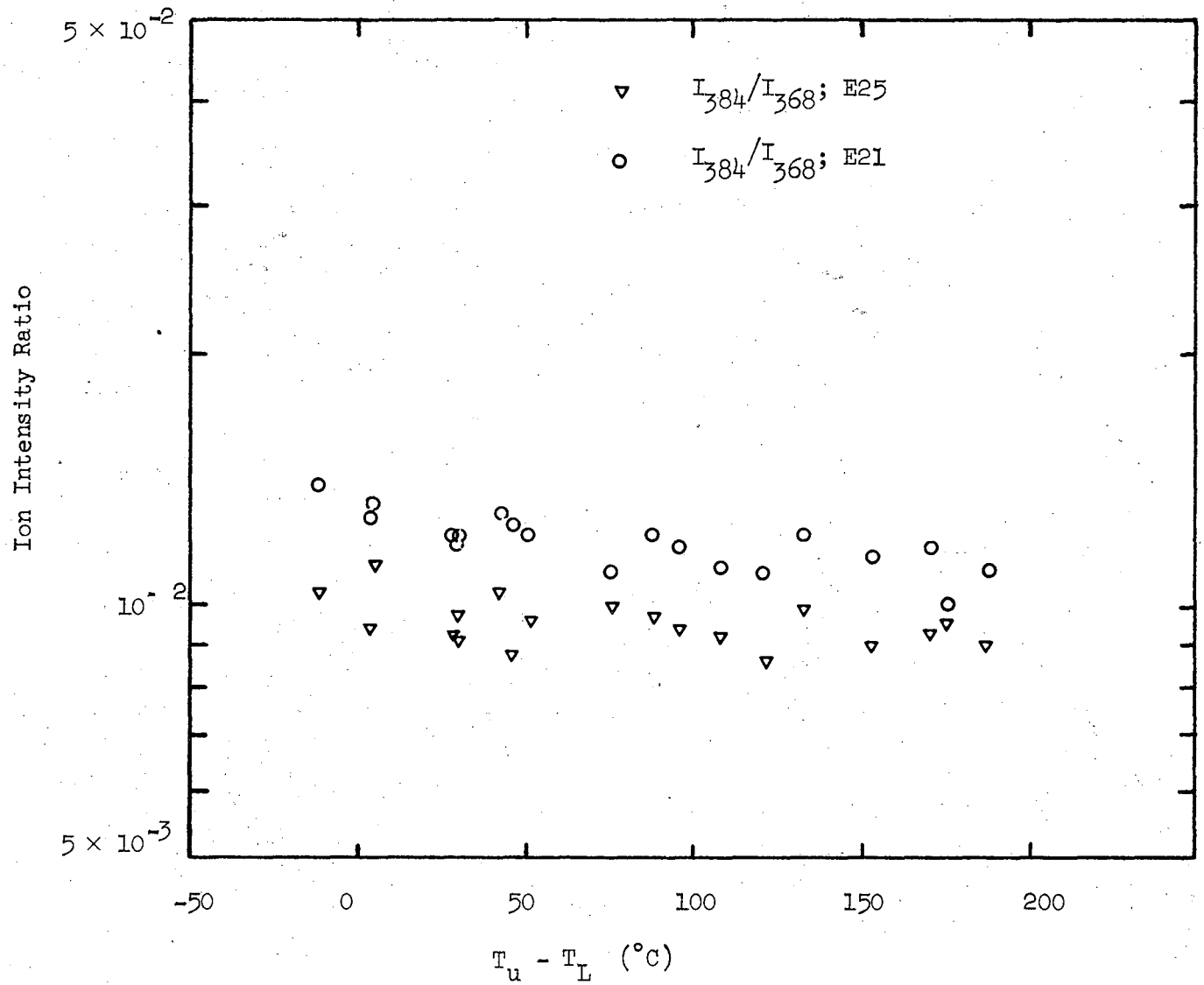
I_{384}/I_{368}; E25
I_{384}/I_{368}; E21
Ion Intensity Ratio
5×10^{-2}
10^{-2}
5×10^{-3}
-50
0
50
100
150
200
$T_u - T_L$ (°C)

Figure 5

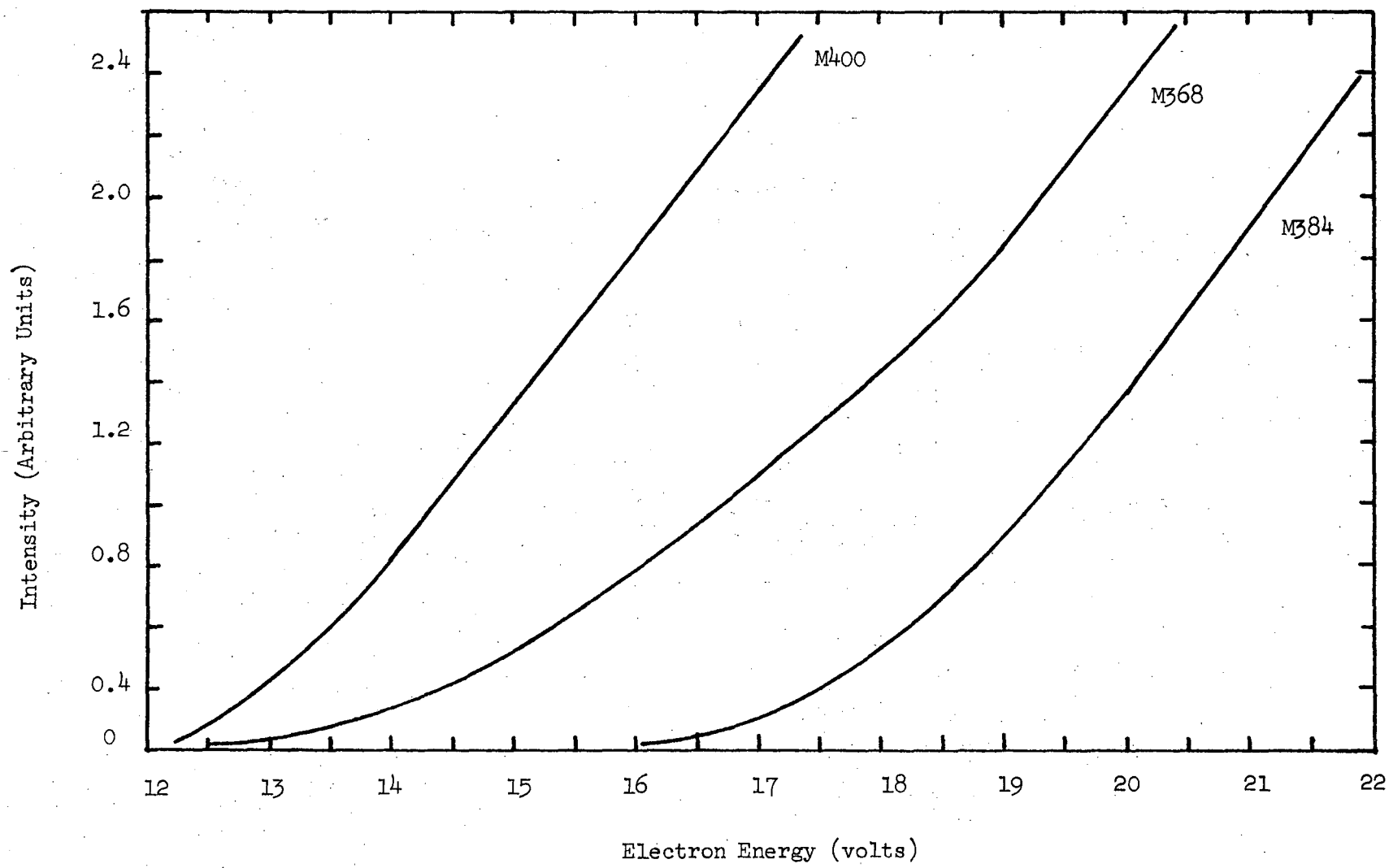
M400
M368
M384
2.4
2.0
1.6
1.2
0.8
0.4
0
Intensity (Arbitrary Units)
12
13
14
15
16
17
18
19
20
21
22
Electron Energy (volts)

Figure 6

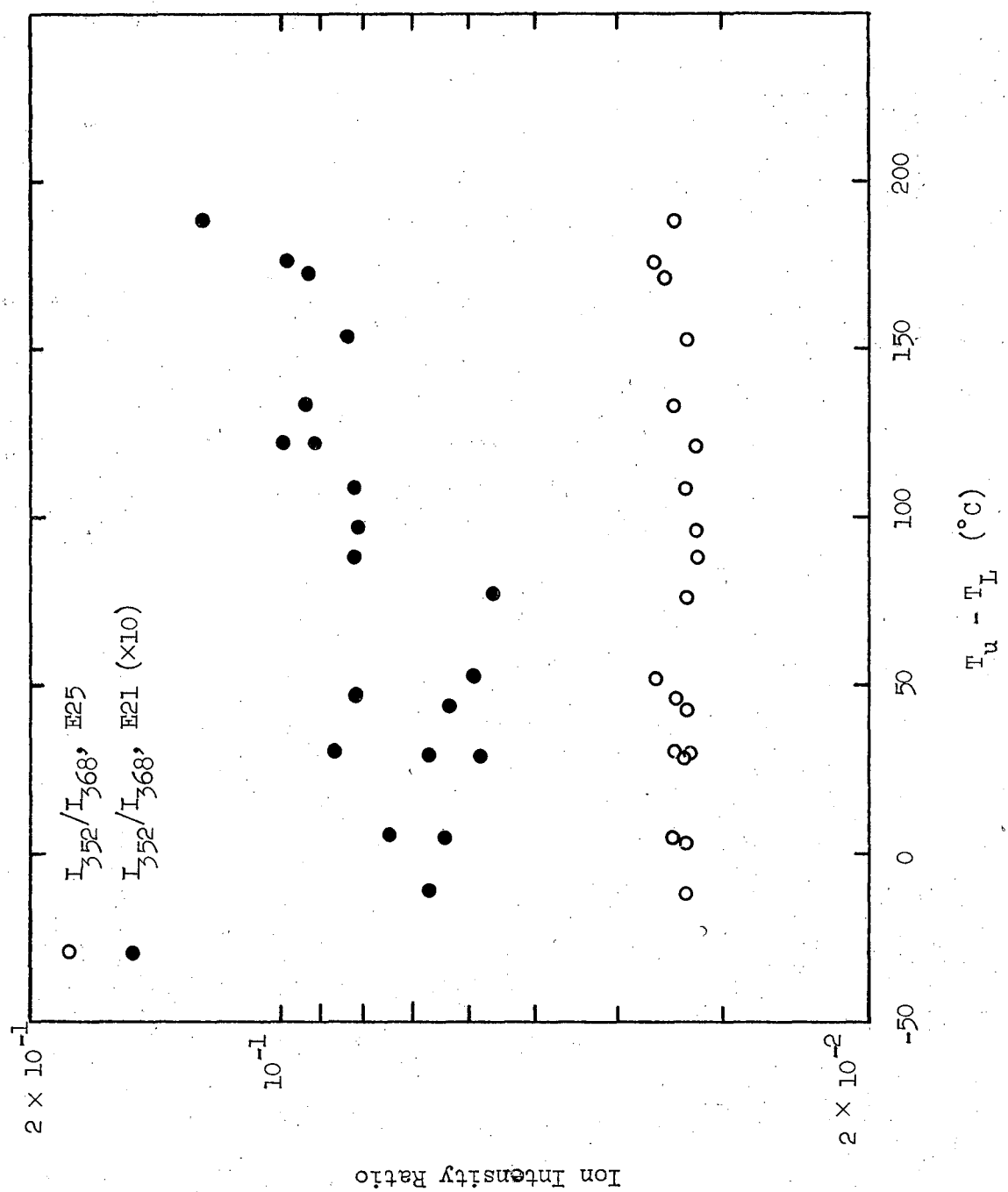
I_{352}/I_{368}, E25
I_{352}/I_{368}, E21 (×10)
2×10^{-1}
10^{-1}
2×10^{-2}
Ion Intensity Ratio
-50
0
50
100
150
200
$T_u - T_L$ (°C)

Figure 7

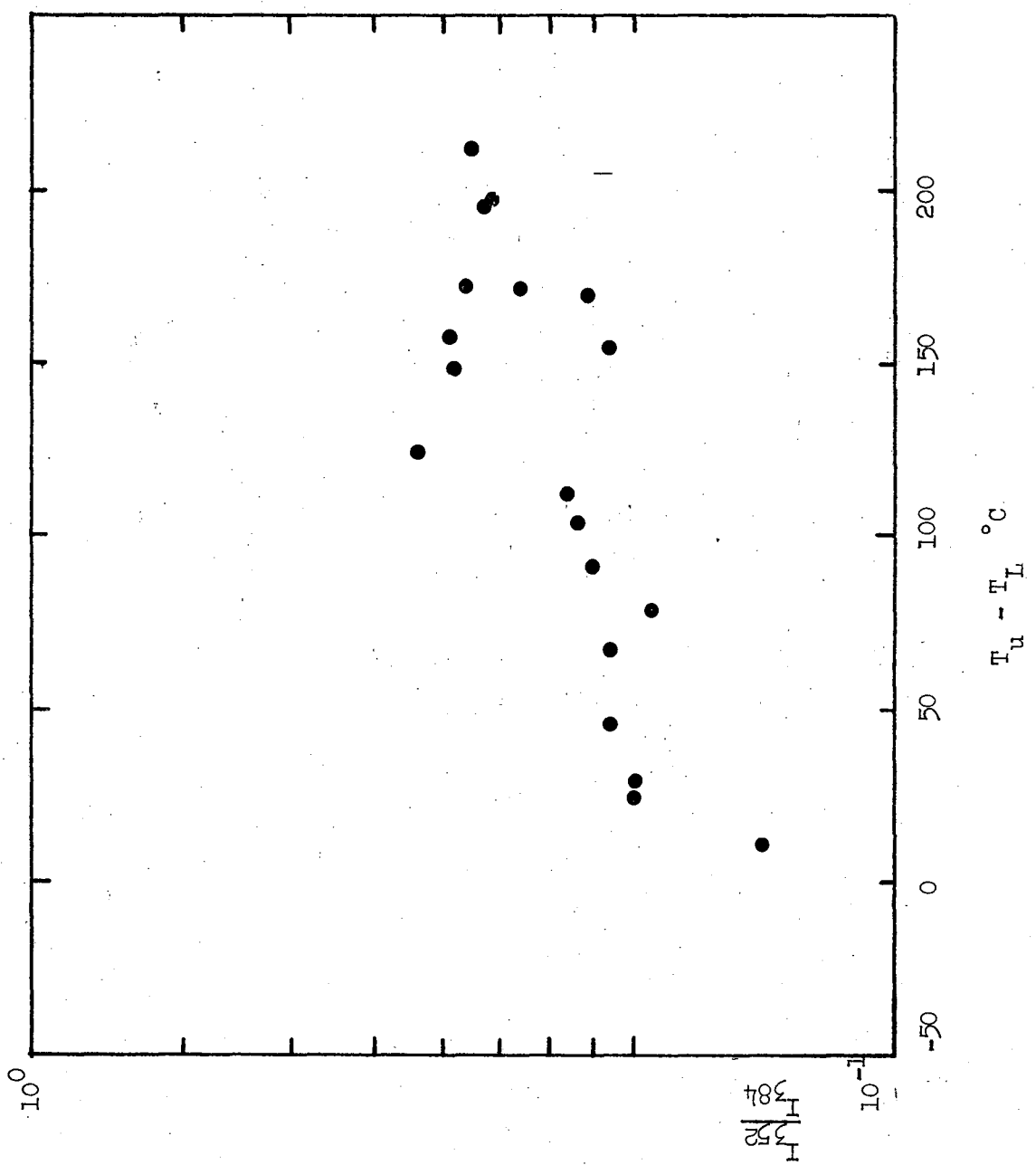

Figure 8

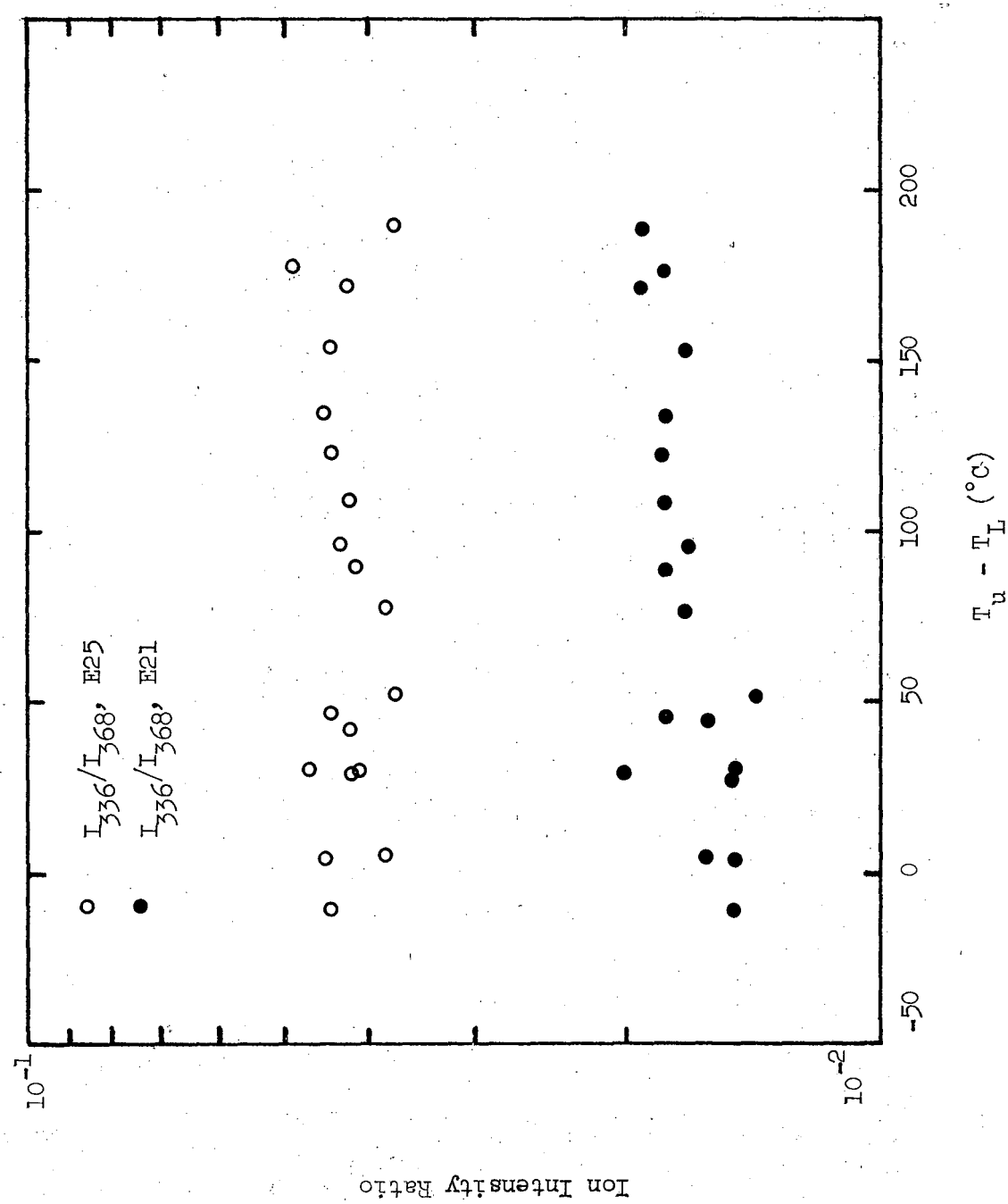
I_{336}/I_{368}, E25
I_{336}/I_{368}, E21
10^{-1}
10^{-2}
Ion Intensity Ratio
-50
0
50
100
150
200
$T_u - T_L$ (°C)

Figure 9

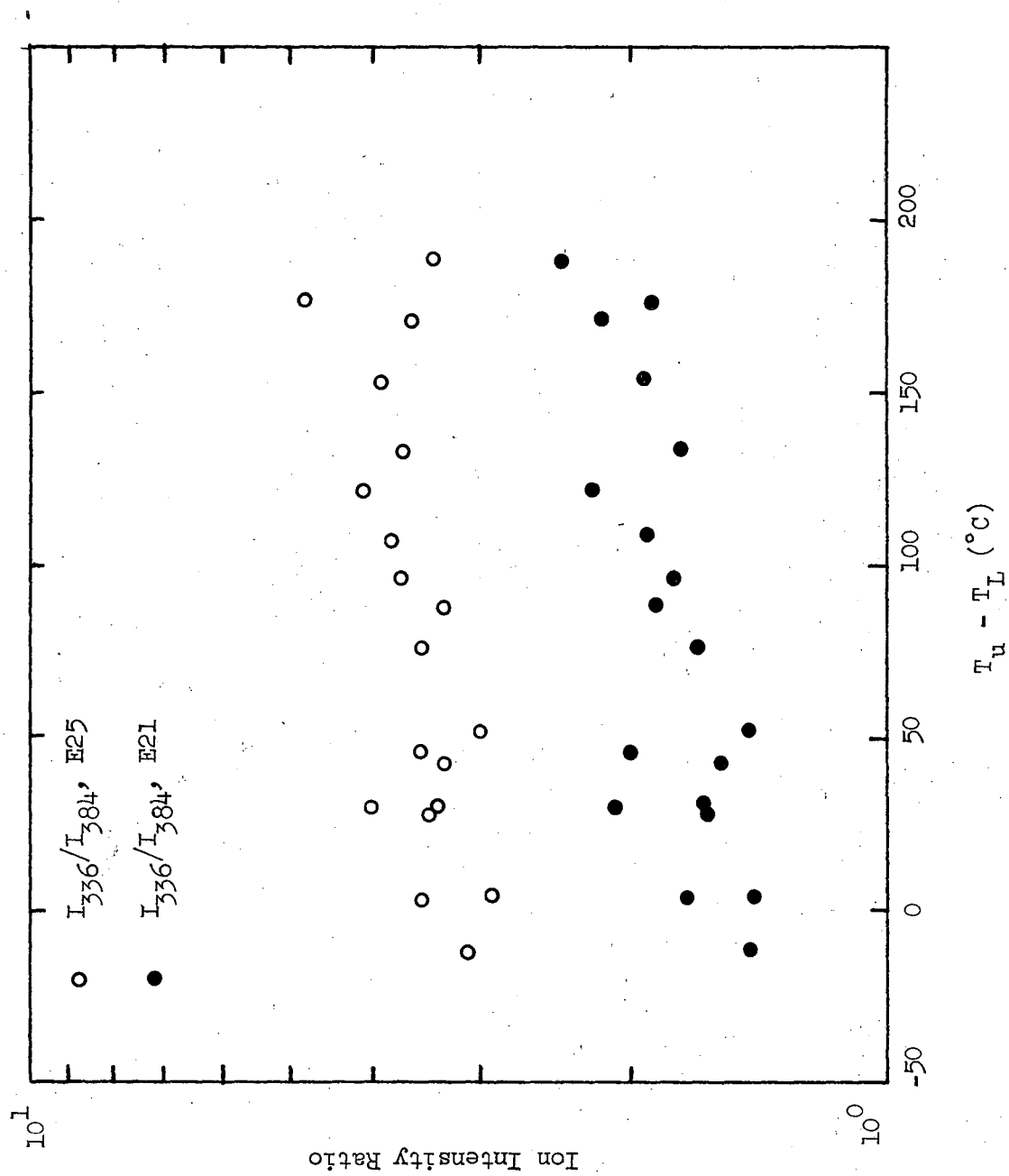
I_{336}/I_{384}, E25
I_{336}/I_{384}, E21
10^1
10^0
Ion Intensity Ratio
-50
0
50
100
150
200
$T_u - T_L$ (°C)

Figure 10

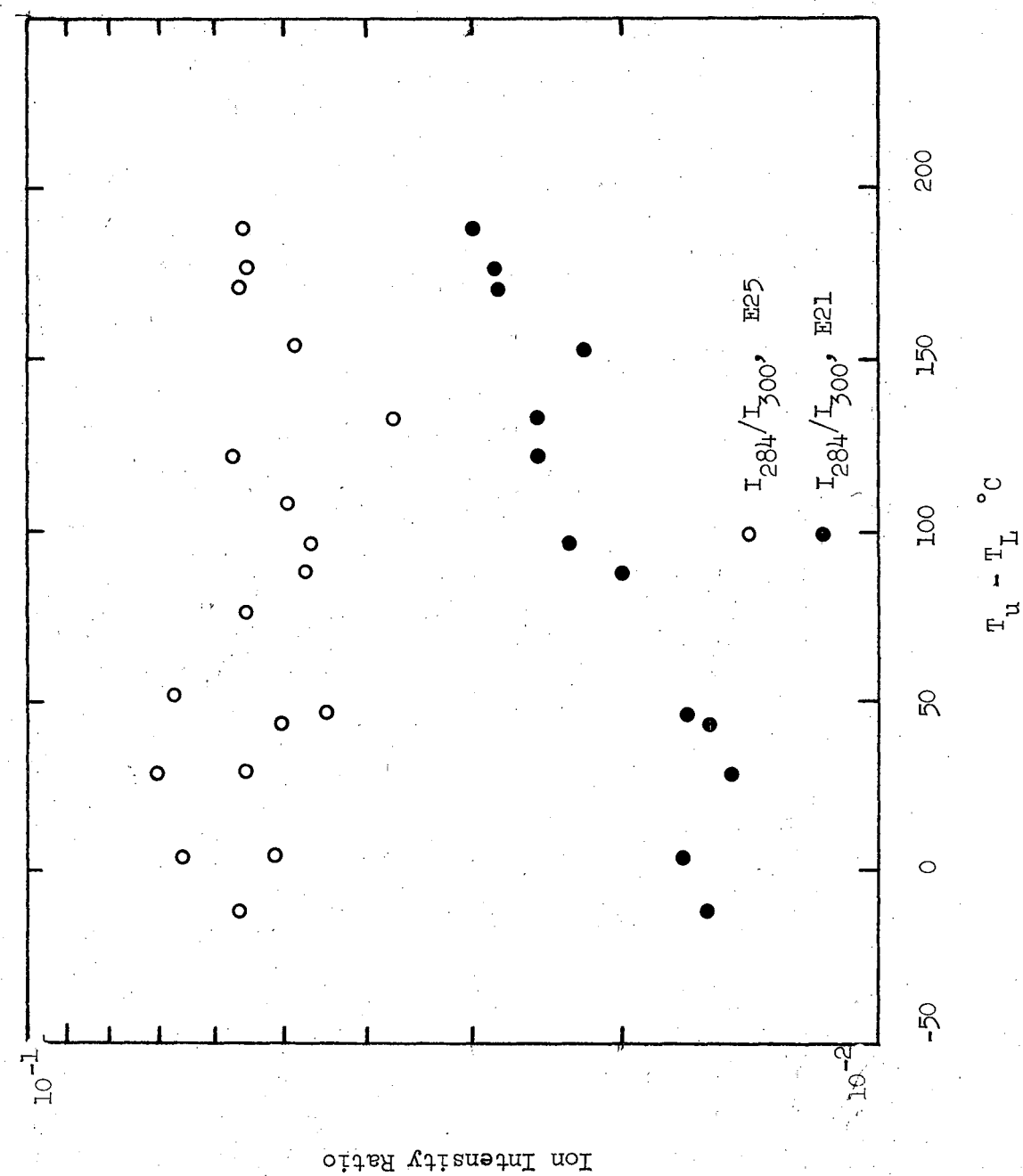
Ion Intensity Ratio
10^{-1}
10^{-2}
-50
0
50
100
150
200
$T_u - T_L$ °C
I_{284}/I_{300}, E25
I_{284}/I_{300}, E21

Figure 11

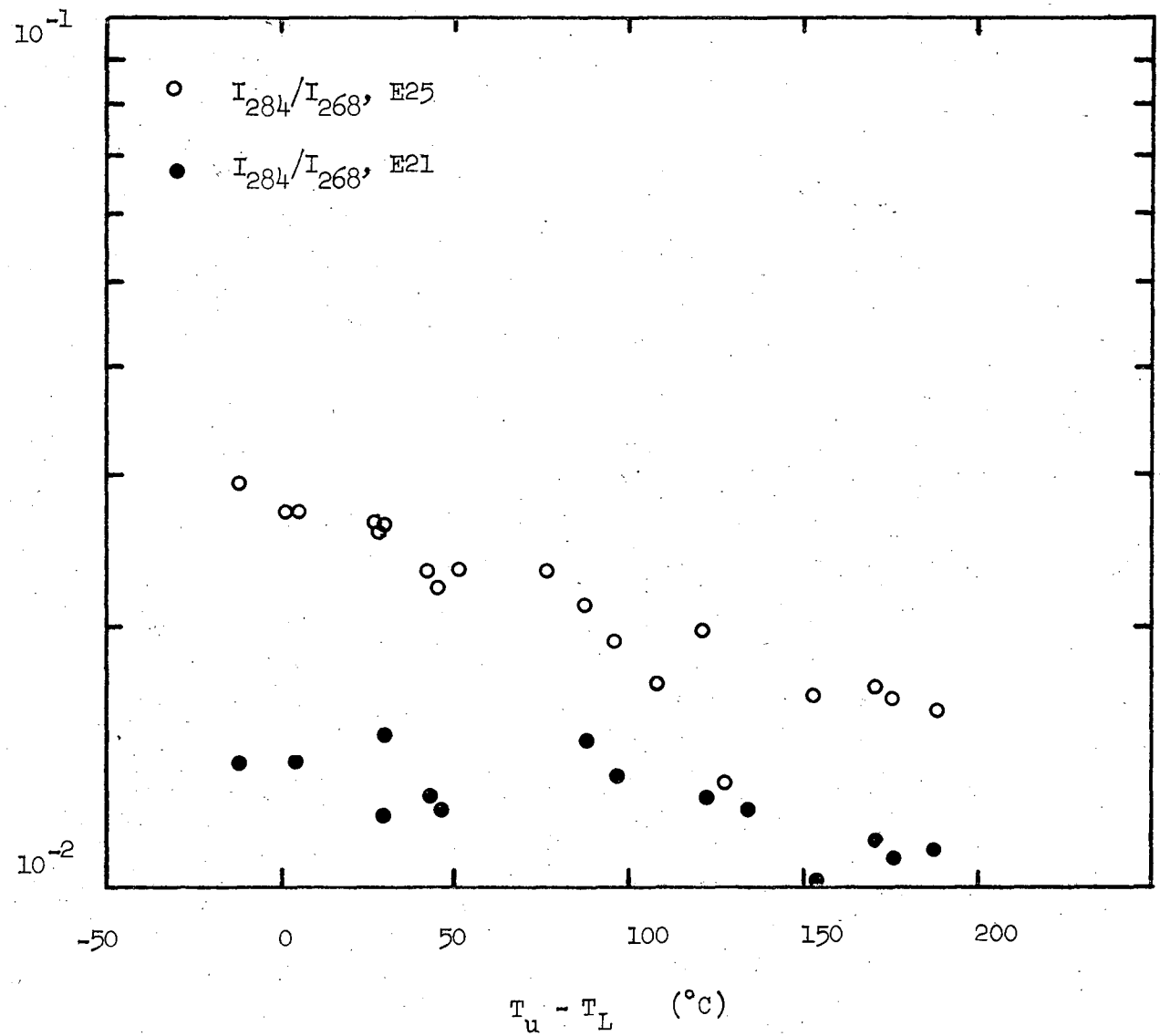
10^{-1}
10^{-2}
I_{284}/I_{268}, E25
I_{284}/I_{268}, E21
Ion Intensity Ratio
-50
0
50
100
150
200
$T_u - T_L$ (°C)

Figure 12

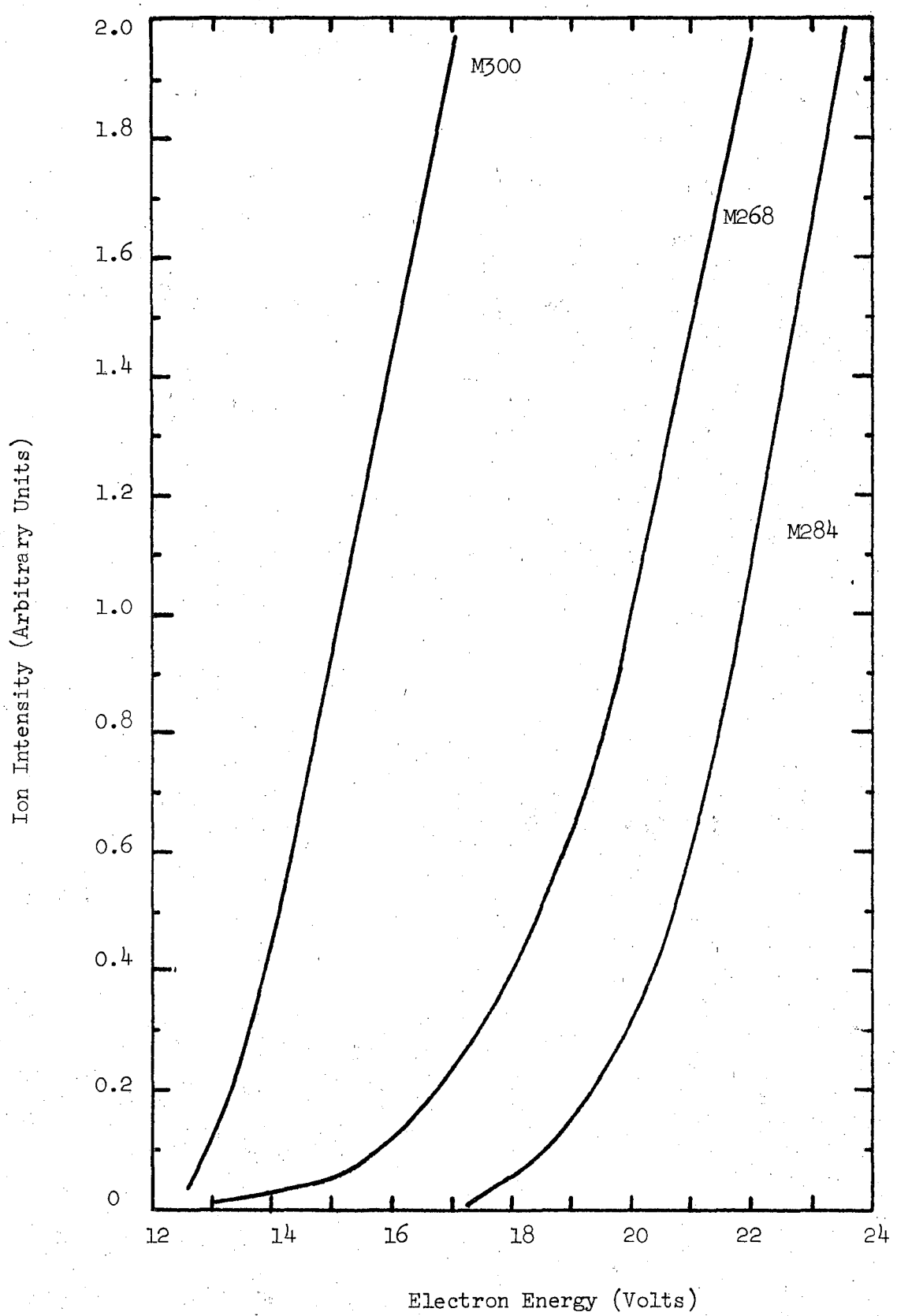
2.0
1.8
1.6
1.4
1.2
1.0
0.8
0.6
0.4
0.2
0
Ion Intensity (Arbitrary Units)
M300
M268
M284
12
14
16
18
20
22
24
Electron Energy (Volts)

Figure 13

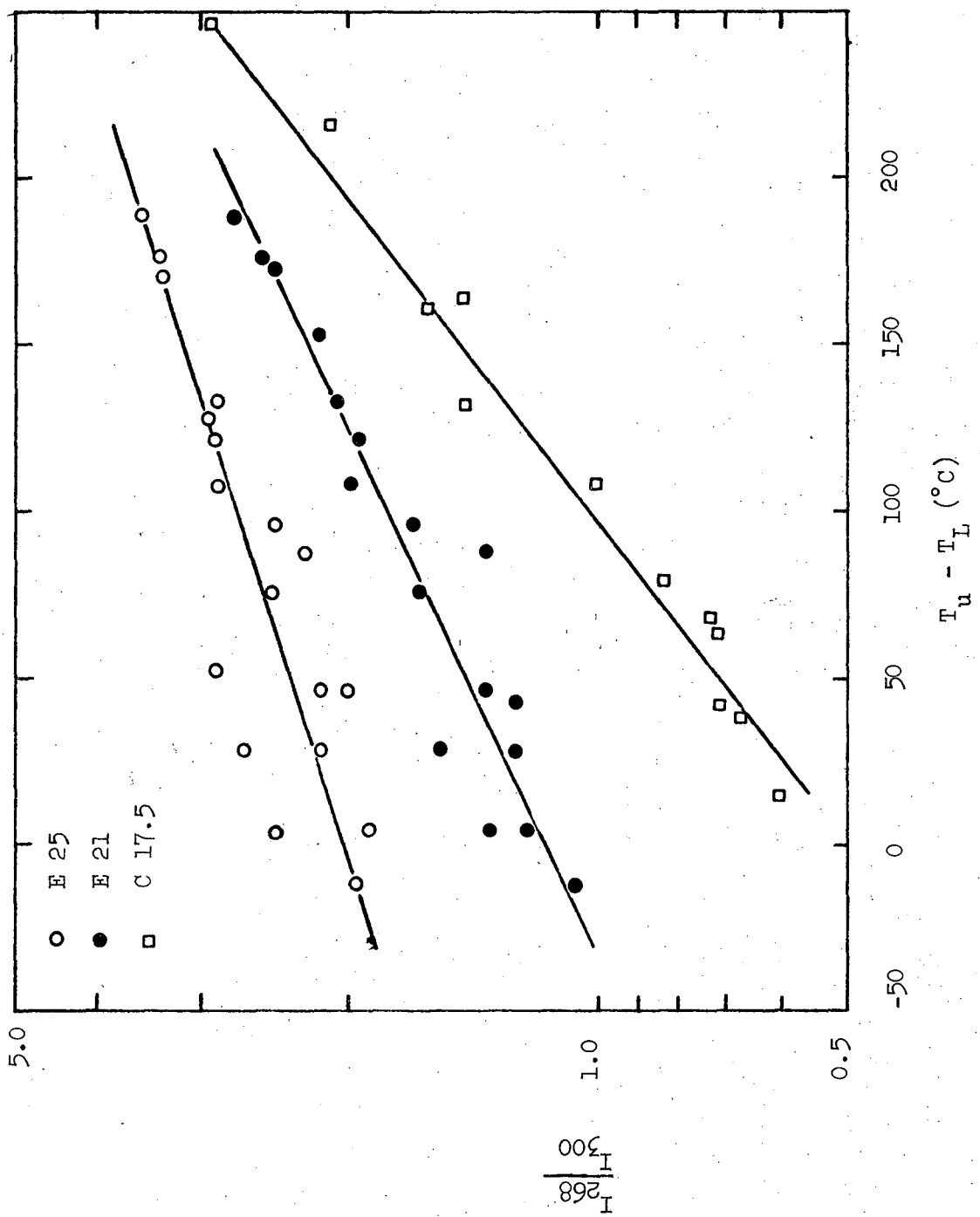

Figure 14

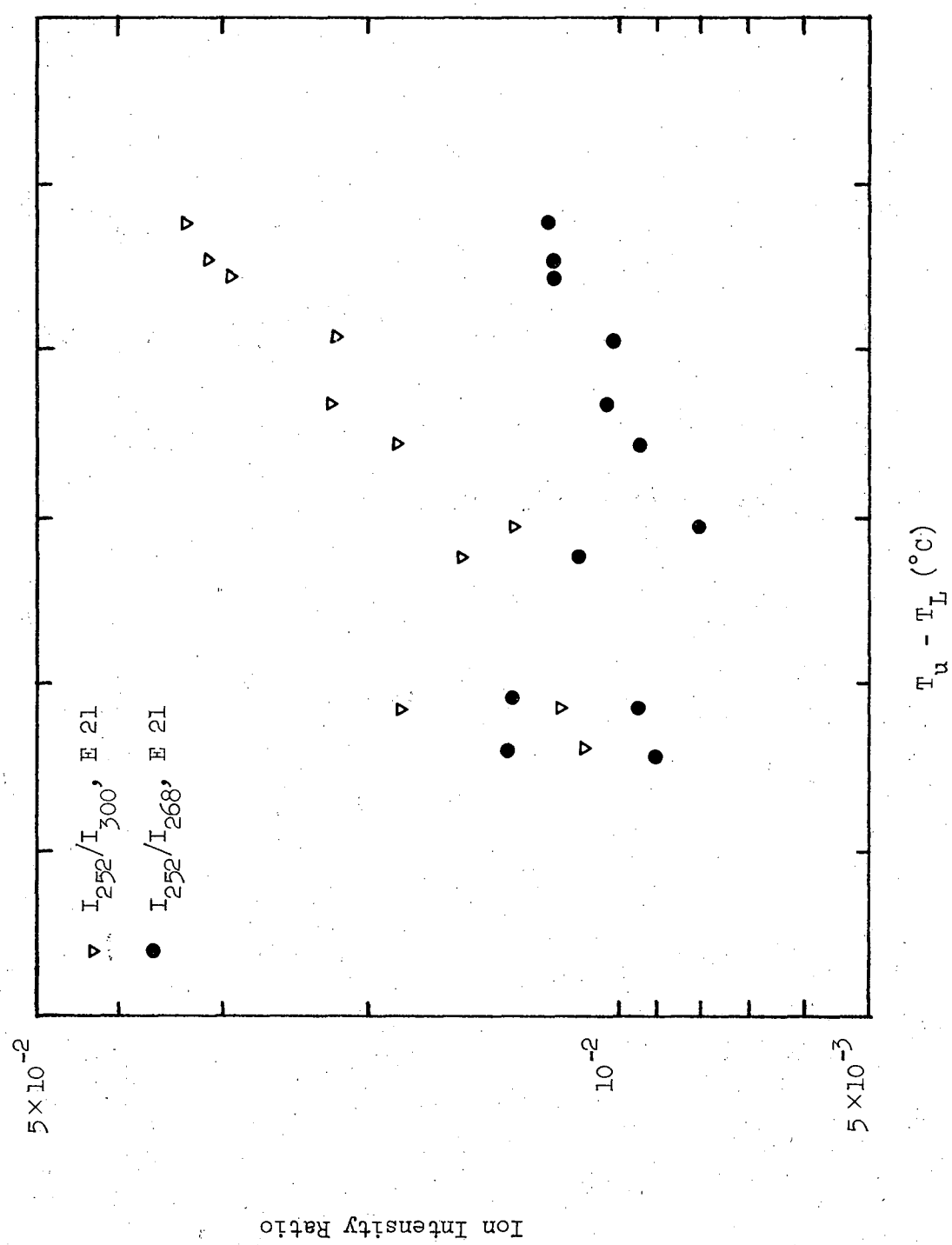
I_{252}/I_{300}, E 21
I_{252}/I_{268}, E 21
5×10^{-2}
10^{-2}
5×10^{-3}
Ion Intensity Ratio
$T_u - T_L$ (°C)

Figure 15

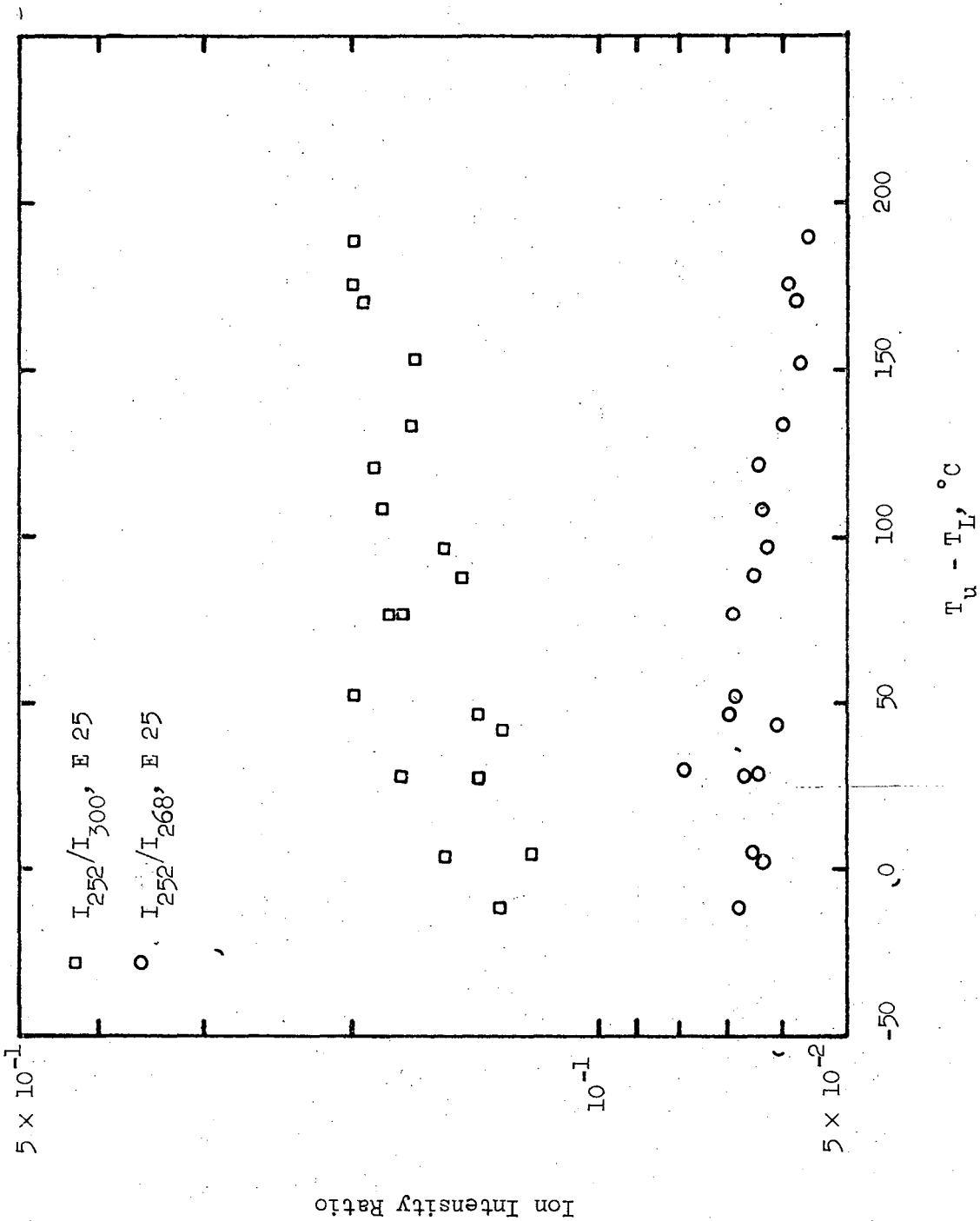
I_{252}/I_{300}, E 25
I_{252}/I_{268}, E 25
5×10^{-1}
10^{-1}
5×10^{-2}
Ion Intensity Ratio
-50
0
50
100
150
200
$T_u - T_L$, °C

Figure 16

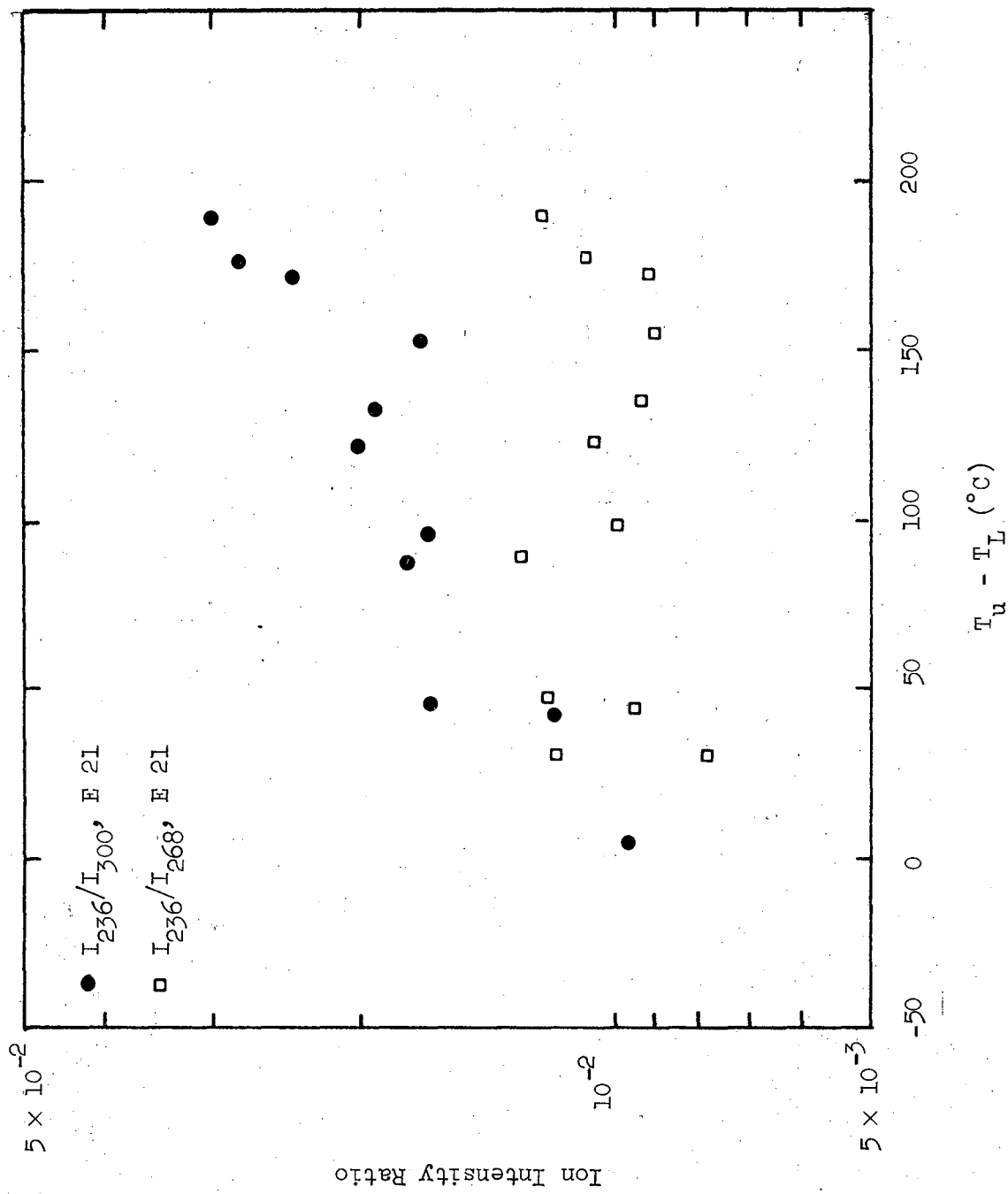
I_{236}/I_{300}, E 21
I_{236}/I_{268}, E 21
5×10^{-2}
10^{-2}
5×10^{-3}
Ion Intensity Ratio
-50
0
50
100
150
200
$T_u - T_L$ (°C)

Figure 17

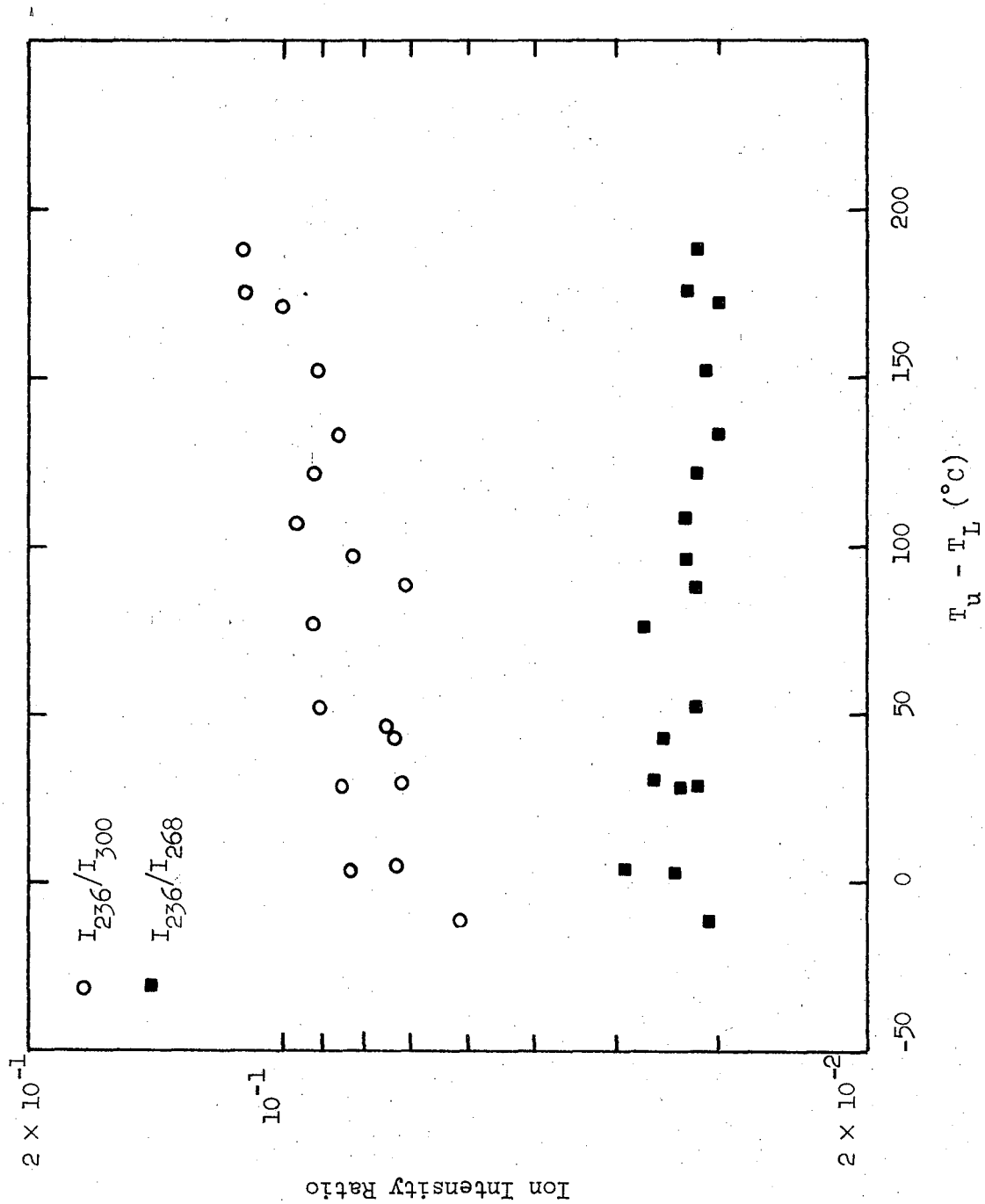
Ion Intensity Ratio
2 × 10^-1
10^-1
2 × 10^-2
-50
0
50
100
150
200
T_u - T_L (°C)
I236/I300
I236/I268

Figure 18

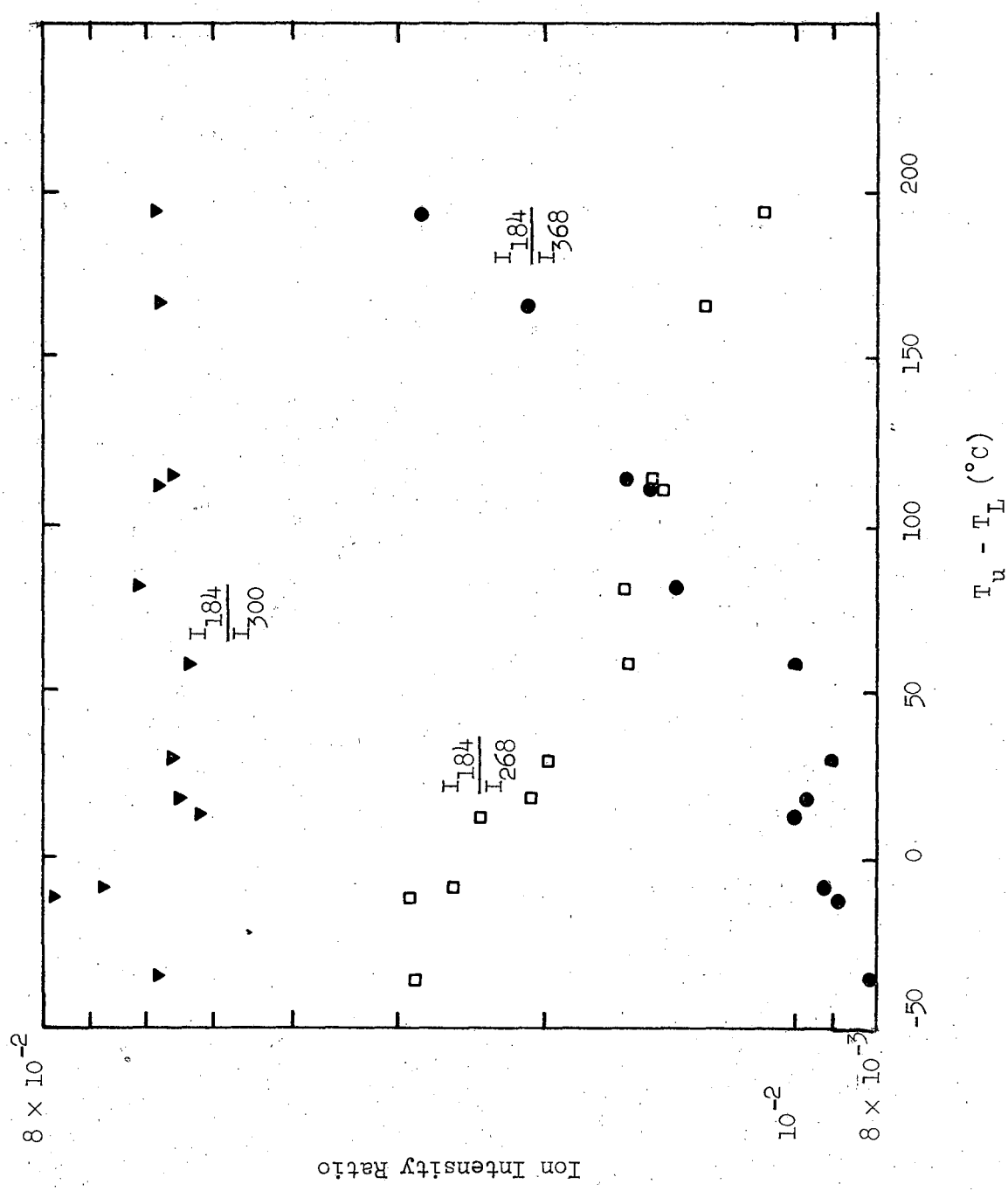
Ion Intensity Ratio
8 × 10^-2
10^-2
8 × 10^-3
-50
0
50
100
150
200
T_u - T_L (°C)
I184/I300
I184/I268
I184/I368

Figure 19

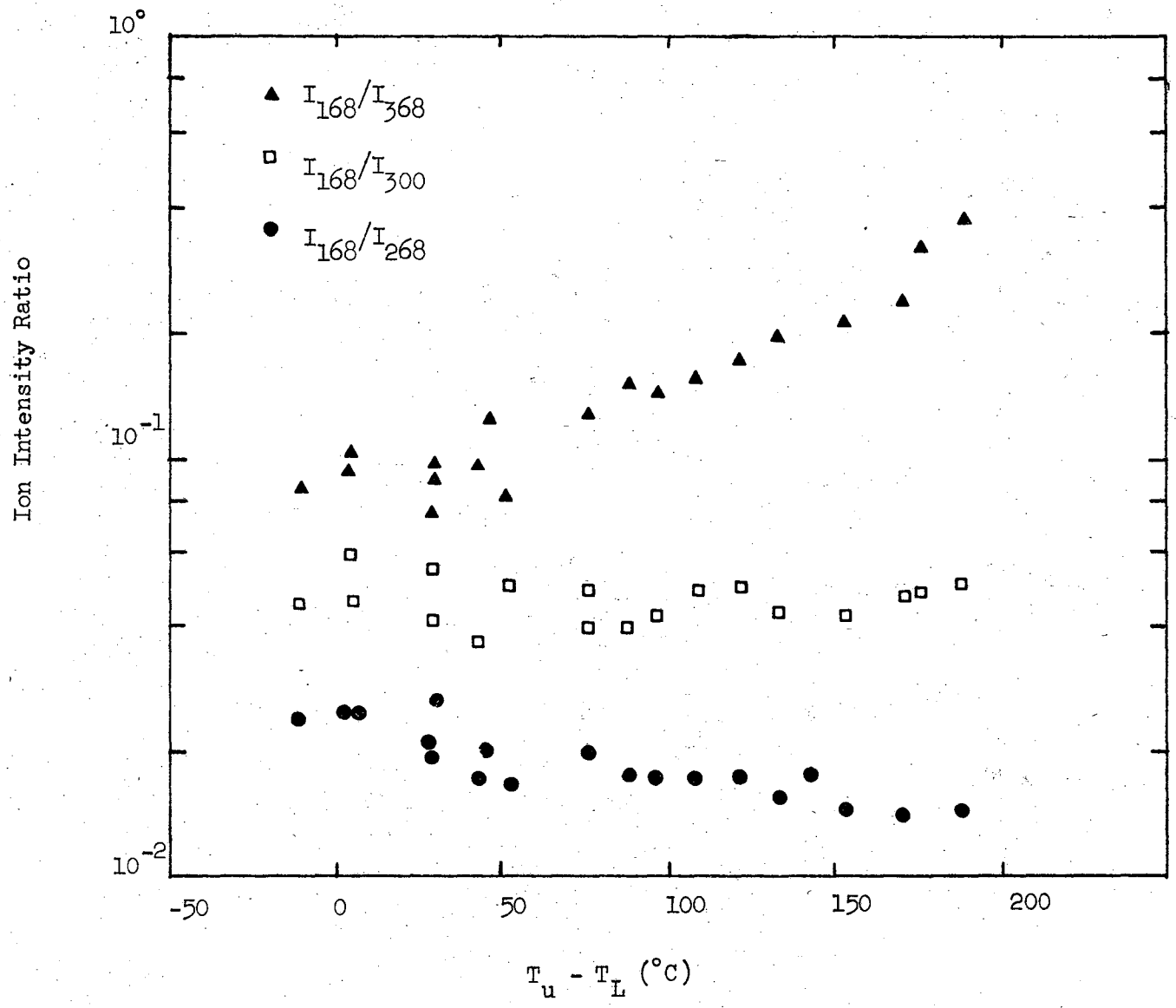
10^{0}
10^{-1}
10^{-2}
Ion Intensity Ratio
I_{168}/I_{368}
I_{168}/I_{300}
I_{168}/I_{268}
-50
0
50
100
150
200
$T_u - T_L$ (°C)

Figure 20

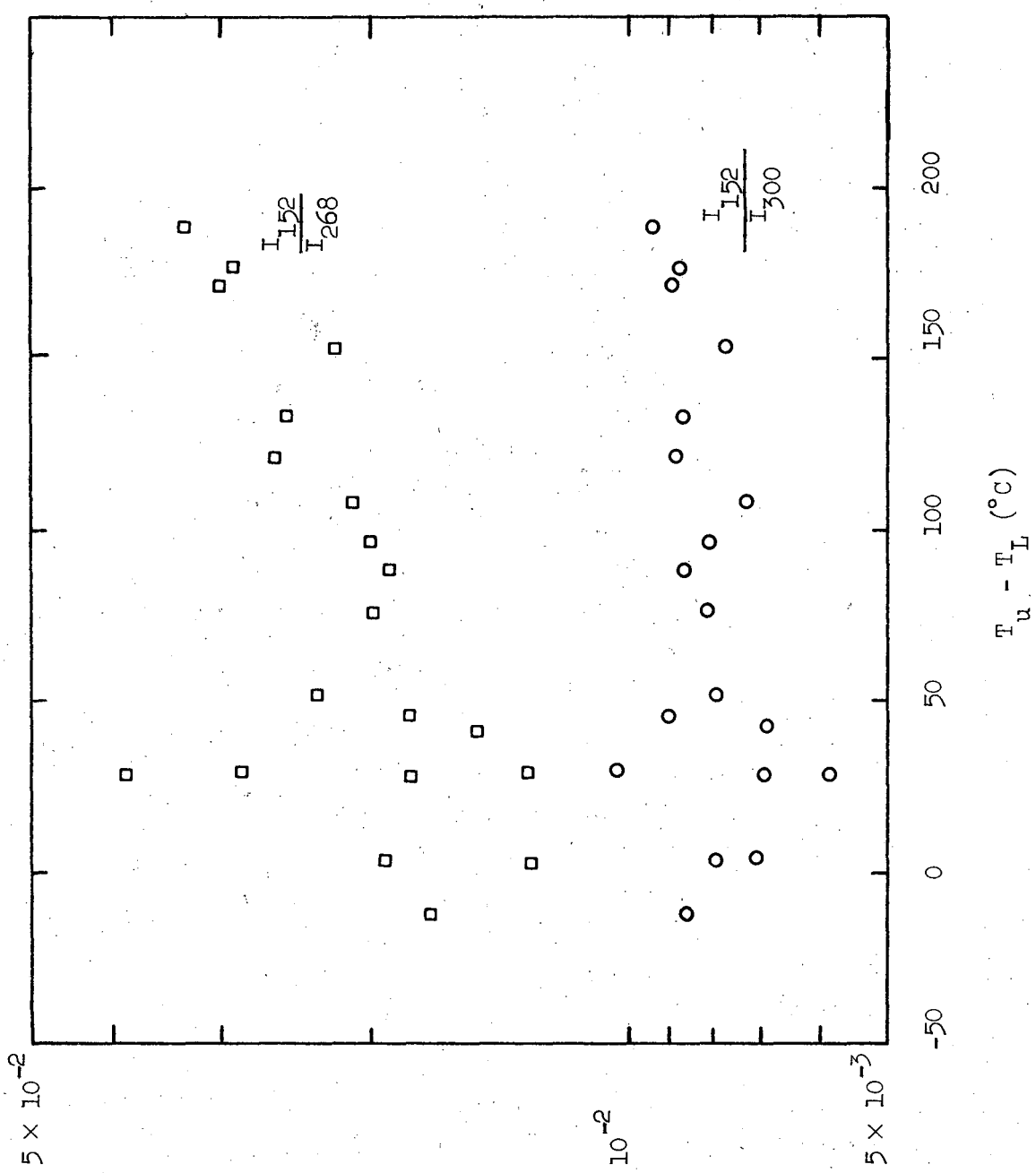
I_{152}/I_{268}
I_{152}/I_{300}
5×10^{-2}
10^{-2}
5×10^{-3}
-50
0
50
100
150
200
$T_u - T_L$ (°C)
Ion Intensity Ratio

Figure 21

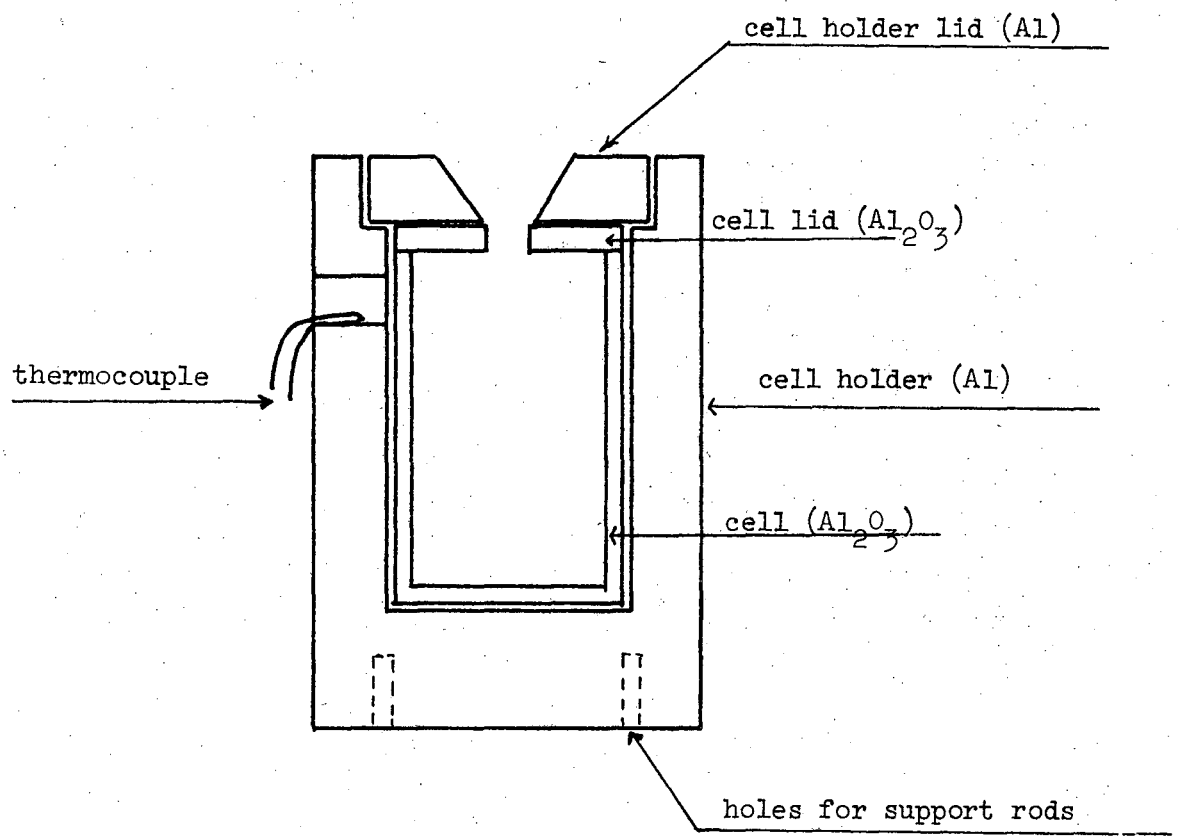
cell holder lid (Al)
cell lid (Al_2O_3)
thermocouple
cell holder (Al)
cell (Al_2O_3)
holes for support rods

Figure 22

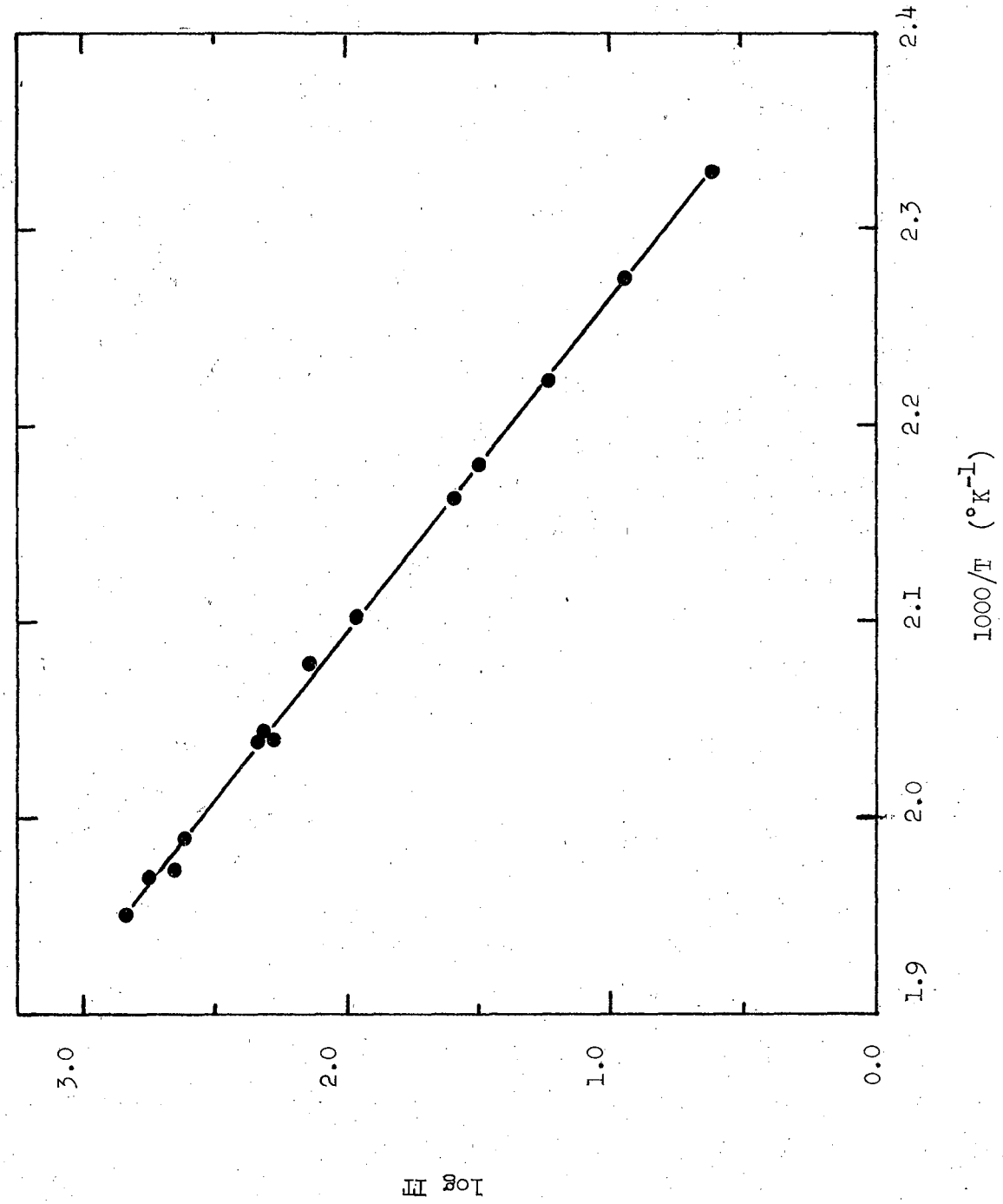

Figure 23

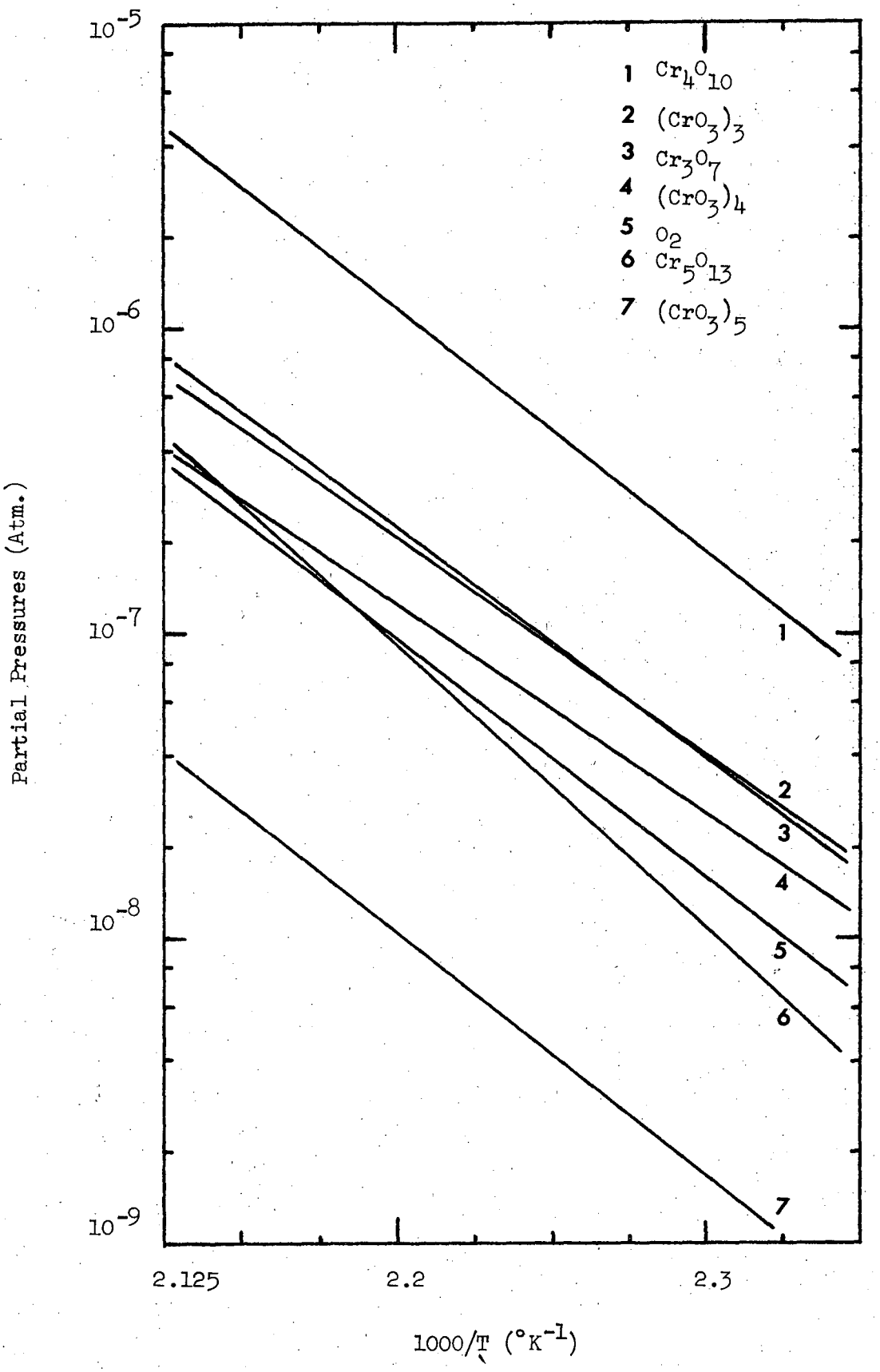
10^{-5}
10^{-6}
10^{-7}
10^{-8}
10^{-9}
Partial Pressures (Atm.)
1 Cr_4O_{10}
2 $(CrO_3)_3$
3 Cr_3O_7
4 $(CrO_3)_4$
5 O_2
6 Cr_5O_{13}
7 $(CrO_3)_5$
1
2
3
4
5
6
7
2.125
2.2
2.3
1000/T (°K^{-1})

Figure 24

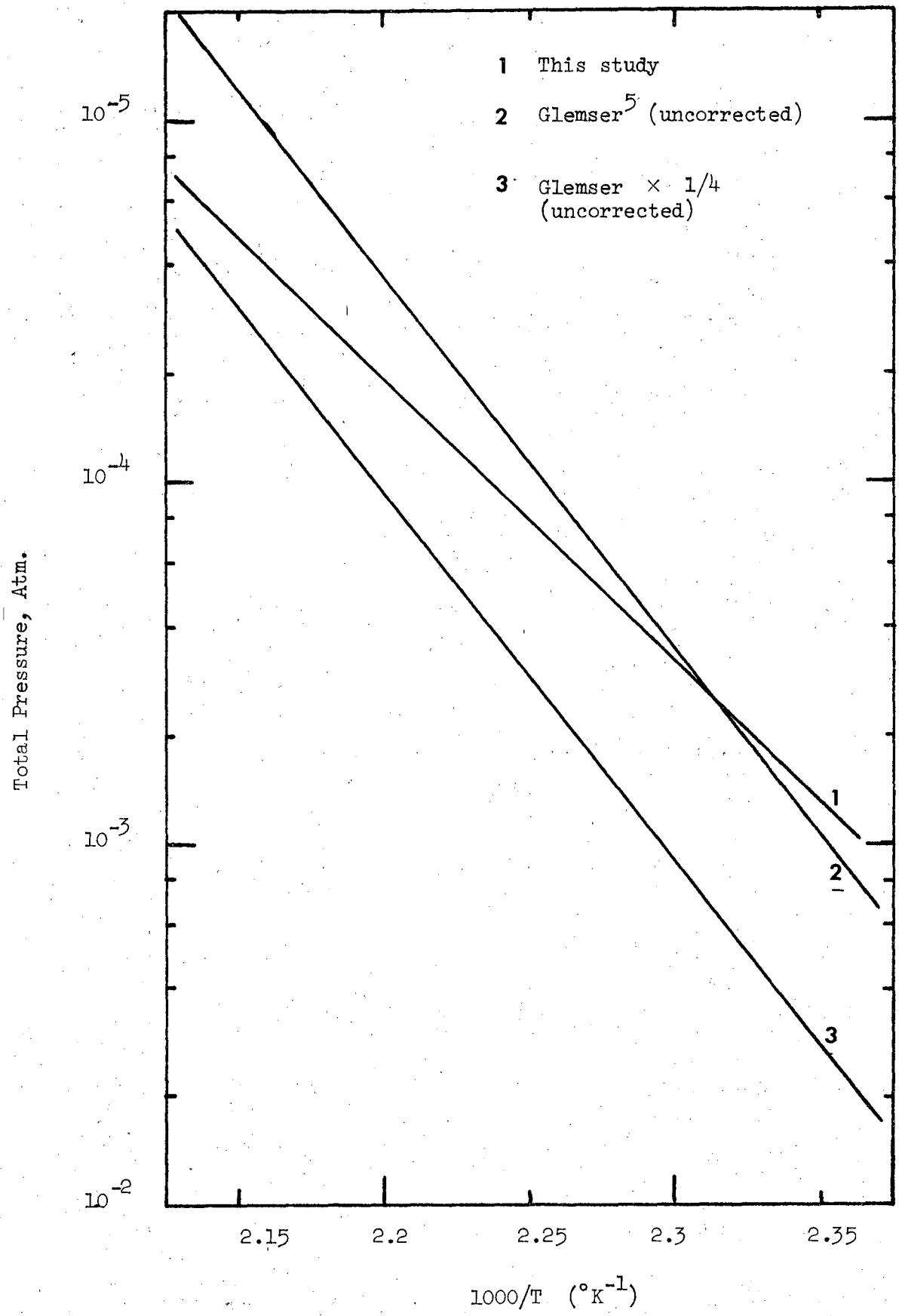
1 This study
2 Glemser[5] (uncorrected)
3 Glemser × 1/4 (uncorrected)
10^{-5}
10^{-4}
10^{-3}
10^{-2}
Total Pressure, Atm.
1
2
3
2.15
2.2
2.25
2.3
2.35
1000/T (°K^{-1})

Figure 25

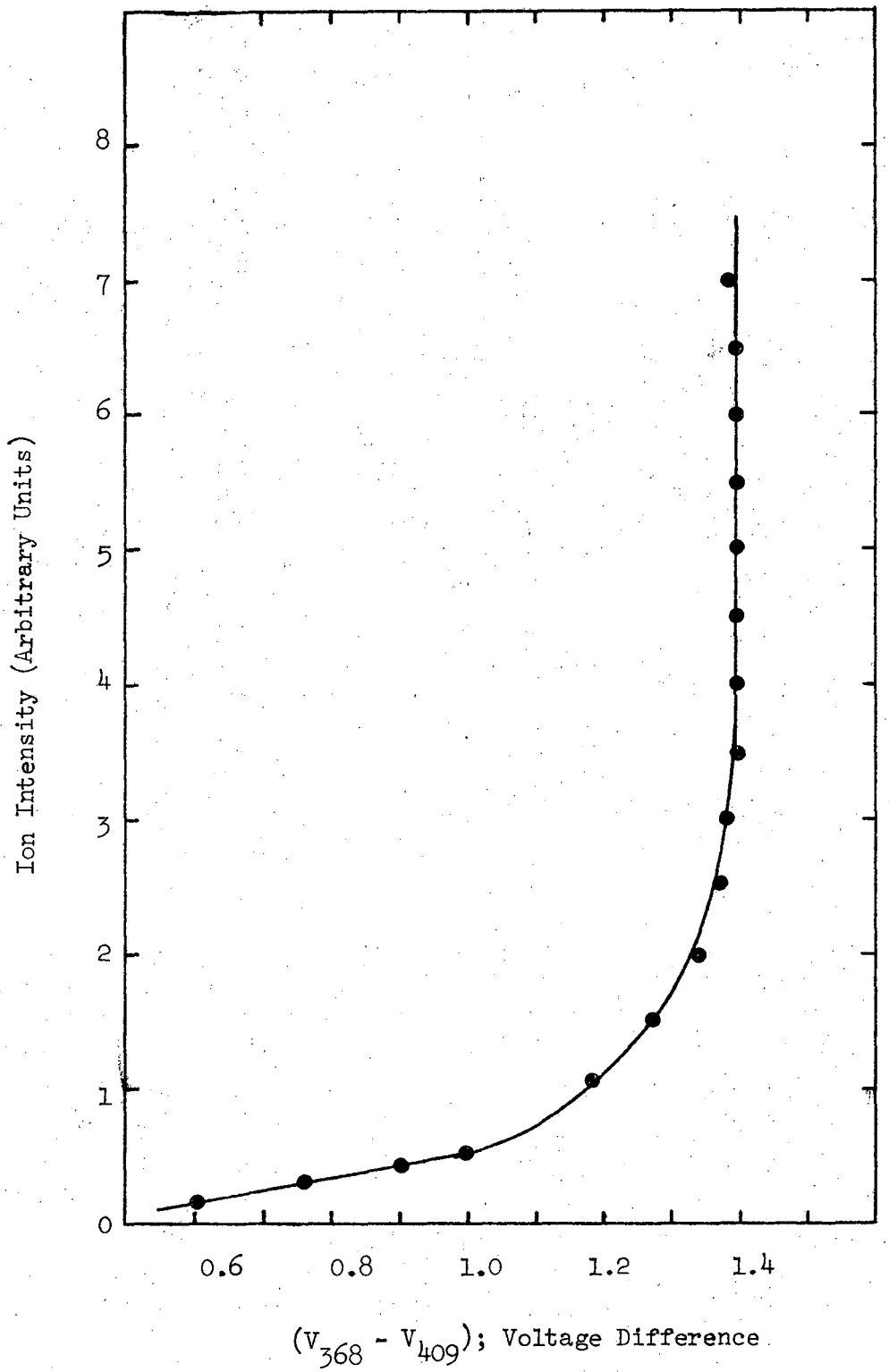
Ion Intensity (Arbitrary Units)
0
1
2
3
4
5
6
7
8
0.6
0.8
1.0
1.2
1.4
$(V_{368} - V_{409})$; Voltage Difference

Figure 26

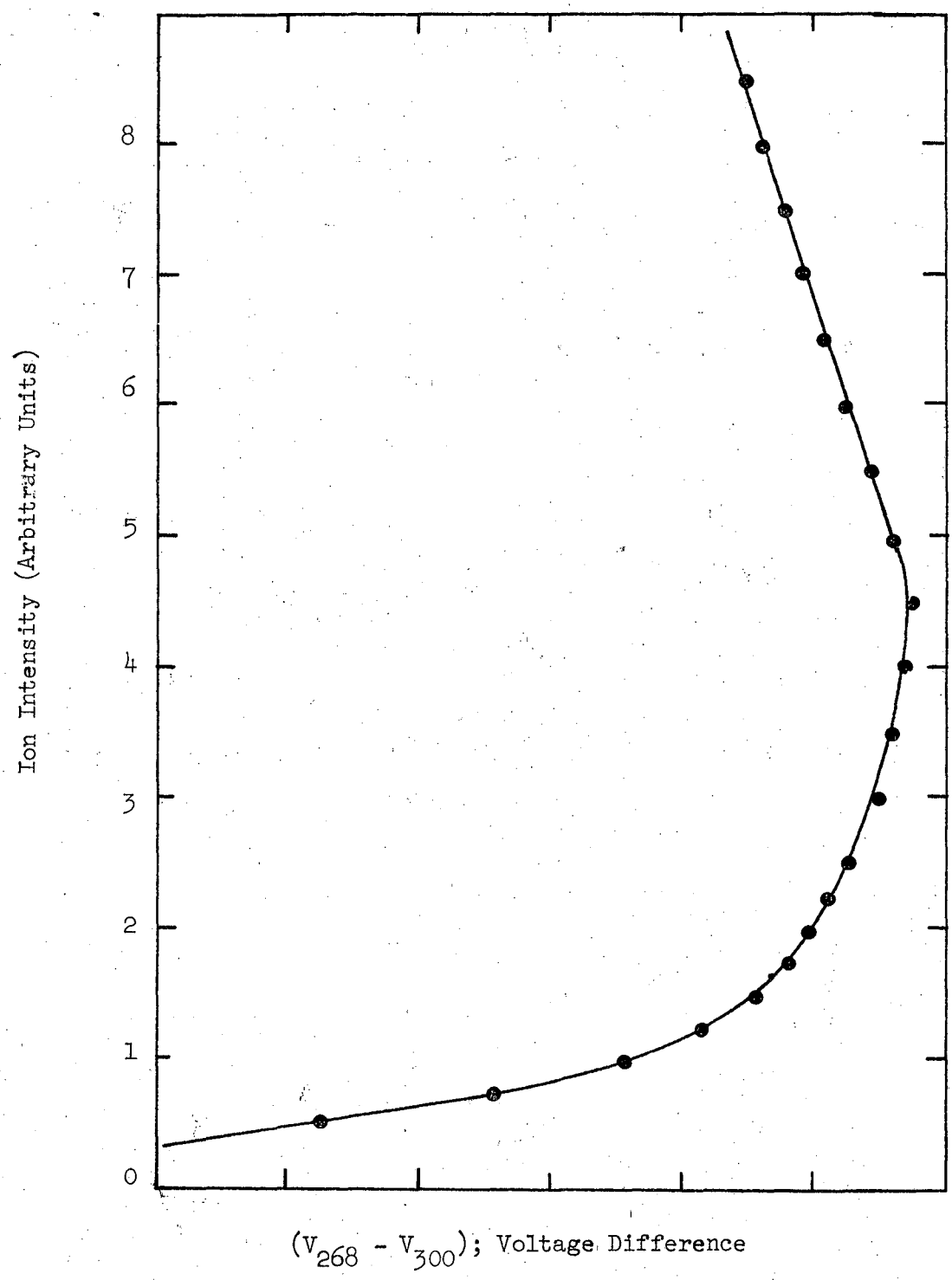
Ion Intensity (Arbitrary Units)
0
1
2
3
4
5
6
7
8
$(V_{268} - V_{300})$; Voltage Difference

Figure 27

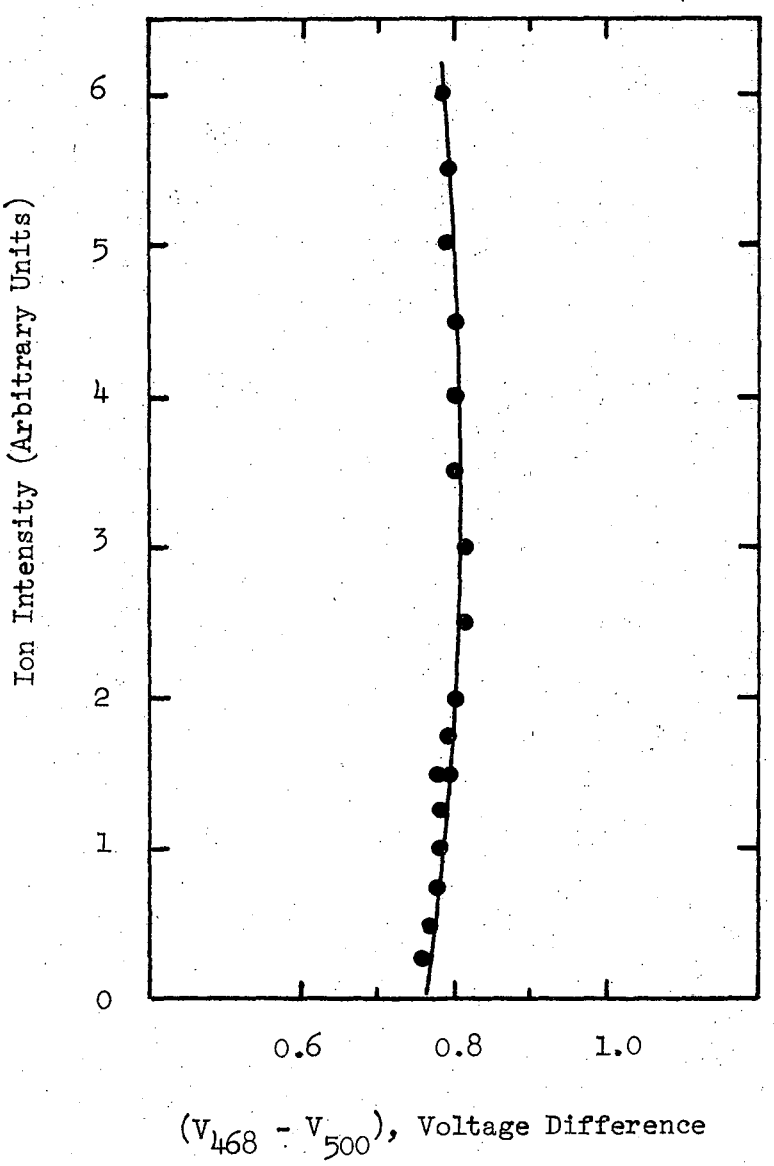
Ion Intensity (Arbitrary Units)
0
1
2
3
4
5
6
0.6
0.8
1.0
$(V_{468} - V_{500})$, Voltage Difference

Figure 28

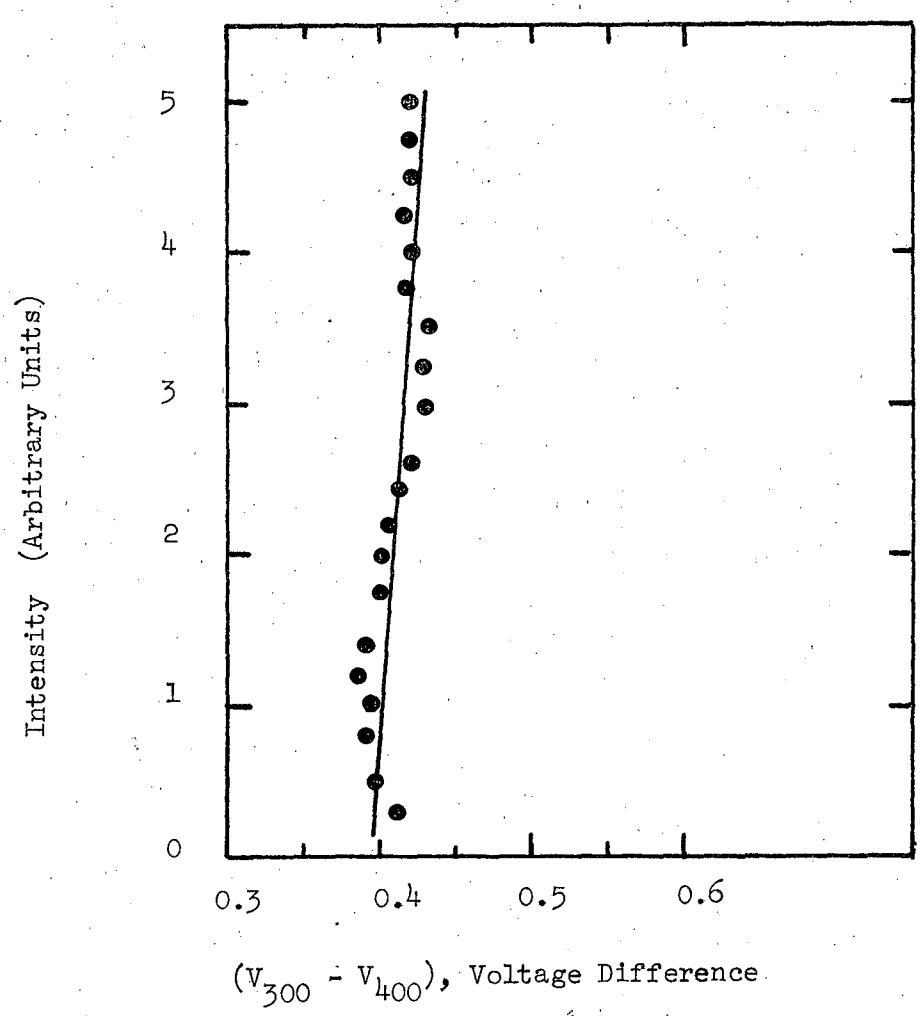
5
4
3
2
1
0
Intensity (Arbitrary Units)
0.3
0.4
0.5
0.6
$(V_{300} - V_{400})$, Voltage Difference

Figure 29

LEGAL NOTICE

This report was prepared as an account of Government sponsored work. Neither the United States, nor the Commission, nor any person acting on behalf of the Commission:

A. Makes any warranty or representation, expressed or implied, with respect to the accuracy, completeness, or usefulness of the information contained in this report, or that the use of any information, apparatus, method, or process disclosed in this report may not infringe privately owned rights; or

B. Assumes any liabilities with respect to the use of, or for damages resulting from the use of any information, apparatus, method, or process disclosed in this report.

As used in the above, "person acting on behalf of the Commission" includes any employee or contractor of the Commission, or employee of such contractor, to the extent that such employee or contractor of the Commission, or employee of such contractor prepares, disseminates, or provides access to, any information pursuant to his employment or contract with the Commission, or his employment with such contractor.

TECHNICAL INFORMATION DIVISION
LAWRENCE RADIATION LABORATORY
UNIVERSITY OF CALIFORNIA
BERKELEY, CALIFORNIA 94720